The role of mtDNA damage in mitochondrial dysfunction

by

Amy Marie Furda

B.S. Biology, Bethany College, 2006

Submitted to the Graduate Faculty of

University of Pittsburgh School of Medicine in partial fulfillment

of the requirements for the degree of

Doctor of Philosophy

UNIVERSITY OF PITTSBURGH

SCHOOL OF MEDICINE

This dissertation was presented

by

Amy Marie Furda

It was defended on

December 8th, 2011

and approved by

Chairperson: Guillermo Romero, Ph.D., Associate Professor, Department of Pharmacology & Chemical Biology

Laura Niedernhofer, M.D., Ph.D., Associate Professor, Department of Microbiology & Molecular Genetics

Alicia Palladino, Ph.D., Research Assistant Professor, Department of Pharmacology & Chemical Biology

Sruti Shiva, Ph.D., Assistant Professor, Department of Pharmacology & Chemical Biology

Robert W. Sobol, Ph.D., Assistant Professor, Department of Pharmacology & Chemical Biology

Dissertation Advisor: Bennett Van Houten, Ph.D., Professor, Department of Pharmacology & Chemical Biology

THE ROLE OF MTDNA DAMAGE IN MITOCHONDRIAL DYSFUNCTION

Amy Marie Furda

University of Pittsburgh, 2011

Mammalian mitochondria have a 16.5 kb genome encoding for 13 polypeptides, 2 rRNAs, and 22 tRNAs essential for mitochondrial function. Mutations and deletions in mitochondrial DNA (mtDNA) are implicated in some hereditary diseases as well as aging, cancer and neurodegeneration. Here, we examine the role of DNA ligase in mtDNA maintenance, and the role of mtDNA damage inflicted by hydrogen peroxide (H_2O_2) or methyl methanesulfonate (MMS) in mitochondrial dysfunction. We establish that mitochondrial DNA ligase activity is essential for survival, persistent mtDNA damage is not sufficient to induce rapid mtDNA loss and mitochondrial dysfunction. We removed and replaced the normal mitochondrial DNA ligase III with different forms of mitochondrially-targeted DNA ligase, and found that mitochondrial DNA ligase activity is necessary for cellular survival and that any type of DNA ligase activity in the mitochondria is sufficient to maintain mtDNA integrity and copy number. To study the relationship between mtDNA integrity and mitochondrial function, we treated cells with H_2O_2 or with the alkylating agent MMS, both of which resulted in persistent mtDNA lesions. However, only the H_2O_2-treated cells showed mtDNA loss and mitochondrial dysfunction by 8 hours post-treatment, indicating that persistent mtDNA damage does not necessarily cause a rapid loss of mtDNA or mitochondrial function. These data suggest that oxidants are more efficient than alkylating agents at driving mtDNA loss and mitochondrial dysfunction.

We then addressed the cause of H_2O_2-induced loss of mtDNA 8 hours following treatment. We hypothesized that this loss of mtDNA is dependent upon mitochondrial fission and mitophagy. In order to test this hypothesis, we treated cells with the fission inhibitor mdivi-1. Mdivi-1 protected mtDNA against oxidative-induced mtDNA damage but not MMS-induced mtDNA damage. Because mdivi-1 is thought to act through inhibition of Drp1, we performed siRNA-mediated knockdown (KD) of Drp1 and observed that the knockdown did not recapitulate mdivi-1 treatment in protecting against H_2O_2-induced mtDNA damage. Furthermore, treating Drp1 KD cells with mdivi-1 still showed the protective effects of mdivi-1 on mtDNA damage. These results suggest that the mdivi-1 mediated protection of oxidant-induced mtDNA damage may be independent of its role in inhibiting mitochondrial fission.

TABLE OF CONTENTS

LIST OF SCHEMA

LIST OF TABLES

LIST OF FIGURES

PREFACE

Abbreviations

5'-dRP	5'deoxyribose-5-phosphate
8-oxoG	8-hydroxyguanine
AP site	Apurinic/apyrimidinic site
APE	Apurinic/apyrimidinic endonuclease
BCNU	Bis-chloroethylnitrosourea
BER	Base excision repair
Cu,Zn-SOD/SOD1	Copper,zinc-superoxide dismutase
Dna2	DNA helicase 2
DNM1	Mitochondrial division dynamin
Drp1	Dynamin-related protein 1
ETC	Electron transport chain
EXOG	Exonuclease G
$FADH_2$	Flavine adenine dinucleotide
Fe^{2+}	Ferrous iron
Fe^{3+}	Ferric iron
FEN1	Flap endonuclease 1
FeS	Iron-sulfur

Fis1	Fission 1
GPDH	Glycerol-3-phosphate dehydrogenase
GPX	Glutathione peroxidase
GSH	Reduced glutathione
GSSG	Oxidized glutathione
H_2O_2	Hydrogen peroxide
HDAC6	Histone deacetylase 6
KD	knockdown
LC3	Light chain 3
Lig3	DNA Ligase III
LP-BER	Long-patch base excision repair
LPO	Lipid peroxidation
mdivi-1	Mitochondrial division inhibitor-1
Mff	Mitochondrial fission factor
Mfn	Mitofusin
MGMT	O^6-methylguanine methyltransferase
MLS	Mitochondrial localization sequence
MMS	Methyl methanesulfonate
MnSOD/SOD2	Manganese superoxide dismutase
MNU	*N*-methyl-*N*-nitrosourea
MPG	*N*-methylpurine glycosylase
mtDNA	Mitochondrial DNA
MYH	mutY homolog

NADH	Nicotinamide adenine dinucleotide
NADPH	Nicotinamide adenine dinucleotide phosphate
nDNA	Nuclear DNA
NEIL1	Nei endonuclease VIII-like 1
NTH1	Nth endonuclease III-like 1
O^6-MeG	O^6-methylguanine
OGG1	8-oxoguanine DNA glycosylase
OMM	Outer mitochondrial membrane
Opa1	Optic atrophy 1
PHGPX	Phospholipid hydroperoxide glutathione peroxidase
PINK1	Phosphatase and tensin homolog (PTEN)-induced putative kinase 1
Polγ/POLG	DNA polymerase γ
ROS	Reactive oxygen species
SAM	S-adenosylmethionine
SOD	Superoxide dismutase
SP-BER	Short-patch base excision repair
TIM	Translocase of the inner membrane
TMZ	Temozolomide
TOM	Translocase of the outer membrane
UNG1	Uracil-DNA glycosylase
VDAC1	Voltage-dependent anion channel 1

$\Delta\Psi$	Mitochondrial membrane potential

ACKNOWLEDGMENTS

First, I would like to thank the person whose wisdom and advice singlehandedly transformed my graduate career. Dr. Bruce Freeman was the person to first introduce me to my mentor, Dr. Ben Van Houten. Joining Dr. Ben Van Houten's lab reacquainted me with the passion I have always had for science and Dr. Van Houten's mentoring style instilled confidence in me to do science and to have faith in myself. His trust in me and in the data I generated allowed for he and I to speculate on what the results meant and to then design experiments to test these speculations. My happiest and most rewarding times in graduate school occurred during my time in his lab. In short, Dr. Ben Van Houten's mentoring style has been optimal for my growth and development as a scientist.

The Van Houten lab of past and present consists of wonderful and helpful people. The hour-long debates with Harshad Ghodke over experimental design and interpretation of results were not only fun, but a challenge that induced me to argue like a scientist. Similarly, my discussions with Atif Towheed, Vera Roginskaya, Dr. Michelle Barbi de Moura, and Dr. Wei Qian established my lab coworkers as my work family. I thank them for their help and companionship.

I am grateful to my committee members Dr. Guillermo Romero, Dr. Laura Niedernhofer, Dr. Alicia Palladino, Dr. Sruti Shiva, and Dr. Robert Sobol for guiding me through the past couple of years. They ensured that my thesis work was on track and gave me the encouragement I needed to finish my thesis. The department of pharmacology was extremely helpful in my graduate school journey, especially Dr. Bruce Freeman and Pat Smith, who through their actions and advice, have truly changed my life for the better. I am very thankful for the funding I have

received during my time at Pitt, including a pharmacology training grant, a departmental fellowship, and a UPCI fellowship. Without this funding I would not have been able to do research.

I thank my grandparents for being proud of me and for the phone calls and visits that increased my spirits and pushed me forward. Most especially, I thank my parents and my boyfriend Merle. They listened to my rants, encouraged me when I was disheartened, and cheered me on when I succeeded. My parents have never wavered in their support of my goals and dreams, beginning with my undergraduate studies at a tiny rural college to a graduate career at a huge urban university. My mother stayed home with me throughout my childhood and her teachings in those early years developed my insatiable eagerness to learn and a constant curiosity about how things work. My dad has instilled in me the drive to not quit a project until it is complete. He also taught me that self-reliance is the way to ensure that something is done the correct way. I am where I am today because of their constant love and support. I love you all so dearly and I could not have done this without you.

This dissertation is dedicated to my Papap. He suffered through many hardships growing up but was a wonderful family man and grandfather to me. He loved his family dearly, always saw the positive in everything, never complained, and had a cute saying to explain every situation in life. I wish he could have seen me when I graduated from high school and college, but I especially wish that he could see me receiving my doctoral degree. I wonder what cute saying he would come up with to describe this event. I miss you and I love you, Papap.

1.0 INTRODUCTION

1.1 MITOCHONDRIAL STRUCTURE

Mitochondria are double-membrane organelles located in the cytoplasm of most mammalian cells. Their outer membrane contains transporters such as porin (VDAC-1) and the translocase of the outer membrane (TOM)(1). Between the outer and inner membranes of mitochondria is an intermembrane space with enzymes such as copper,zinc-superoxide dismutase (Cu,Zn-SOD)(2) and cytochrome *c* (3) as well as an accumulation of protons that establish an electrochemical gradient across the impermeable inner membrane. Embedded within the inner membrane are inner membrane translocases (TIM) and the complexes of the electron transport chain, which participate in ATP production via oxidative phosphorylation (1). The innermost space of the mitochondria is the matrix, which in humans contains 2-10 copies of the mitochondrial genome (mtDNA), a circular 16.5 kb molecule (4) as well as matrix antioxidants. The mtDNA is not protected by histones like nuclear DNA (nDNA) and is instead associated with the protein mitochondrial transcription factor A (TFAM) and single-strand binding proteins (5). The mitochondrial genome encodes 13 polypeptides, 22 transfer RNAs and 2 ribosomal RNAs; these gene products are essential for oxidative phosphorylation. The mitochondrial DNA polymerase, Pol γ, is encoded by the nucleus and is involved in both DNA replication and repair.

1.2 OXIDATIVE PHOSPHORYLATION

ATP production in the mitochondria is carried out through the process of oxidative phosphorylation. This is accomplished by a series of five complexes embedded in the inner mitochondrial membrane and involves the acceptance of electrons from the reducing agents nicotinamide adenine dinucleotide (NADH) or flavine adenine dinucleotide ($FADH_2$) at Complex I and Complex II, respectively. These electrons are passed along the complexes by electron carriers such as ubiquinone and cytochrome *c*. Concurrently with electron transport, protons are transferred across the inner membrane by complex I (NADH dehydrogenase), complex III (cytochrome bc 1 complex), and complex IV (cytochrome c oxidase). The transfer of protons to the intermembrane space establishes an electrochemical proton gradient due to the pH difference between the mitochondrial matrix and the intermembrane space (reviewed in (6)). Complex V (ATP synthase) harnesses the proton gradient to produce ATP (reviewed in (7)). The ATP synthase can also run in reverse, converting ATP to ADP in an attempt to restore the proton gradient in the intermembrane space (reviewed in (7)). Molecular oxygen is the final electron acceptor during oxidative phosphorylation and is reduced to water in a four-electron reduction.

1.3 MITOCHONDRIA AND ROS

1.3.1 Mitochondrial ROS

The two major forms of ROS in the mitochondria are superoxide and H_2O_2. These are produced normally during oxidative phosphorylation and are increased during ischemia-reperfusion and other instances of oxidative stress (8). In the mitochondrial matrix the normal steady-state concentration of superoxide ($O_2^{\bullet -}$) is estimated to be 5- to 10-fold higher than it is in the cytoplasm and nucleus (9,10).

Mitochondrial superoxide is generated during respiratory chain activity (Scheme 1, reaction 1). Superoxide is reduced to H_2O_2 by manganese superoxide dismutase (MnSOD) and copper,zinc superoxide dismutase (Cu,ZnSOD) in the mitochondria (Scheme 1, reaction 4) and is oxidized to molecular oxygen by cytochrome *c* (Scheme 1, reaction 3) or by molecules containing ferric iron, such as FeS-containing proteins (Scheme 1, reaction 2)(reviewed in (9)). Mitochondrial H_2O_2 is generated via SOD activity (Scheme 1, reaction 4) and by the spontaneous dismutation of superoxide (reviewed in (10)). Hydrogen peroxide is converted to water by glutathione peroxidase (Scheme 1, reaction 5) and peroxiredoxins (Scheme 1, reaction 6)(reviewed in (9)). When H_2O_2 reacts with Fe^{2+}, the hydroxyl radical (HO•) is generated via the Fenton reaction (Scheme 1, reaction 7). The hydroxyl radical is highly reactive with all biomolecules, including nucleic acids, proteins, lipids, and sugars. The reactions and processes that generate superoxide, H_2O_2, and the hydroxyl radical are summarized in scheme 1.

Scheme 1. Chemical reactions in mitochondrial ROS production and metabolism

1. $O_2 + e^- \rightarrow O_2^{\bullet -}$

2. $O_2^{\bullet -} + Fe^{3+} \rightarrow Fe^{2+} + O_2$

3. cyt c-$Fe^{3+} + O_2^{\bullet -} \rightarrow$ cyt c-$Fe^{2+} + O_2$

4. $2O_2^{\bullet -} + 2H^+ \rightarrow H_2O_2 + O_2$

5. $H_2O_2 + 2GSH \rightarrow 2H_2O + GSSG$

6. $2H_2O_2 \rightarrow 2H_2O + O_2$

7. $Fe^{2+} + H_2O_2 \rightarrow Fe^{3+} + OH^{\bullet} + OH^-$

1.3.2 Mitochondrial antioxidant defense system.

MnSOD (SOD2) is the primary enzymatic defense against superoxide produced during mitochondrial oxidative phosphorylation. Each of the three SODs existing in mammalian cells have been knocked out, but it was the loss of SOD2 activity that had the most severe effects, including neonatal lethality, heart defects, and reduced activity of mitochondrial proteins, including complex I, complex II, aconitase, and citrate synthase (11-13). In humans, polymorphisms in the *Sod2* gene have been linked to several diseases including type I diabetes and various cancers (14-16), and in recent years SOD2 has been suggested to be a tumor suppressor (17). The intermembrane space of mitochondria typically contains Cu,Zn-SOD (SOD1) (2), which converts superoxide in the intermembrane space to H_2O_2.

Mitochondria have both glutathione peroxidase (GPX) and phospholipid hydroperoxide glutathione peroxidase (PHGPX) activity, which detoxifies H_2O_2 and oxidized lipids, respectively. GPX activity appears to outcompete all other H_2O_2 scavengers in mitochondria (18). In reducing H_2O_2, glutathione peroxidases generate oxidized glutathione (GSSG), which is re-reduced using the enzyme glutathione reductase and the reducing agent NADPH (reviewed in (6)).

In addition to glutathione peroxidase and glutathione to reduce H_2O_2, mitochondria contain peroxiredoxins, which are small thiol-dependent peroxidases (19). At least six isoforms of peroxiredoxin exist in humans, and these isoforms differ in their cellular location, their oligomeric status, and the presence of one or two conserved cysteines required for their function (20,21). The mitochondrial isoforms of peroxiredoxin are peroxiredoxin-III and V (19). Both of these mitochondrial isoforms utilize two conserved cysteine residues to reduce H_2O_2 to H_2O and return the enzyme to its reduced state. Peroxiredoxin-V overexpression in particular has been shown to protect mtDNA against exogenously added H_2O_2 (19).

Glutathione (GSH) is the major endogenous antioxidant and participates directly in reducing free radicals and ROS, keeping exogenous antioxidants such as vitamins E and C in their reduced forms, and directly binding xenobiotics and carcinogens (reviewed in (22)). The reduced form of glutathione (GSH) makes up 90% of the glutathione pool in healthy cells and tissue (23). There are two major pools of glutathione in the cell: the cytosolic pool and the mitochondrial pool (24). The mitochondrial pool of glutathione composes 10-15% of the total cellular glutathione at a concentration similar to that of cytosolic glutathione (10-14 mM)(reviewed in (22)). After GSH reacts with an oxidant in a direct or glutathione peroxidase-catalyzed reaction, the oxidized form of glutathione readily reacts with another molecule of

glutathione to form GSSG, thus preventing oxidants from damaging important biomolecules. In fact, an increased GSSG-to-GSH ratio is considered to be an indication of oxidative stress (25).

In addition to the antioxidant Cu,Zn-SOD (2), the intermembrane space of mitochondria contains cytochrome *c*, which in its oxidized form (cyt c-Fe^{3+}) can oxidize superoxide to molecular oxygen (reviewed in (26)).

Though catalase is chiefly known for its role in the peroxisome and to a lesser extent in the cytoplasm, it has been detected in the mitochondria of rat heart and liver (27-29). However, its presence in the mitochondria and its role there remains controversial (27).

1.3.3 Sources of mitochondrial ROS

Several superoxide-generating sites in mitochondria have been discovered by using inhibitors of the electron transport chain on isolated mammalian mitochondria or submitochondrial particles (reviewed in (10)). Unlike when using intact mitochondria, submitochondrial particles are mainly devoid of the mitochondrial matrix antioxidant enzymes (30,31), and so ROS are not metabolized by the matrix antioxidants and are able to be detected and measured. In this same vein, studies in isolated mitochondria do not take into account the effects of cytosolic antioxidants and other cellular components in the production and metabolism of mitochondrially-generated ROS. Therefore, measurements made of mitochondrial ROS generation rates *in vivo* under normal conditions are indirect ((32), reviewed in (6)).

An increase in ROS can be seen experimentally by treating cells with rotenone. Rotenone inhibits complex I by blocking the enzyme near the binding site for its electron acceptor ubiquinone (33). This inhibition increases the reduction of complex I's NADH dehydrogenase site, which faces the matrix side of the inner mitochondrial membrane (34),

leading to enhanced electron leak and superoxide production in that compartment (35). Rotenone treatment of intact mitochondria with complex I substrates does not lead to increased H_2O_2 production, and yet in submitochondrial particles, H_2O_2 production was increased, indicating that (1) complex I is the source of rotenone-induced ROS production and that (2) the ROS produced by complex I are metabolized by matrix antioxidants (36). ROS produced by complex I are released into the mitochondrial matrix and can then cause mitochondrial damage or be inactivated by matrix antioxidants (30,37). The specific sites of complex I that generate superoxide are proposed to be the NADH-binding site (site IF) and the ubiquinone reduction site (site IQ), but these sites still remain controversial (10).

Treatment of cells with 3-nitroproprionic acid as well as mutations in complex II have been shown to cause superoxide overproduction through complex II (38-40), but under normal conditions, superoxide from complex II is insignificant (10).

Complex III is a major site of mitochondrial superoxide generation (41-44). It has two main ROS-producing regions: the Q_o center, which faces the intermembrane space; and the Q_i center, which faces the mitochondrial matrix from its position in the inner mitochondrial membrane. The complex III inhibitor antimycin A acts at the Q_i center of complex III and increases superoxide production from the Q_o center (42,44-46). Unlike superoxide produced at the Q_i site of complex III, which most likely is released into the mitochondrial matrix, superoxide produced at the Q_o site of complex III is released into the mitochondrial intermembrane space (43,45,46). Studies in both mitochondrial and submitochondrial particles using antimycin A to inhibit complex III increased H_2O_2 production, supporting the idea that superoxide produced at the Q_o center is released into the intermembrane space and is not metabolized by matrix antioxidants (36,41). Complex III is considered to be the dominant site of

mitochondrial ROS production, with 70% of the superoxide it generates released into the matrix and 30% released into the intermembrane space (36).

Conversely, inhibiting complex IV does not lead to increased ROS production at complex IV (47-49) but causes increased electron leak and ROS production from complexes I and III (50). Studies of submitochondrial particles treated with the complex IV inhibitor azide suggest that complex I is the major site of ROS production in this case because H_2O_2 production was enhanced in the presence of complex I substrates, but not in the presence of the complex II substrate succinate and complex I inhibitor rotenone (36).

Though the flavoprotein monoamine oxidase is found on the mitochondrial outer membrane, its oxidative deamination of amines contributes to the steady-state concentration of H_2O_2 both in the cytosol and in the mitochondrial matrix (reviewed in (9)). Hydrogen peroxide produced during the reaction between monoamine oxidase and catecholamines is proposed to damage the mitochondrial membrane and contribute to neurodegenerative diseases like Alzheimer's and Parkinson's (reviewed in (9)).

Another mitochondrial enzyme contributing to ROS production is glycerol-3-phosphate dehydrogenase (GPDH), an enzyme present in tissues such as the brain, adipose tissue, heart muscle, placenta, and fibroblasts (51). A cytosolic and mitochondrial isoform of GPDH work to oxidize NADH back to NAD+ and to recycle the byproducts. The mitochondrial isoform of GPDH is located on the mitochondrial inner membrane facing the intermembrane space and is proposed to produce superoxide both in the mitochondrial intermembrane space and in the mitochondrial matrix, similar to complex III (52).

The matrix dehydrogenases pyruvate dehydrogenase and 2-oxoglutarate dehydrogenase also contribute to mitochondrial ROS, introducing superoxide species to the

mitochondrial matrix; however, the method of ROS production by these enzymes is poorly understood (10).

1.3.4 The effects of ROS on biomolecules

1.3.4.1 Effects of ROS on proteins

Ferrous iron released from Fe-S clusters by superoxide readily binds both DNA and polypeptides, and so, when the Fenton reaction (Scheme 1, reaction 7) occurs at these sites, these proteins are expected to be damaged by the resultant hydroxyl radical ($OH^{\bullet}$)(53). Of the wide variety of protein oxidation products, carbonyls are often measured as an indicator of protein oxidation due to their being most easily quantified (54). The oxidation of most amino acids, aside from sulfur-containing residues, seems to be irreversible, and thus the oxidatively-modified protein likely undergoes proteolytic degradation. The hydroxyl radical generated during Fenton chemistry targets cysteine and methionine more than other amino acid residues because these residues (1) readily react with hydroxyl radicals and (2) can be directly oxidized by H_2O_2 without the involvement of Fenton chemistry (53,55). In general, however, the speed of H_2O_2-mediated cysteine and methionine oxidation is very low and thus, the direct oxidation of amino acids by H_2O_2 is unlikely to cause major effects at physiological H_2O_2 concentrations (56,57). Particular mitochondrial proteins shown to be inactivated by H_2O_2 include aconitase (58). Superoxide is also known to be highly reactive with the [4Fe-S] cluster in aconitase (9). Another enzyme targeted by mitochondrial ROS is citrate synthase, and in fact there is a decrease in citrate synthase activity in the heart mitochondria of SOD2 mutant mice (13).

1.3.4.2 Effects of ROS on lipids

The ROS-mediated oxidation of lipids is just one of three distinct methods of lipid peroxidation (LPO), the others being enzymatic oxidation and nonenzymatic oxidation by nonradical sources such ozone.

Superoxide is not active enough to directly oxidize lipids, but when superoxide reacts with nitric oxide (NO•) to form peroxynitrite ($ONOO^-$), this product is able to initiate lipid peroxidation (reviewed in (59)). Superoxide may also indirectly contribute to LPO by reducing Fe^{3+} to Fe^{2+} (scheme 1, reaction 2), which can then react with H_2O_2 in the vicinity of lipids and generate hydroxyl radicals (scheme 1, reaction 7) that readily oxidize nearby lipids and other biomolecules.

The reaction of ROS with lipids generates products that can be both detrimental and beneficial to the cell. Lipid peroxidation can lead to biomembrane disturbances as well as protein and DNA modifications, but products of lipid peroxidation have been shown to regulate gene expression and redox signaling and enhance oxidative stress tolerance. The lipid hydroperoxides resulting from lipid oxidation can become DNA-adducting electrophiles, thus propagating ROS damage (60)(reviewed in (61)).

1.3.4.3 Effects of ROS on polysaccharides

The effects of ROS on polysaccharides have been studied much more extensively in plants and fungi than in animals. The major ROS that reacts with polysaccharides is the hydroxyl radical. However, hyaluronic acid, a component of connective tissue in mammals, has been shown to be oxidatively depolymerized by H_2O_2 and Fe^{2+} *in vitro* [62].

1.3.4.4 Effects of ROS on nucleic acids

Superoxide can only indirectly damage DNA by releasing ferrous iron (Fe^{2+}) from Fe-S clusters. This ferrous iron (Fe^{2+}), some of which readily complexes with DNA, is directly oxidized by H_2O_2 in the Fenton reaction to generate the extremely reactive $OH^{\bullet}$ (scheme 1, reaction 7)(62,63). $OH^{\bullet}$ reacts readily with all biomolecules near the site of its production at a rate limited only by diffusion, and when the site of $OH^{\bullet}$ production is a ferrous iron-DNA complex, DNA damage results (53). Guanine is a particular target of $OH^{\bullet}$, though $OH^{\bullet}$ can attack any base (64). The major product formed in an $OH^{\bullet}$-DNA reaction is 8-hydroxyguanine (8-oxoG), though other products can include thymine glycols, formamidopyrimidines, single-strand breaks, and abasic sites. Treatment of cells with H_2O_2 generates ten times more strand breaks and abasic sites in mtDNA than base substitutions (65). Mitochondrial DNA (mtDNA) is particularly susceptible to attack by oxygen radicals due to (1) its close proximity to the sites of superoxide production by the respiratory chain and (2) its lack of histone protection. In fact, studies in which cells were treated with H_2O_2 at concentrations at 200 μM or less observed significantly more mtDNA damage than nuclear DNA (nDNA) damage (32,66-68), illustrating the increased ROS vulnerability of mtDNA compared to nDNA.

1.3.5 ROS-associated pathologies

A wide range of human diseases has been linked to oxidative stress and mitochondrial dysfunction, including cancers (breast, colorectal, gastric, kidney, etc.), diabetes mellitus, ischemia-reperfusion injury, atherosclerosis, and neurodegenerative diseases such as Alzheimer's disease (AD), Lou Gehrig's disease, Friedreich's Ataxia, Huntington's disease, and Parkinson's

disease (reviewed in (8) and (69)). Mutations in the mitochondrial genome and altered expression of mitochondrially-encoded proteins have been implicated in many of the aforementioned diseases (reviewed in (70-72)). Alterations in mitochondrial mass, morphology, mtDNA copy number, and mitochondrial function have all been linked to neurodegenerative diseases. For example, a decrease in mtDNA content and mitochondrial mass is an early indicator of Alzheimer's disease (73,74). Two studies generated cytoplasmic hybrids (cybrids) by destroying the mtDNA of SH-SY5Y neuroblastoma cells and repopulating the cells with the mtDNA of control or Alzheimer's patients (75,76). These studies observed AD-like amyloid-β accumulation and mitochondrial dysfunction such as reduced mitochondrial membrane potential, altered mitochondrial morphology and increased oxidative stress in cybrids containing AD mtDNA (75,76). Chronic exposure of rodents to the complex I inhibitor rotenone mimics the symptoms of Parkinson's disease (77-79).

1.4 MITOCHONDRIA AND ALKYLATING AGENTS

1.4.1 Alkylating agents

There are three main categories of alkylating agents. Nucleophilic alkylating agents are typically composed of a metal such as lithium or copper bound to carbons (organometallics). They can displace molecules such as Cl^- and add themselves to electron-deficient carbons. Carbene alkylating agents can attack even alkane C-H bonds and are extremely reactive. These two types of agents are generally used for the industrial production of polymers and will not be discussed further. The third category of alkylating agent, the electrophilic alkylating agent,

attaches an alkyl group to nucleophiles such as the free nitrogens of nucleic acids, which can be mutagenic (80). The first anti-cancer chemotherapy developed was in the form of electrophilic alkylating agents; these include cyclophosphamide (a nitrogen mustard), methyl methanesulfonate (MMS) and temozolomide (TMZ). Electrophilic alkylating agents can block DNA replication and are thus toxic to rapidly dividing cells, namely cancer cells.

Endogenous sources of alkylation include S-adenosylmethionine (SAM), which has roles in amino acid and polyamine biosynthesis. SAM has been shown to methylate DNA *in vitro* as well as proteins and lipids (81).

1.4.2 The effects of alkylating agents on biomolecules

1.4.2.1 Effects of alkylating agents on proteins

Protein alkylation by alkylating agents has not been investigated as comprehensively as DNA alkylation. In an *in vitro* study in 2005 with hemoglobin and the agents *N*-methyl-*N*-nitrosourea (MNU) or MMS, the authors observed that MMS formed methylated protein adducts with histidine or N-terminal valine residues (80). This preferential alkylation of histidines by MMS may be due to the nitrogens of histidine being stronger nucleophiles than the nitrogen of lysine. In addition to histidine and valine methylation by MMS, earlier *in vivo* studies observed cysteine and histidine methylation in rodent hemoglobin by MMS (82,83). Importantly, studies with glutathione (GSH) showed that MMS rapidly methylates glutathione *in vitro*, which generates the product S-methyl glutathione (84). S-methylglutathione has a blocked –SH group

and unlike reduced GSH, does not aid in the reduction of oxidized peroxiredoxin (85), suggesting that glutathione methylation can increase oxidative stress.

1.4.2.2 Effects of alkylating agents on nucleic acids

MMS directly reacts with nucleophilic targets such as nucleic acids as well as amino acids with no metabolic activation needed (82). Alkylating agents typically attach an alkyl group to guanine in DNA on N-7. MMS methylates DNA on the N-7 or O-6 of guanine and the N-3 of adenine via an S_N2 mechanism (reviewed in (86)). Approximately 81% of the lesions caused by MMS are N7-methylguanine, which are not toxic to the cell and can be removed by BER. Other measured DNA lesions include N3-methyladenine adducts, which make up 0.3% of total MMS-induced DNA lesions and are proposed to cause stalling of replication forks (87), and O^6-methylguanine (O^6-MeG), which makes up 10.4% of total MMS-induced DNA lesions and is the lesion responsible for the carcinogenic effect of MMS. If the O^6-methylguanine lesion is not removed, it can be mispaired with thymine, leading to DNA mutagenesis and/or repair by the mismatch repair pathway, which does not remove the O^6-methylguanine but instead removes the thymine opposite it, leaving the possibility for another O6-MeG-T mismatch and another cycle of repair (reviewed in (88)).

1.5 MTDNA REPAIR

Until recently, it had been proposed that mitochondria only possessed a short-patch base excision repair (SP-BER) pathway (89). It is now apparent that mtDNA repair occurs through

several pathways also existing in the nucleus; these pathways include mismatch repair (MMR), homologous recombination, and nonhomologous end-joining (NHEJ), as well as the key pathways involved in removal of oxidative and alkylation lesions, SP-BER and long-patch BER (LP-BER)(reviewed in (89)).

Though mismatched bases are able to be removed in mtDNA (90), whether mitochondria have mismatch repair is controversial. The presence of homologous recombination repair and non-homologous end-joining in mammalian mitochondria has been suggested in a couple of recent studies by the presence of Holliday junction-like species in human heart DNA (91) and end-joined products in isolated mitochondria, respectively (92). However, these pathways have not been further elucidated in terms of identifying the specific proteins involved with this process (91-93), and it is only ligase III that has been suggested to participate in mtDNA end-joining (92,94).

Base excision repair is the main pathway that removes oxidation- and alkylation-induced lesions in DNA. The presence of SP-BER in the mitochondria was established in studies showing that uracil and other types of oxidative damage could be removed from mtDNA (66,95,96). The components of mitochondrial SP-BER include lesion-specific DNA glycosylases, an AP endonuclease I (Ape), DNA polymerase γ (Polγ), and DNA ligase III (reviewed in (97)). In mitochondrial SP-BER, a DNA glycosylase removes the damaged base to generate an AP site. AP sites can also be generated via spontaneous hydrolysis of a sugar-base linkage. Following the removal of the base, Ape1 cleaves the sugar-phosphate backbone 5' to the AP site; this results in the production of a 3'-hydroxyl and a 5'deoxyribose-5-phosphate (5'-dRP) residue on either side of the abasic site. Polγ is primed by the 3'-hydroxyl residue to insert a nucleotide into the abasic site, followed by the Polγ-mediated removal of the 5'-dRP residue.

Repair is completed when DNA ligase III seals the nick in the sugar-phosphate backbone (reviewed in (89)). The LP-BER pathway discovered in mitochondria also repairs oxidative base damage but differs from SP-BER in that the 5'-dRP flap left after Ape1 cleavage cannot be cut by Polγ after base insertion. Three enzymes have been identified in mitochondria that can process the 5'-dRP flap; these include FEN1, EXOG, and the helicase Dna2 (98-101). The nick is then sealed by DNA ligase III (reviewed in (89)). The mtDNA repair of oxidative and alkylation lesions are summarized in Fig. 1.

All of the glycosylases found in mitochondria recognize and remove oxidative mtDNA lesions. Lesion-specific glycolyases identified in mitochondria include the following: OGG1, which removes oxidized guanines such as 8-oxoG and formamidopyrimidine (102-104); UNG1, which removes uracil from DNA (105); MYH, which removes adenine across from 8-oxoG (106,107); and the glycosylases NTH1 and NEIL1, which remove oxidized pyrimidines such as thymine glycols (108,109). Some of these glycosylases have redundant functions to remove base lesions (reviewed in (110)). The mitochondrial localization of mitochondrial DNA repair proteins such as UNG1 and the mitochondrial forms of OGG1, NTH1, MYH, polymerase γ and ligase III is due to the presence of a mitochondrial localization sequence (MLS) on these proteins (94,103,111-115). An alternative splice site in the gene generates an MLS for several glycosylases, including the mitochondrial forms of UNG (UNG1), MYH, and OGG1 (103,105,106).

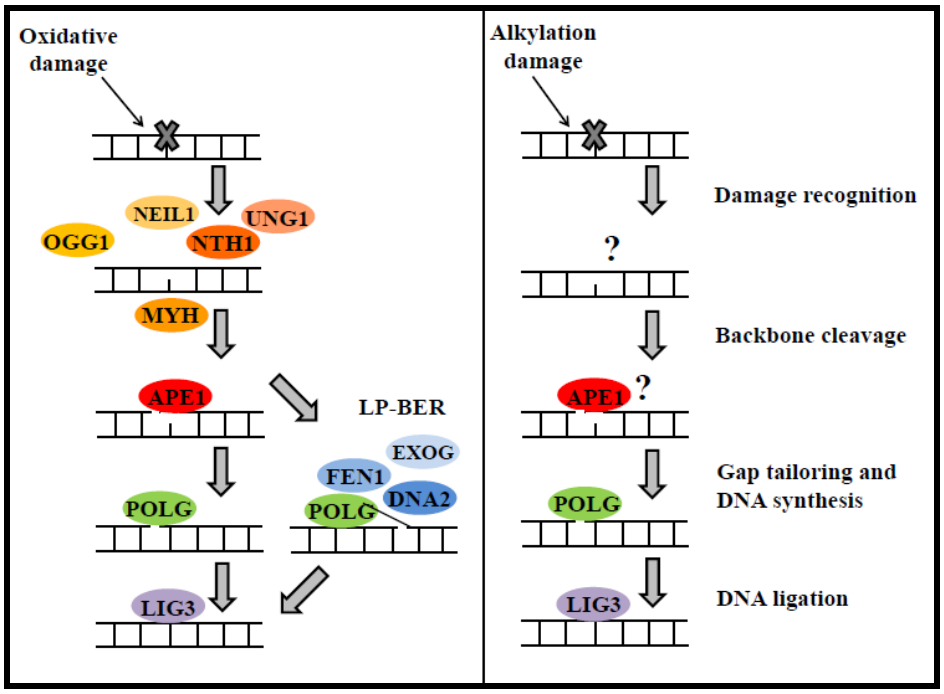

Figure 1. Repair of oxidative and alkylation lesions in mtDNA

Glycosylases involved in the removal of oxidatively-damaged mtDNA include OGG1, NEIL1, NTH1, UNG1, and MYH. After removal of the damaged base to generate an AP site, APE1 prepares the site for POLG, which performs gap filling in the abasic site and cleaves the 5'dRP residue. When two or more consecutive bases are damaged, EXOG, FEN1, and DNA2 are involved in removing the resultant 5'dRP flap. The glycosylases and/or proteins involved in recognition and removal of alkylation damage in mtDNA are unknown. APE1 likely functions in the preparation of an AP site resulting from the removal of methylated bases. POLG and Lig3 are the only known mitochondrial polymerase and DNA ligase, respectively, and they likely function in gap filling and ligation of the DNA strand.

The removal of alkylation lesions in mtDNA is not well understood. Mammalian mitochondria have not been shown to possess *N*-methylpurine glycosylase (MPG), the glycosylase that recognizes alkylation lesions such as N3-methyladenine, N3-methylguanine and hypoxanthine, or MGMT, a direct reversal protein of alkylation lesions such as O^6-methylguanine (reviewed in (89)). They have, however, been shown to repair alkylation lesions

from MMS, MNU and streptozotocin (65,116-118). Studies in yeast indicate that MMS is repaired in mtDNA without a loss of mitochondrial mass or mtDNA copy number, indicating that MMS lesions are not being "diluted" from mtDNA (119). Mitochondrial targeting of the O^6-methylguanine DNA methyltransferase (MGMT) in mammalian cells increases cell survival after treatment with the alkylating agents MMS, TMZ, and BCNU (120,121). In contrast, cells transfected with mitochondrially-targeted MPG show decreased cell survival and induction of apoptosis (122,123). This is attributed to 'imbalanced repair' via the accumulation of cytotoxic BER intermediates such as single strand breaks and abasic sites (122,124,125). Despite the aforementioned studies shedding light on alkylation-induced mtDNA repair, the mechanism of alkylation repair in mtDNA is still largely unknown.

Two forms of human APE have been discovered, APE1, the major AP endonuclease in the nucleus (126), and APE2, which has weak AP endonuclease activity. APE1 possesses an unconventional MLS in its C-terminus and several studies show it to localize and have activity in mitochondria (127-129), specifically as a 33 kDa N-terminally cleaved product in beef liver mitochondria (130). A connection between oxidative stress and mitochondrial BER was exemplified in a study in Raji B lymphocytes showing the H_2O_2-dependent translocation of APE1 to mitochondria (131). A 2001 study by Tsuchimoto and colleagues found a putative MLS in APE2, and this same study found both nuclear and mitochondrial localization of APE2 (132).

Two key enzymes involved in mtDNA replication and repair are DNA polymerase γ, the sole mitochondrial DNA polymerase, and DNA ligase III (Lig3), the source of mitochondrial DNA ligase activity. It was in 1976 that DNA ligase activity in mammalian mitochondria was first proposed (133), but it was not until a putative mitochondrial presequence was recognized

within the gene for Lig3 that the source of mitochondrial ligase activity was first discovered (134). It has since been established that alternate translation initiation in the Lig3 gene generates a nuclear form and a mitochondrial form of Lig3, the latter of which contains an MLS (94). Lig3 is the only DNA ligase found in mammalian mitochondria, and is the source of all mitochondrial DNA ligase activity during the replication and repair of mtDNA (reviewed in (89)).

1.6 MITOPHAGY

Defective mitochondria are potentially harmful to a cell, generating increased amounts of ROS, hydrolyzing ATP in an attempt to maintain a proton gradient, and releasing proapoptotic factors such as cytochrome *c*. As with other dysfunctional and aged organelles in the cell, these mitochondria are eliminated by autophagy. Autophagy is a pathway in which organelles are enveloped by autophagosomes and are transferred to lysosomes to be degraded in response to nutrient deprivation or damage (reviewed in (135)). Since the first evidence of mitochondria in liver autophagosomes was observed in 1962, scientists have been trying to understand the pathways that lead to the autophagosomal engulfment of mitochondria (136).

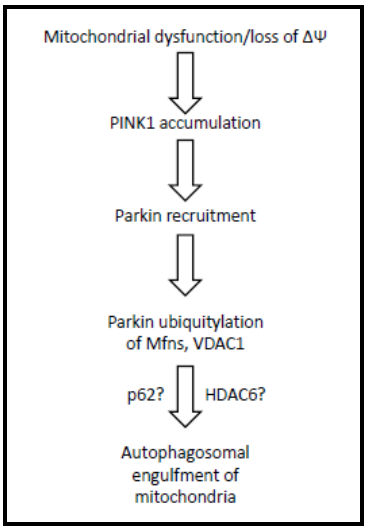

Figure 2. Mechanism of selective mitophagy

Loss of ΔΨ precedes mitophagy but is not sufficient to cause mitophagy. PINK1 levels are stabilized in response to mitochondrial dysfunction and/or loss of ΔΨ, and accumulate on the damaged mitochondria. Subsequent recruitment of Parkin to the damaged mitochondria is dependent on PINK1. Parkin ubiquitinates mitofusins and VDAC1 on the damaged mitochondria. After parkin accumulation on damaged mitochondria, the ubiquitin-binding adaptor p62 and the histone deacetylase HDAC6 accumulate on mitochondria, but their precise role in mitophagy is not well understood.

Until recently, mitochondrial autophagy was thought to occur randomly, but several recent studies have suggested selective mitochondrial autophagy, or mitophagy, as it was coined in 2005 by Dr. John Lemasters (137). Selective mitophagy in mammalian cells is proposed to occur through phosphatase and tensin homolog (PTEN)-induced putative kinase 1 (PINK1) and the E3 ubiquitin ligase parkin (reviewed in (138)). Both PINK1 and Parkin have been shown to harbor mutations in autosomal recessive Parkinson's disease, suggesting a role for mitophagy in neurodegeneration (reviewed in (138)). The only recognizable domain in PINK1 is a serine-threonine kinase domain (139). PINK1 has an MLS and spans the outer membrane of mitochondria with its kinase domain facing the cytoplasm (140), but is normally very rapidly

degraded by proteolysis (reviewed in (138)). However, when mitochondria are damaged, PINK1 proteolysis is inhibited and PINK1 accumulates on the damaged mitochondria (Fig. 2)(141,142). Parkin is normally localized in the cytoplasm (142), but it is selectively recruited to mitochondria displaying dysfunction and low membrane potential (143,144). This translocation of parkin to dysfunctional or uncoupled mitochondria is dependent on PINK1 (Fig. 2)(139,141-143,145). Increasing PINK1 expression (146,147) or increasing PINK1 accumulation on mitochondria (148) is sufficient to induce both the translocation of parkin and mitophagy. Likewise, overexpressing parkin in heteroplasmic cybrids leads to the selective elimination of mitochondria with detrimental mutations in their mtDNA (144). The interaction of PINK1 and parkin has been suggested to occur through direct binding (145,148,149) or PINK1-induced phosphorylation of parkin (146,150), but the precise mechanism by which PINK1 recruits parkin to mitochondria is not yet understood (reviewed in (138)). In addition to PINK1 and parkin, the ubiquitin-binding adaptor p62 and the histone deacetylase HDAC6 have been suggested to participate in mitophagy due to their accumulation on mitochondria after parkin recruitment, but the role(s) and requirement of these proteins in mitophagy is controversial (Fig. 2)(reviewed in (138)).

Parkin is proposed to induce mitophagy by ubiquitylating mitochondrial targets such as the mitofusins (151-153) and VDAC1 (145) (Fig. 2)(reviewed in (138)). The involvement of mitofusin ubiquitylation in mitophagy is one of many links between mitochondrial dynamics and mitophagy; this will be discussed in greater detail below.

1.7 MITOCHONDRIAL DYNAMICS

The word “mitochondria” derives from the Greek terms for thread (mitos) and grains (chondros), reflecting the vast differences in mitochondrial morphology. Mitochondrial morphology is fluid and is constantly being altered by the fission and fusion of mitochondria. The process of mitochondrial fission generates mitochondria that are more grain-like and fragmented, and the process of mitochondrial fusion generates an elongated, tubular network of mitochondria. Proteins essential for mitochondrial fusion include the mitofusins (Mfn1 and Mfn2) of the outer mitochondrial membrane as well as the inner membrane protein optic atrophy protein 1 (OPA1) (154-156). Critical players in mitochondrial fission include Dynamin-related protein 1 (Drp1) and mitochondrial fission factor (Mff)(157,158). OPA1, Mfn1, Mfn2, and Drp1 are all large GTPases in the dynamin-related protein family (reviewed in (159)). GTPase activity and oligomerization are essential for the activities of Mfn1, Mfn2, and Drp1 in mitochondrial dynamics (154,160).

1.7.1 Mitochondrial fusion

Mitochondrial fusion is mediated by OPA1, Mfn1, and Mfn2. Eight OPA1 isoforms of different lengths are generated by alternative splicing of the OPA1 gene and differential processing of the OPA1 protein by mitochondrial proteases (reviewed in (161)). OPA1 is anchored to the IMM and faces the intermembrane space (162). It is proposed to be responsible for inner membrane fusion and cristae folding by forming oligomers with other OPA1 proteins (162-164). Mfn1 and Mfn2 are located in the OMM and their oligomerization with mitofusins on other mitochondria is suggested to allow for the OMM fusion of multiple mitochondria

(165,166). In the presence of mutated OPA1 or a lack of ΔΨ, inner membrane fusion was shown to occur independently of outer membrane fusion (163,167). However, it is possible that under normal conditions these processes are coordinated (161).

1.7.2 Mitochondrial fission

Drp1 is in the dynamin-related GTPase family and its homologs in yeast and mice are Dnm1 and Dlp1, respectively. The mammalian Drp1 protein consists of two GTPase domains, one at its n-terminus and one at its c-terminus (reviewed in (161)). The c-terminus GTPase domain of Drp1 functions in self-assembly (reviewed in (161)). Drp1 is mostly cytosolic in mammalian cells but is able to translocate to mitochondrial tubules where it oligomerizes to create a "belt" around the targeted mitochondrion (157,168). The oligomerized "belt" twists upon GTP cleavage *in vitro*, constricting the mitochondrion (168).

Drp1 is regulated by phosphorylation, ubiquitylation, and SUMOylation (reviewed in (161)). Phosphorylation of human Drp1 has been shown to occur on at least two serine residues, Ser618 and Ser637, which upregulate and inhibit Drp1 activity/fission, respectively (169,170). The dephosphorylation of Ser637 on Drp1 by calcineurin induces Drp1 translocation to mitochondria (171). Ubiquitylation and SUMOylation of Drp1 have been shown to increase Drp1 activity/fission (reviewed in (161)).

Drp1 was proposed to interact with a protein called Fis1 on the mitochondrial outer membrane (172,173). The requirement for Fis1 in Drp1 mitochondrial localization was controversial, as Fis1 knockdown did not change the mitochondrial targeting of Drp1 (174). It was not until 2010 that mitochondrial fission factor (Mff), a protein anchored on the OMM, was found to be essential for the recruitment of Drp1 to mitochondria (158). The authors of the 2010

study found that (1) Drp1 and Mff physically interact *in vitro* and *in vivo*, that (2) knocking down Mff decreased mitochondrial fission, and (3) that overexpressing Mff stimulated Drp1 mitochondrial targeting and fission (158). Conversely, knocking down Fis1 did not inhibit fission and thus, the authors concluded that Fis1 is not necessary for mitochondrial fission (158).

1.7.3 Mitochondrial dynamics and mitophagy

In addition to the aforementioned parkin-mediated ubiquitylation of mitofusins, mitochondrial dynamics and mitophagy are interrelated. Deleting the fission gene Dynamin 1 (DNM1), which is a homolog of the human DRP1 gene, was shown to inhibit mitophagy in yeast (175). Parone and colleagues knocked down Drp1 in mammalian cells and observed a reduced incidence of mitochondria-LC3 colocalization, an indication of mitophagy; this suggested that Drp1 plays a part in autophagy in mammalian cells (176). When individual expression levels of mitochondrial fission and fusion components were manipulated, it was found that the pro-fusion protein OPA1 inhibits mitophagy and that the pro-fission proteins Fis1 and Drp1 work in mitophagy (177). Fission is proposed to generate metabolically dissimilar daughter mitochondria; it is the membrane potential of the daughter units that determines their fate—either to re-fuse or to be degraded by autophagy (177). Membrane potential alone, however, is not the sole determinant of a mitochondrion's fate. In cells that are dependent on oxidative phosphorylation, like neurons, mitophagy does not occur when mitochondria are depolarized (178).

1.8 MAJOR HYPOTHESIS

Previous studies have indicated a role for mtDNA damage, mtDNA loss and mitochondrial dysfunction in many human pathologies ranging from cancer to neurodegenerative diseases. The cause, interdependency, and the kinetics of persistent mtDNA damage relative to mtDNA loss and mitochondrial dysfunction are not known.

This thesis tested three major hypotheses: (1) that persistent mitochondrial DNA (mtDNA) damage leads to mitochondrial dysfunction through a loss in mtDNA copy number, and this loss is dependent on mitophagy; (2) that a compound that inhibits mitophagy, mdivi-1, prevents mitochondrial dysfunction by preventing mtDNA loss, and (3) that general mitochondrial DNA ligase activity similar to Ligase III activity is essential for cell survival.

2.0 MATERIALS AND METHODS

2.1 MATERIALS

2.1.1 General materials

Pipetmen were manufactured by Gilson. The multi-channel pipettor was manufactured by Socorex. The microcentrifuge was manufactured by and purchased from Thermo Scientific. The centrifuge for 15 mL and 50 mL tubes was manufactured by Sorvall. Pipette tips were manufactured by VWR (10 μL) and Molecular BioProducts (20, 200, 1000 μL) and purchased from VWR and Molecular BioProducts, respectively. BD Falcon serological pipets, aspirating pipets, and tubes were purchased from BD Biosciences. Microcentrifuge tubes were manufactured by Eppendorf. The black-bottomed 96 well assay plates (Costar) used in the QPCR assay, Amplex Red assay and ATPlite assay were purchased from Fisher. The plate reader used with the aforementioned black-bottomed plate was manufactured by and purchased from BioTek.

2.1.2 Cell culture materials

Cell lines for this work were 92TAg MEFs (a gift from Dr. Robert Sobol) and Mito-GFP transfected MCF7 cells. The MCF7 cells were acquired from ATCC. DMEM high glucose and

Glutamax were manufactured by Gibco and purchased from Invitrogen. RPMI 1640 (Lonza) was purchased from Fisher. Fetal bovine serum (Tet system approved) was manufactured by and purchased from Clontech. Penicillin/streptomycin, 1X PBS and 1X trypsin EDTA were manufactured by CellGro and purchased from Mediatech. BD Falcon dishes and flasks were purchased from BD Biosciences. Hydrogen peroxide was manufactured by and purchased from Sigma-Aldrich. MDIVI-1 was purchased from Calbiochem. The CASY cell counter, CASYton and CASYcups were manufactured by and purchased from Innovatis.

2.1.3 QPCR materials

The QIAcube, Qiagen Genomic-tip kit buffers G2, QBT, QC and QF and 20/G and 100/G genomic-tips, DNeasy Blood & Tissue kit, QIAamp DNA Mini kit, Proteinase K and RNase A were manufactured by and purchased from Qiagen. Tris-EDTA (10 mM Tris and 1 mM EDTA, pH 8.0) and isopropanol was manufactured by and purchased from Fisher. HaeII and PvuII restriction enzymes and related components were manufactured by and purchased from New England Biolabs. Lambda (λ)/HindIII DNA (Gibco) for the DNA standard curve was purchased from Invitrogen. Picogreen (Molecular Probes) was purchased from Invitrogen. Thermocyclers were manufactured by and purchased from Biometra. QPCR water (Sigma) was purchased from Sigma. The GeneAmp XL PCR kit and dNTPs were manufactured by and purchased from Applied Biosystems. Bovine serum albumin (Roche) was purchased from Roche. QPCR primers were purchased from IDT. PCR tubes were purchased from USA Scientific. Ethanol was manufactured by Pharmco-Aaper. The PCR enclosure was manufactured by and purchased from Labconco. Agarose, ethidium bromide, the horizontal gel

apparatus and 10X TAE were manufactured by and purchased from BioRad. The DNA loading dye (GelPilot) and DNA marker (GelPilot) were purchased from Qiagen.

2.1.4 Seahorse materials

The Seahorse Extracellular Flux Bioanalyzer and Seahorse cartridges and plates were manufactured by and purchased from Seahorse Biosciences. Oligomycin, FCCP, rotenone, 2-deoxyglucose (2-DG), DMEM base for making unbuffered media, and dimethyl sulfoxide (DMSO) were purchased from Sigma.

2.1.5 Western blot materials

PVDF membranes were purchased from Millipore. Nitrocellulose membranes, voltage packs, the vertical gel apparatus, gel transfer boxes, Bradford assay dye, BSA for protein standards, Laemmli sample buffer, 10X Tris-Glycine, 10X Tris-Glycine-SDS, Tween 20, PROTEAN TGX gels and ReadyGels (Tris-Glycine and Tris-HCl) were manufactured by and purchased from BioRad. NP-40 was purchased from Pierce. Sodium vanadate (Na_3VO_4) was purchased from Sigma. The protease inhibitor cocktail set III was purchased from Calbiochem. 1 M Tris pH 7.4 was purchased from Sigma. Dry milk was purchased from Santa Cruz. Protein marker (SeeBlue) was purchased from Invitrogen. Porin antibody was purchased from Mitosciences, β-actin from Sigma, complex V α subunit antibody from Invitrogen/Mitosciences, Drp1 antibody from BD Biosciences, and ND4 antibody from Santa Cruz. Mouse and rabbit secondary antibodies were purchased from Sigma. The Supersignal West Femto Maximum Sensitivity Substrate developing kit and x-ray film was purchased from Thermo Scientific.

2.1.6 Amplex Red materials

The Amplex Red Hydrogen Peroxide assay kit was manufactured by and purchased from Invitrogen.

2.1.7 siRNA transfection materials

Oligofectamine (Invitrogen) and OPTI-MEM media (Gibco) were purchased from Invitrogen. siRNA constructs were purchased from Qiagen.

2.2 CELL CULTURE

The simian virus 40 (SV40)-transformed mouse embryonic fibroblast cell line, 92TAg, a gift from Dr. Robert Sobol Jr., was maintained in a 37°C incubator at 5% CO_2 and grown in Dulbecco's Modified Eagle Medium, 10% fetal bovine serum (FBS), 1% penicillin/streptomycin (100 units penicillin/100 μg streptomycin per mL), and 2% Glutamax in 100 mM dishes. The cells were routinely split 2 times a week to a cell density of 1-2 $x10^4$ cells/mL. An MCF7 luminal breast cancer cell line previously transfected with a Mito-GFP construct was maintained in a 37°C incubator at 5% CO_2 and grown in RPMI supplemented with 10% FBS and 1% Penicillin/Streptomycin in 250 mL vent cap flasks. The cells were routinely split 2 times a week to a cell density of $4x10^4$ cells/mL.

2.3 DRUG TREATMENTS

For H_2O_2 treatment, 92TAg MEFs or MCF7s were plated at a density from 5-6x10^5 cells/dish in duplicate 60 mm dishes for each treatment type the evening before treatment. H_2O_2 (30%, Sigma) was first diluted into serum-free media to a concentration of 0.1 M, and then further diluted in serum-free media to the treatment concentration (50-400 μM). To each plate, 6.25 mL of serum-free media +/- H_2O_2 was added, and then cells were incubated in the media for 15 or 60 min at 37°C (Scheme 2, # 1 and 2). The original plating media (conditioned media) was saved before the H_2O_2-containing media was added to the plates, kept in a 37°C water bath, and put back on the plates after treatment for harvest times of 1 hr, 4 hr, and 8 hr (Scheme 2, # 1 and 2). Cells were harvested at 0 hr (immediately following H_2O_2 treatment), 1 hr, 4 hr, 8 hr (Scheme 2, # 1 and 2). Cells were also harvested at 1.5 hr and 24 hr for different experiments (not shown on Scheme 2). For harvest times of 1, 1.5, 4, 8 and 24 hours, H_2O_2-containing media was aspirated from the cells following the treatment and replaced with conditioned media (Scheme 2, # 1 and 2).

For MMS treatment, 92TAg MEFs were plated at a density of 6x10^5 cells/dish in duplicate 60 mm dishes for each treatment type the evening before treatment. MMS (Sigma) was diluted into serum-free media to the treatment concentration (1-3 mM). To each plate, 6.25 mL of serum-free media +/- MMS was added, and then cells were incubated in the media for 60 min at 37°C (Scheme 2, # 3). The original plating media (conditioned media) was saved before the MMS-containing media was added to the plates, kept in a 37°C water bath, and put back on the plates after treatment for harvest times of 1 hr, 4 hr, and 8 hr (Scheme 2, # 3). Cells were harvested at 0 hr (immediately following MMS treatment), 8 hr, and 24 hr. For harvest times of

1, 4, and 8 hrs, MMS-containing media was aspirated from the cells following the treatment and replaced with conditioned media.

For mdivi-1 treatment, mdivi-1 powder had first been dissolved in DMSO at a concentration of 50 mM and aliquots of it were stored at -20°C. 92TAg MEFs or MCF7 cells were plated at a density of $6x10^5$ cells in duplicate 60 mm dishes for each treatment type the evening before treatment. To prepare for the mdivi-1 treatment of cells, the 50 mM mdivi-1 stock was thawed and directly added to serum-free media to make a final mdivi-1 concentration of 10-50 µM. To each 60 mm dish, 6.25 mL of serum-free media +/- mdivi-1 was left on for 1 hour, followed by a 1 hour treatment +/- mdivi-1 +/- 200 µM H_2O_2 (Scheme 2, # 4). Cells were harvested immediately following treatment or 8 hours later (Scheme 2, # 4). In some experiments, mdivi-1 was added to the conditioned media after the treatment at a concentration of 10-50 µM (Scheme 2, # 5)

Scheme 2: Experimental design of cell treatments

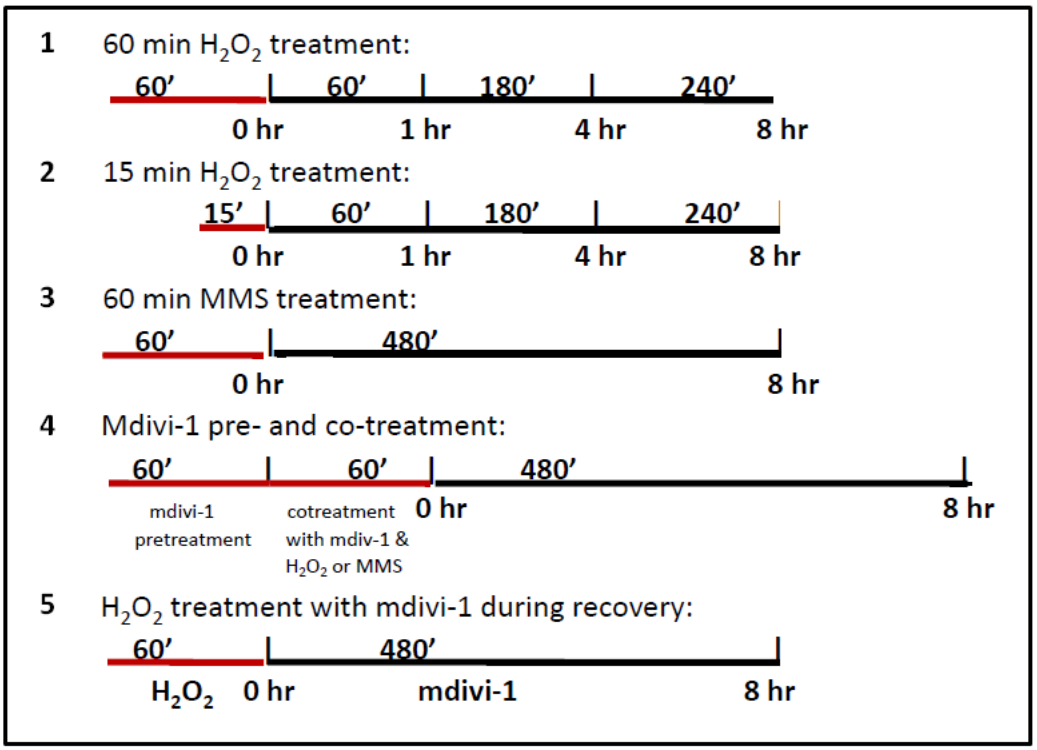

2.4 SEAHORSE EXTRACELLULAR FLUX BIOANALYZER

92TAg MEFs or Mito-GFP-transfected MCF7 cells were seeded in 24-well Seahorse tissue culture microplates in regular growth media at a density of $4x10^4$ cells per well and incubated overnight at 37°C in 5% CO_2. To a separate plate containing the Seahorse cartridge, each well was filled with Seahorse calibrant and placed at 37°C, 0% CO_2 overnight to hydrate. The next day, cells were inspected for confluency and treated with H_2O_2 as described in section 2.3. Before all H_2O_2 treatments, wells were washed with serum-free media, except for the 0-hour recovery treatments, in which wells were washed with unbuffered media. For 0-hour recovery cells, the H_2O_2 treatment was performed in unbuffered media at 37°C with 0% CO_2. The cell plate was immediately loaded into the Seahorse following H_2O_2 treatment, with no wash or change of media. For 1-hour recovery cells, the H_2O_2 treatment was performed in serum-free media at 37°C with 5% CO_2, and after a wash with unbuffered media, unbuffered media was added to the wells for 1 hour preceding the Seahorse run and plates were put at 37°C with 0% CO_2. For 4-hour and 8-hour recovery cells, the H_2O_2 treatment was performed in serum-free media at 37°C with 5% CO_2, and after a wash with serum-free media, conditioned media was added back to the wells for 3 hours and 7 hours, respectively, and plates were put at 37°C with 5% CO_2. After this incubation, wells were washed with unbuffered media and then unbuffered media was left on the cells for 1 hour at 37°C with 0% CO_2 preceding the Seahorse run.

In the hour immediately preceding the Seahorse run, the Seahorse cartridge was loaded with 75 µL of compounds dissolved in unbuffered media in the four ports per well. Unbuffered

media alone was put into each of the four ports for temperature control wells and 'blank' wells. Final concentrations of compounds in the Seahorse wells are as follows: oligomycin, 1 μM; FCCP, 300 nM; 2-DG, 100 mM; and rotenone, 1 μM.

The first 3-4 measurements of the Seahorse machine were used to establish a baseline OCR (oxygen consumption rate) and ECAR (extracellular acidification rate). Additional automated measurements were performed after the injection of four compounds affecting bioenergetic capacity: oligomycin at injection port A, FCCP at injection port B, 2-DG at injection port C, and rotenone at injection port D. Experiments were performed by simultaneously measuring OCR and ECAR rates in real time by averaging rate data for 3-6 replicate wells for each treatment type. Data was reported in pmol/min for OCR and mpH/min for ECAR. After the completion of the experiment, cells were immediately trypsinized and counted with the CASY Cell Counter to normalize individual well rate data to cell counts.

2.5 DNA ISOLATION AND QUANTITATIVE PCR (QPCR)

High molecular weight DNA was isolated either manually with the QIAGEN Genomic-tip kit or automatically with the QIAcube instrument, the QiaAmp DNA Mini Kit and the appropriate animal/human protocol as described by the manufacturer. The concentration of total cellular DNA was determined by PicoGreen fluorescence and was read using a plate reader with an excitation filer at 485 nm and an emission filter at 528 nm. λ/*Hind*III DNA was used as a standard. When using QIAcube-extracted DNA with mitochondrial primer sets, 225 ng DNA was digested with HaeII restriction enzyme (for mouse) or PvuII restriction enzyme (human) for 1 hour (for mouse) or 2 hours (human) at 37°C in a 50 μL digest mix containing 1X BSA and 20

units of restriction enzyme. After the digest, PicoGreen was used to quantitate the DNA. For mouse samples, 15 ng DNA for the QPCR assay was removed directly from the restriction digest mix. For human samples, 7.5 ng DNA was mixed at a 1:1 ratio with 1X TE before adding to QPCR reaction tubes, due to an apparent inhibition of the QPCR reaction by PvuII.

QPCRs were performed in a Biometra Professional standard thermocycler 96 with the GeneAmp XL PCR kit. Reaction mixtures contained 15 ng of template DNA, 1.2 mM $Mg(AOc)_2$ for use with the large mito and β-polymerase primers and 1.1 for use with the small mito primers, 100 ng/μ BSA (Roche, Basel, Switzerland), 0.2 mM deoxynucleotide triphosphates (Applied Biosystems, Foster City, CA), 20 pM primers and 1 unit of r*Tth* DNA polymerase, XL (Applied Biosystems, Foster City, CA). For human DNA, 1.1 mM $Mg(AOc)_2$ was used with the large mito primers and 1.2 mM $Mg(AOc)_2$ was used with the β-polymerase primers and small mito primers. For mouse, the primer nucleotide sequences were as follows: for the 6.6-kb fragment of the β-polymerase gene (GenBank database accession number AA79582), 5'-TATCTCTCTTCCTCTTCACTTCTCCCCTGG-3'and 5'-CGTGATGCCGCCGTTGAGGGTCTCCTG-3'; for the 10-kb fragment of the mouse mitochondrial genome, 5'-GCCAGCCTGACCCATAGCCATAATAT-3'and 5'-GAGAG ATTTTATGGGTGTAATGCGG-3', and for the 117-bp fragment of the mouse mitochondrial genome, 5'-CCCAGCTACTACCATCATTCAAGT-3'and 5'-GATGGTTTGGGAGATTGGTTGATGT-3'. For human, the primer nucleotide sequences were as follows: for the 221-bp fragment of the human mitochondrial genome, 5'-CCCCACAAACCCCAT TACTAAACCCA -3' and 5'-TTTCATCATGCGGAGATGTTGG ATGG-3', for the 8.9-kb fragment of the human mitochondrial genome (GenBank database accession number J01415), 5'-TCTAAGCCTCCTTATTCGAGC CGA-3' and 5'-

TTTCATCATGCGGAGATGTTGGATGG-3', and for the 12.2 kb region of the DNA polymerase β gene (GenBank database accession number L11607), 5'-CATGTCACCAC TGGACTCTGCAC-3' and 5'-CCTGGAGTAGGAACAAAAATTGCTG-3'. For the 6.6-kb and 10-kb mouse fragments and for all the human fragments, the PCR was initiated with a 75°C hot start addition of the polymerase. For the 117-bp mouse fragment, polymerase was added before the tubes were placed in the thermocycler. The samples underwent thermocycler parameters as described in table 1 (179).

To ensure quantitative conditions within the linear range of fragment amplification, a 50% control containing half the concentration of template DNA was included with each sample set. To ensure a lack of contamination in the PCR reaction components, a 'no template' control was included with each sample set, and contained a volume of 1X TE equal to the volume of DNA samples in the other reactions. PCR products were quantified using PicoGreen fluorescence and a plate reader. The fluorescence of the 'no template' control was subtracted from the average fluorescence of triplicate reads for each PCR reaction. PCR products were run on an 0.8% agarose gel (for large mito and β-pol fragments) or a 1.8% agarose gel (for small mito fragments) to ensure correct size of the PCR product and the absence of product in the 'no template' lane. DNA lesion frequencies were calculated relative to the control-treated samples. After subtracting the 'no template' fluorescence from the fluorescence values of the control and treated samples, the fluorescence values of treated samples (F_T) were divided by the fluorescence values of control samples (F_C). The resulting ratio is the relative amplification of damaged to control samples. If lesions are assumed to be randomly distributed, then nondamaged templates can be set as the zero class in the Poisson equation and can be used to calculate the lesion frequency per DNA strand of treated samples: $\lambda = -\ln F_T/F_C$.

Table 1. QPCR conditions

Primer pair	organism	Denaturation temperature (°C)	Annealing temperature (°C)	Extension temperature (°C)	Number of cycles
Small mitochondrial fragment	mouse	94	60	72	18
	human	94	60	72	19
Large mitochondrial fragment	mouse	94	64	64	16
	human	94	64	64	18
β-polymerase	mouse	94	64	64	26
	human	94	64	64	26

2.6 WESTERN ANALYSIS

Cell pellets were resuspended in two volumes of NP-40 lysis buffer (1% NP-40, 10% glycerol, 20 mM Tris pH 7.4, 137 mM NaCl) with freshly added sodium vanadate (2 mM) and protease inhibitor cocktail set III (1%) and lysed for 2 hours at 4°C on a tube rotator. Lysates were centrifuged at 4°C for 15 minutes at 13000 rpm, and the supernatant was removed and put in a pre-chilled tube on ice. Protein concentrations were measured using the Bradford assay (BioRad) and a BSA standard curve. Samples were adjusted to the same volume and concentration using 1X PBS and 2X Laemmli buffer + 5% β-mercaptoethanol. Samples of equal volumes and concentrations were separated by molecular weight on an SDS-PAGE 4-15% Tris-HCl gel and transferred overnight to a 0.45 μm nitrocellulose membrane (BioRad). Blots were blocked in 20% dry milk in PBST (, 1X PBS, pH 7.4, 1% Tween-20) for 2 hours at room temperature or overnight at 4°C depending on the affinity of the antibody. Blots were then

incubated with primary antibody diluted in 10% PBST milk for 1-2 hours at room temperature or overnight at 4°C depending on the affinity of the antibody. Blots were rinsed with PBST 3 times for 5-10 minutes each and were then incubated with peroxidase-conjugated mouse or rabbit IgG in 10% PBST milk for 30 minutes to 1 hour at room temperature depending on the primary antibody. Blots were rinsed with PBST 3 times for 5-10 minutes each and were then developed using the SuperSignal West Femto Maximum Sensitivity Substrate (Thermo Scientific) onto X-ray film (Thermo Scientific) and were analyzed using ImageJ software.

2.7 AMPLEX RED ASSAY

Cells were plated and treated with H_2O_2 and/or MDIVI-1 as described in other sections. Amplex Red solutions (1X reaction buffer, HRP stock solution, Amplex Red solution) were prepared as described by the manufacturer. At 5-10 minute increments after the H_2O_2 treatment had commenced, the plate was swirled around and a small sample of media was removed and placed into ice cold 1X reaction buffer. At the end of the treatment, each sample was mixed briefly and pipetted into a 96-well plate, along with the standards for a H_2O_2 standard curve that had been previously prepared in reaction buffer in H_2O_2 concentrations ranging from 0 to 20 μM. Amplex Red solution was combined with 1X reaction buffer and HRP stock solution to make a working solution that was then pipetted into the 96-well plate. The plate was then incubated at room temperature for 30 minutes, protected from light. A plate reader with excitation in the range of 530-560 nM and emission at 590 nM was used to read the resulting fluorescence. The H_2O_2 concentration of each sample was calculated using the H_2O_2 standard curve.

2.8 SIRNA-MEDIATED KNOCKDOWN OF DRP1

MCF7 cells + Mito-GFP were plated the night before transfection in 100 mM dishes at a cell density of 2.5 x 10^5 cells per dish. On the day of transfection, Opti-MEM and oligofectamine were combined in a tube and incubated at room temperature for 5 minutes. Opti-MEM was mixed with siRNA for either Drp1 or scrambled, combined with the oligofectamine/Opti-MEM, mixed and incubated at room temperature for 20 minutes. The Drp1 siRNA sequence is as follows: 5'-AACGCAGAGCAGCGGAAAGAG-3', targeting amino acids 96-116 in the human Drp1 open reading frame (180). Before transfection, the cell plates were washed two times with RPMI media without FBS or antibiotics, and then 8 mL RPMI was added to the plates. After the 20-minute incubation period, the Opti-MEM/siRNA/oligofectamine was then added dropwise to each plate and the plate was swirled. Plates were placed at 37°C for 6 hours. After 6 hours, FBS was added to the plate and swirled around to mix, and then the cell media was removed and replaced with fresh growth media. Three days after siRNA transfection, the cells were harvested for western blots or QPCR.

2.9 TRANSMISSION ELECTRON MICROSCOPY

92TAg MEFs were seeded in a 6-well plate at 1x10^5 cells per plate and incubated overnight at 37°C, 5% CO_2. The next day, the cells were treated for 60 minutes with 200 μM H_2O_2 and allowed to recover for 0 or 8 hours, then rinsed in PBS and fixed with 2.5% glutaraldehyde in PBS at room temperature for 1 hour. Fixed cells were then washed 3 times for ten minutes each in PBS buffer, then post-fixed for 1 hour at 4°C in 1% OsO_4 with 1%

potassium ferricyanide followed by three ten-minute washes in PBS. Cells were then dehydrated in a graded series of alcohol for ten minutes at each grade (30%, 50%, 70%, and 90%) with three 15-minute changes in 100% ethanol. This was followed by three 1 hour incubations in the epoxy embedding media epon. The last change of epon was then removed and beam capsules full of resin were inverted over the cells and polymerized at 37°C overnight and then for 48 hours at 60°C. The beam capsules were then removed and the cell layers were sectioned at 70 nm and stained with 1% uranyl acetate and 1% lead citrate. TEM images were taken of 4-6 cells per treatment on a JEM 1011 transmission microscope (JEOL, Peabody. MA).

2.10 STATISTICAL ANALYSIS

For statistical analysis of more than two samples, one-way Analysis of Variance (ANOVA) and Tukey test was utilized. The unpaired Student's *t* test was utilized for statistical analysis of two samples, with a p value < 0.05 being statistically significant (*), < 0.01 very significant (**), and < 0.001 extremely significant (***).

3.0 OXIDANTS AND NOT ALKYLATING AGENTS INDUCE RAPID MTDNA LOSS AND MITOCHONDRIAL DYSFUNCTION

3.1 INTRODUCTION

Oxidative stress has been implicated in many human pathologies and involves the imbalance of reactive oxygen species (ROS) and cellular antioxidants. ROS are produced by both exogenous and endogenous sources and include such molecules as superoxide anion ($O_2^{-\bullet}$), hydrogen peroxide (H_2O_2) and the extremely reactive hydroxyl radical ($OH^{\bullet}$). Mitochondria are the major source of endogenous ROS and produce as much as 90% of the cellular ROS during oxidative phosphorylation (reviewed in (181)). Mitochondrial DNA (mtDNA) is particularly susceptible to oxidative stress due to (1) its location on the inner mitochondrial membrane near the ROS-generating electron transport chain and (2) its lack of protective nucleosome structure; in fact, several studies have shown that inducing oxidative stress conditions in cells leads to greater levels of mtDNA damage than nuclear DNA damage (32,66,182-185). Oxidative stress and mitochondrial dysfunction are implicated in premature aging (186,187), retinal degeneration (188), neurodegenerative diseases such as Alzheimer's and Parkinson's disease (189,190), and various cancers (191-193)(also reviewed in (69)).

Hydrogen peroxide is freely diffusible and widely used to induce oxidative stress in cells. Treatment of cells with H_2O_2 causes a wide range of effects based on concentration and cell type,

including an increase in mtDNA damage compared to nDNA damage (nuclear DNA) (32,66-68,184), mtDNA degradation (65), increased mitochondrial mass (194), cell growth arrest (66,195-199), apoptosis (32,199-201), autophagy (201), increased secondary ROS such as superoxide (202), and decreased antioxidant activity (203,204). The only study linking oxidative stress to a decrease in mitochondrial function is a 2001 study by Szweda and Nulton-Persson, which suggested that H_2O_2 treatment of isolated rat heart mitochondria caused a reversible decline in oxidative phosphorylation (204).

Humans are primarily exposed to alkylating agents via cancer chemotherapy or through environmental sources such as tobacco smoke. These agents add an alkyl group to modify both nucleic acids and proteins. Alkylating agents such as chlorambucil and cyclophosphamide have been used in cancer chemotherapy (reviewed in (205)). Endogenous sources of alkylation include S-adenosylmethionine (SAM), which has been shown to methylate nucleic acids, proteins, and lipids *in vitro* (81).

Typically alkylating agents modify DNA by attaching an alkyl group to guanine in DNA on N-7. MMS in particular methylates DNA on the N-7 and O^6 of guanine and the N-3 of adenine. Although N7-methylguanine is thought to be an innocuous lesion, N3-methyladenine is toxic and leads to stalling of replication forks, and O^6-methylguanine can lead to G-C to A-T transversions (206,207). Alkylating agents such as diethylnitrosamine (DEN), dimethylnitrosamine (DMN), and N-methyl-N-nitrosourea (MNU) have been examined in the context of mtDNA damage and repair (65,116,117,208,209). A study in 1970 by Wunderlich et al used ^{14}C-labeled MNU to show that mtDNA is preferentially targeted by alkylators (208). In addition, the authors of a 1985 study with DEN and DEM gave mice a single dose of ^{14}C-labeled DEN and DMN, and mtDNA isolated from these mice showed a 10-90-fold enrichment of ^{14}C compared to nDNA,

and they also concluded that mtDNA was preferentially targeted (209). These studies may be an underestimate because the authors did not account for the DNA repair that may have occurred before the harvesting of the tissues. It was not until 1988 that mtDNA repair of alkylating lesions was addressed in a study by Myers and colleagues in which the authors found that (1) O^6-MeG lesions were present at higher levels in mtDNA than in nDNA and were repaired in mtDNA at similar rates to nDNA, and yet (2) butyl adducts on mtDNA were repaired very slowly (116). In a 1991 study, Pettepher and coworkers showed that in mammalian mtDNA, the alkali-labile sites produced by the alkylating agent streptozotocin were 55% repaired by 8 hours following treatment, and 70% repaired by 24 hours following treatment (117). A 2009 study by Shokolenko and coworkers demonstrated in HeLa cells that mtDNA damage generated during a 30 minute treatment with 1 mM MMS and 2 mM MMS is 86% repaired and 50% repaired, respectively, by 6 hours following treatment (65). However, the effect of this damage on mitochondrial function was not addressed.

Mechanisms of protecting and maintaining mtDNA integrity include scavenging of ROS through antioxidants and repair of oxidative and alkyl lesions through base excision repair (BER)(89). When complexes I and III generate superoxide anions during oxidative phosphorylation, superoxide dismutase (SOD2 A.K.A. MnSOD) converts these species to H_2O_2 (210,211), which can be further reduced to water through the action of glutathione peroxidase or peroxiredoxins. Once mtDNA damage has occurred, mitochondrial BER can repair oxidative lesions and lesions produced by alkylating agents (see (89) for review). BER enzymes are encoded in the nuclear DNA and must be imported into mitochondria, an action dependent upon the presence of a protein-encoded mitochondrial targeting sequence and the mitochondrial membrane potential. However, if mtDNA damage is persistent and extensive, it has been

suggested that mtDNA can be selectively destroyed (65,212). This study seeks to elucidate the effects of the oxidant H_2O_2 and the alkylating agent MMS on mtDNA and mitochondrial function.

3.2 RESULTS

The goal of this study was to understand the relationship between persistent mtDNA damage and mitochondrial function. To accomplish this goal, we utilized a QPCR assay to quantify DNA damage and mtDNA copy number in H_2O_2- and MMS-treated samples relative to control mock-treated samples, western blots to measure cellular levels of nuclear and mitochondrially-encoded proteins, and the Seahorse Extracellular Flux Analyzer to measure cellular glycolysis and oxidative phosphorylation.

Hydrogen peroxide and MMS cause persistent mtDNA damage. 92TAg MEFs were incubated in H_2O_2-containing media for 15 minutes (Fig. 3A) or 60 minutes (Fig. 3B), with a wide range of H_2O_2 concentrations (50-400 μM for 15 minutes or 50-200 μM for 60 minutes). As observed previously, initial mtDNA lesions were dependent on concentration and influenced by the treatment time (32,66). For example, a 15-minute treatment with 100 μM H_2O_2 initially caused 1.1 lesions/10kb, which were repaired almost completely by 8 hours (Fig. 4A). In contrast, a 60 minute treatment with 100 μM H_2O_2 initially caused 1.6 lesions/10kb, which were incompletely repaired, even after 8 hours (0.65 lesions/10kb remaining)(Fig. 4A). These data indicate that persistent mtDNA damage depended more upon the treatment time (15 versus 60 minutes) than on H_2O_2 concentration (Fig. 4A). To further illustrate the differences in mtDNA repair rates between 15- and 60-minute treated cells, the number of mtDNA lesions after a 15- or

60-minute treatment with 200 μM H_2O_2 was measured at 0, 1, 4, and 8 hours recovery (Fig. 4A). While the initial mtDNA lesion frequencies are comparable (Fig. 4A), the 60-minute treated cells show persistent mtDNA damage at 8 hours (Fig. 4B). In regards to nDNA damage, amplification of a nuclear DNA fragment near the β-polymerase gene indicated that nDNA damage inflicted by the H_2O_2 treatment was below the detection range of this assay, ~1 lesion/10^5 bases (data not shown).

Once persistent mtDNA lesions had been observed in an oxidant model of damage, 92TAg MEFs were treated with the alkylating agent MMS to determine if a non-oxidant model of damage would lead to mtDNA lesions persisting at 8 hours. Based on the observation that a 60-minute H_2O_2 was able to cause persistent mtDNA lesions, a 60-minute treatment time with MMS was employed. After performing a dose-response experiment with MMS to establish a moderate initial lesion frequency (1-2 lesions/10kb mtDNA)(Fig. 5), 2 mM MMS was used to treat 92TAg MEFs. A 60-minute treatment with 2 mM MMS caused 1.5/10kb initial mtDNA lesions, and by 8 hours following treatment, 71% of these lesions persisted (Fig. 6A). Additionally, this same concentration and treatment time of MMS caused 2.1/10kb nDNA lesions (Fig. 6B). Unlike the mtDNA damage, nDNA damage was more effectively repaired (61% reduction in nDNA lesions) by 8 hours recovery. MMS caused both persistent mtDNA and nDNA damage.

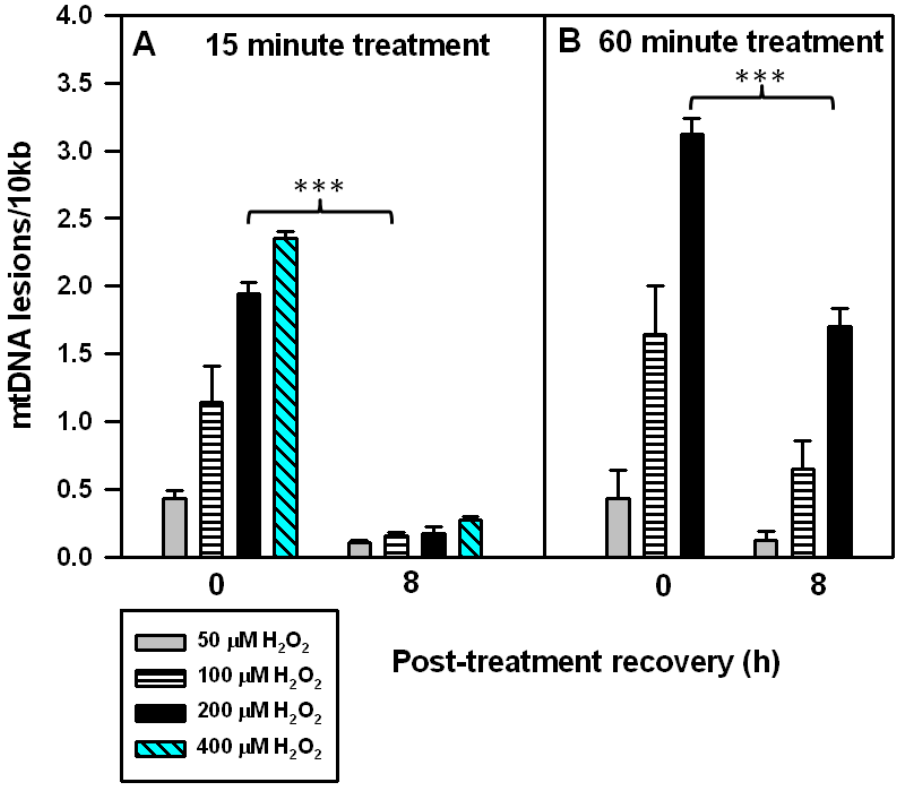

Figure 3. A 60 minute treatment with H_2O_2 causes persistent mtDNA damage

Cells were plated and the following day were treated for 15 or 60 minutes with various concentrations of H_2O_2, as in Scheme 2, #1 and 2. After the treatment, the media was replaced with conditioned media and the cells were allowed to recover for 0 or 8 hours. Cells at 0 hour recovery were harvested immediately following treatment. mtDNA lesions at 0 and 8 hours after a (A) 15-minute H_2O_2 treatment, (B) a 60-minute H_2O_2 treatment at a range of concentrations. Error bars represent the SEM of n=4-19, with 2-9 biological experiments and 2-3 replicates per treatment type. H_2O_2 at 400 μM was not used to treat cells for 60 minutes. One-sided ANOVA and a Tukey Test were used to analyze these data, $p < 0.05$ (*), < 0.01 (**), and < 0.001 (***).

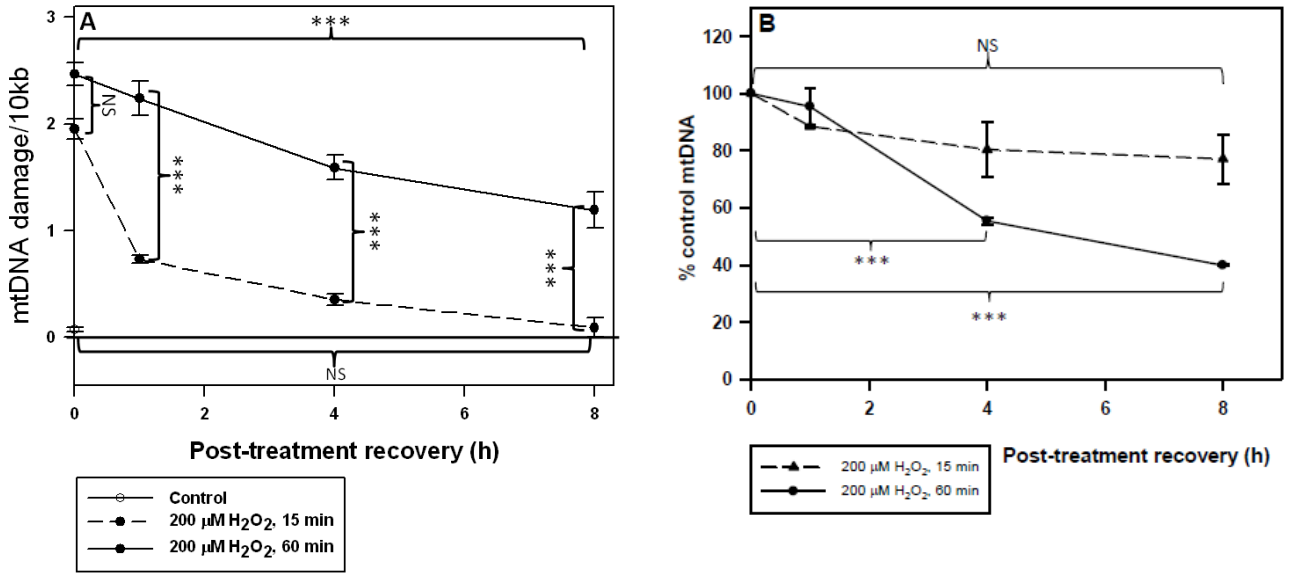

Figure 4. Kinetics of H_2O_2-induced mtDNA repair and mtDNA loss

Cells were plated and the following day were treated for 15 or 60 minutes with H_2O_2 in serum-free media. After the treatment, the media was replaced with conditioned media and the cells were allowed to recover for 1, 4, or 8 hours. Cells at 0 hr recovery were immediately harvested following H_2O_2 treatment. (A) mtDNA lesions at various timepoints after H_2O_2 treatment. Error bars represent the SEM of n=4. (B) Changes in mtDNA copy number after H_2O_2 treatments. Error bars represent the SEM of n=4. A one-sided ANOVA was used to analyze these data, $p < 0.05$ (*), < 0.01 (**), and < 0.001 (***).

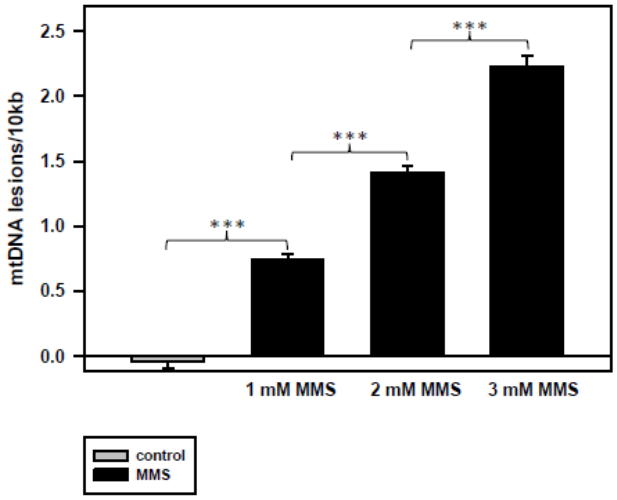

Figure 5. MtDNA damage following a 60 minute treatment with 1-3 mM MMS

Cells were plated and the following day were treated for 60 minutes with 1, 2, or 3 mM MMS in serum-free media (Scheme 2, #3). After the treatment, the cells were immediately harvested. Error bars represent the SD of n=2, with one biological experiment and two replicates per experiment.

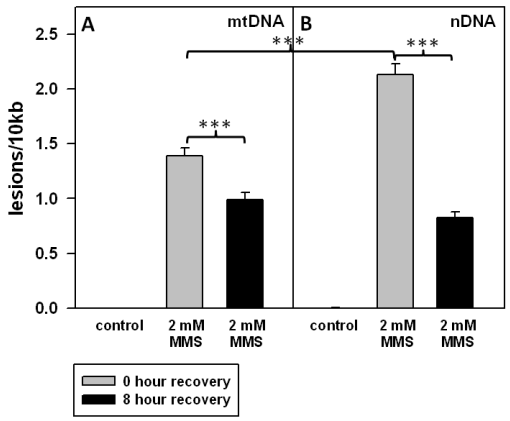

Figure 6. A 60-minute treatment with MMS causes persistent mtDNA damage

Cells were plated and the following day were treated for 60 minutes with 2 mM MMS in serum-free media as in Scheme 2, #3. (A) mtDNA and (B) nDNA lesions at 0 and 8 hours after a 60-minute MMS treatment. Error bars represent the SEM of n=6-8, with 3 biological experiments and 2-4 replicates per treatment type. One-sided ANOVA and a Tukey Test were used to analyze these data, $p < 0.05$ (*), < 0.01 (**), and < 0.001 (***).

A rapid loss of mtDNA occurs after H_2O_2 treatment and not after MMS treatment. Treatment with 200 μM H_2O_2 caused a loss of mtDNA copy number in both 15- and 60-minute treated cells (Fig. 7A and 7B), with the 60-minute treated cells showing increased loss of mtDNA as compared to the 15 minute treated cells. The rate of mtDNA loss in cells treated for 15 or 60 minutes with 200 μM H_2O_2 was measured at 0, 1, 4, and 8 hours following H_2O_2 treatment (Fig. 4B). A 15-minute 200 μM H_2O_2 treatment caused a 29% loss of mtDNA at 8 hours as opposed to the 65% loss of mtDNA in cells treated for 60 minutes with 200 μM H_2O_2, indicating that treatment time influences mtDNA loss more than H_2O_2 dose (Fig. 4B). The initial mtDNA lesions of cells treated for 15 minutes with 200 μM H_2O_2 were similar to the initial mtDNA lesions of cells treated for 60 minutes with 100 μM H_2O_2 (Fig. 4A), but the 15-minute treated cells caused significantly less mtDNA loss (30% versus 52% loss) at 8 hours compared to the 60-minute treated cells (Fig. 4B). These data suggest that it is the treatment duration and not mtDNA lesion frequency that affects loss of mtDNA.

Although a 60-minute treatment with 2 mM MMS caused similar mtDNA lesions to a 60-minute treatment with 100 μM H_2O_2 (1.4 lesions/10kb and 1.6 lesions/10kb, respectively), the MMS treatment did not result in any loss of mtDNA at 8 hours following treatment (Fig. 7C). In fact, there was a slight increase in the mtDNA copy number at 8 hours following MMS treatment. Thus, H_2O_2 treatment or MMS treatment, despite causing similar lesion frequencies, show striking differences in loss of mtDNA.

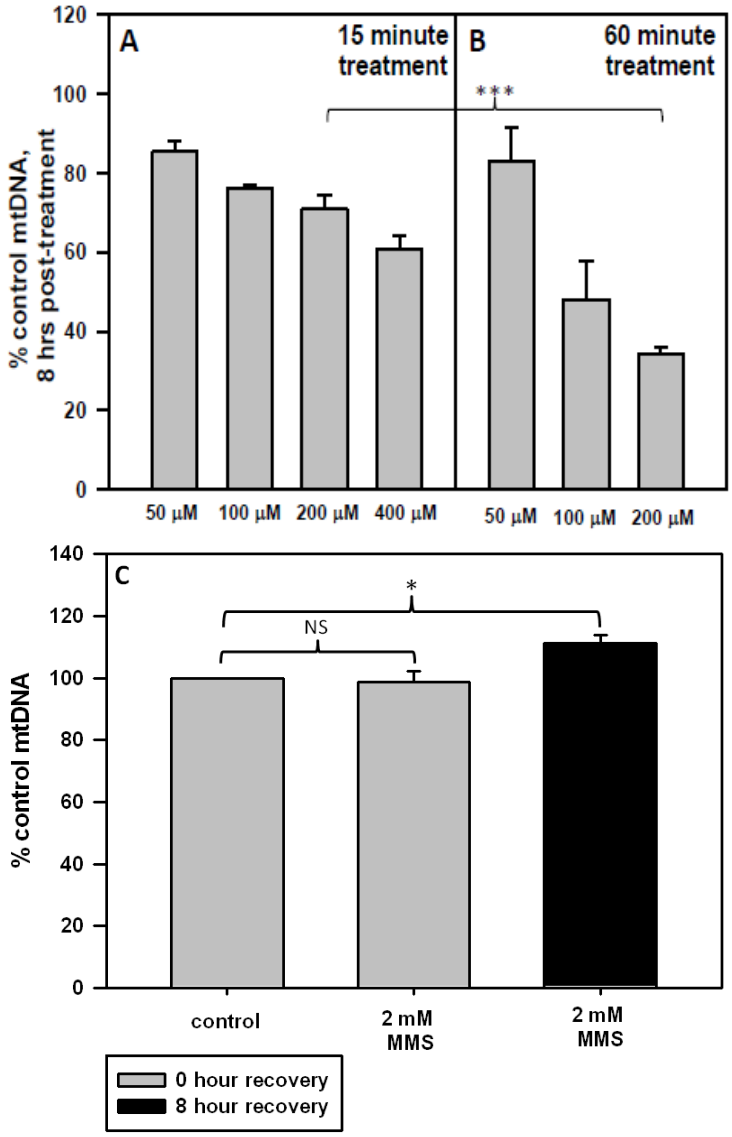

Figure 7. H_2O_2 and not MMS causes rapid loss of mtDNA

92TAg MEFs were treated for 15 or 60 minutes with various concentrations of H_2O_2 (Scheme 2, #1 and 2) or with 2 mM MMS as in Scheme 2, #3. Fraction of mtDNA copy number remaining at 8 hrs after (A) 15-minute H_2O_2 treatments, (B) 60-minute H_2O_2 treatments or (C) 60-minute MMS treatments. Error bars represent the SEM of n=4-19, with 2-9 biological experiments and 2-3 replicates per treatment type. H_2O_2 at 400 µM was not used to treat cells for 60 minutes. There is a significant difference in the mtDNA copy number at 8 hours when comparing cells treated with 200 µM H_2O_2 for 15 minutes to cells treated with 200 µM H_2O_2 for 60 minutes.

A 60 minute treatment with H_2O_2 causes a loss of complex V α subunit. Based on the persistent mtDNA lesions in the 60-minute H_2O_2-treated cells and in the MMS-treated cells, we hypothesized that there would be a decrease in a mitochondrially-encoded protein after these treatments. This hypothesis was further supported by the results of a previous study that did not look at individual mitochondrial protein levels but showed decreased mitochondrial protein synthesis in epithelial cells treated with 200 μM H_2O_2 (67). For this purpose, we determined the levels of ND4, a mitochondrially encoded subunit of complex I, normalized to the nuclear-encoded β-actin (Fig. 8). We found that at 8 hours after a 60-minute treatment with 200 μM H_2O_2, ND4 levels were decreased by 10% compared to control levels (Fig. 8A and 8C). However, at 8 hours after a 60-minute treatment with 2 mM MMS, ND4 levels were decreased by 35%, a significant decrease compared to control (Fig. 8B and 8C). The 15-minute H_2O_2-treated cells did not show a decrease in ND4 levels at 8 hours after treatment.

We measured levels of a nuclear-encoded mitochondrial protein, the α subunit of complex V, and also observed a significant 58% decrease compared to control in the level in cells treated with H_2O_2 for 60 minutes, but not in cells treated with MMS for 60 mins or in cells treated with H_2O_2 for 15 minutes. The significance values compared to control are represented by the stars directly above the bars (Fig. 8C).

In addition to measuring levels of ND4 and complex V α, we measured the levels of the outer membrane transporter porin (VDAC-1) and found that these levels were increased at 8 hours after 60 minute treatments with either H_2O_2 or MMS, but the increase in porin levels was not significant compared to control (Fig. 8C). Histogram data was acquired from 2-3 biological repeats, with 2-3 samples per repeat, and 1-4 westerns performed for each biological repeat.

Included in summary figures are representative blots for the H_2O_2 treatment (Fig. 8A) and MMS treatment (Fig. 8B).

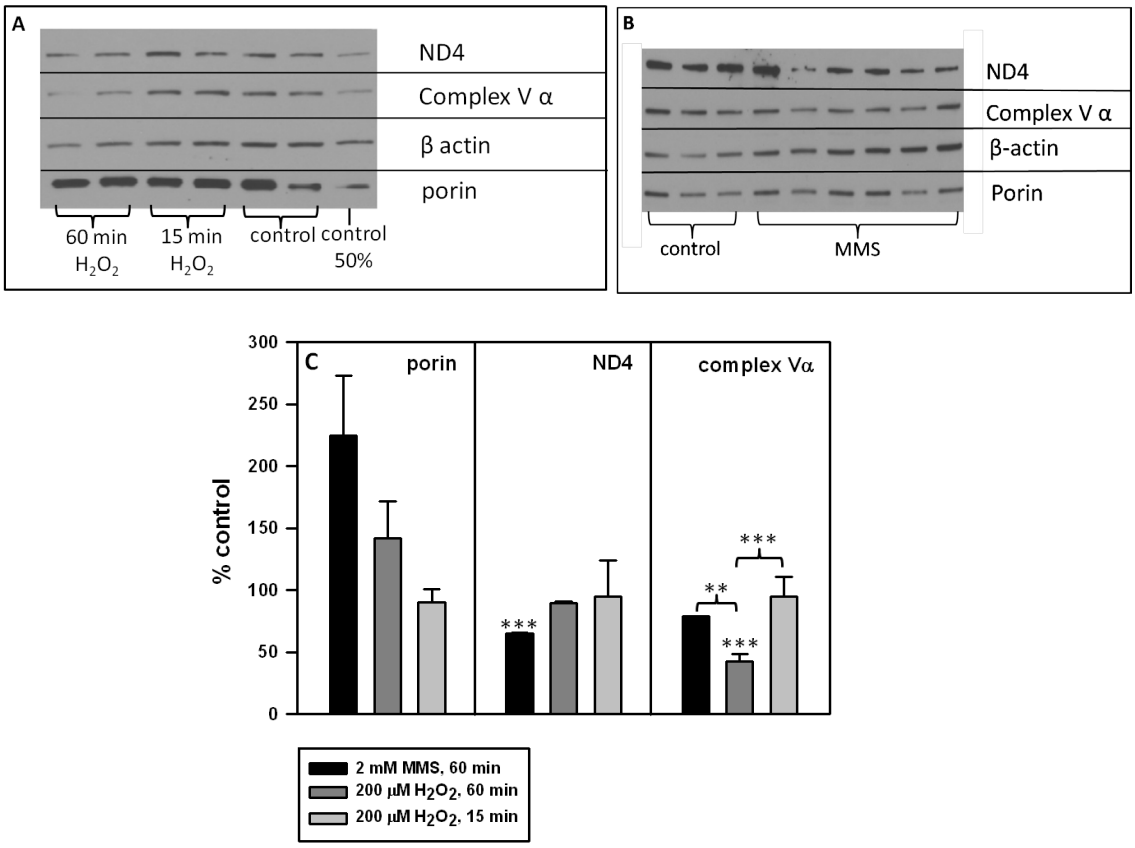

Figure 8. H_2O_2 and MMS affect mitochondrial protein levels differently

Cells were plated and the following day were treated for 15 or 60 minutes with 200 μM H_2O_2 (Scheme 2, #1 and 2) or for 60 minutes with 2 mM MMS (Scheme 2, #3). Cells were harvested at 8 hr and subjected to western blotting. Representative blots 8 hrs after (A) H_2O_2 and (B) MMS treatments. For H_2O_2, the blot is a representative of 3 experiments, with 2 separate gels per experiment and 1-3 replicates per treatment type. For MMS, the blot is a representative of 2 experiments, with 1-2 gels per experiment and 3-4 samples per treatment type. (C) Histogram of porin, ND4 and complex V α subunit levels after H_2O_2 or MMS treatment, normalized to β-actin. Error bars represent standard error of the mean, n=6-10. The stars directly above bars indicate a significant difference from control.

Hydrogen peroxide but not MMS causes a steep decline in oxidative phosphorylation and a concomitant increase in glycolysis. In order to examine mitochondrial function, a combination of four pharmacological inhibitors was used consecutively during the Seahorse extracellular flux analysis. The oxygen consumption rate (OCR) measurements before compound injections are referred to as the basal OCR. The first compound that is injected is oligomycin, which inhibits complex V in the electron transport chain and causes a decrease in respiration. The difference between the resulting OCR and the basal OCR is the ATP-linked OXPHOS (Fig. 9A). The second and third compounds, FCCP and 2-DG, uncouple the mitochondria and inhibit glycolysis, respectively, which drives mitochondrial respiration to its maximal capacity, referred to in this study as the total reserve capacity (Fig. 9A). Finally, rotenone inhibits oxidative phosphorylation at complex I and blocks all mitochondrial oxygen consumption.

We predicted that persistent mtDNA damage in both 60-minute H_2O_2- and MMS-treated cells would result in mitochondrial dysfunction at 8 hours. Figure 9B shows the ATP-linked OXPHOS at 0, 1, 4, and 8 hours following either a 15- or a 60-minute treatment with H_2O_2. Immediately after a 60 minute treatment with hydrogen peroxide, mitochondria become uncoupled, as evidenced by the smaller decrease in oxygen consumption rate after the addition of oligomycin (Fig. 10A), and this is illustrated in Fig. 9B by the 32% drop in ATP-linked OXPHOS. After 1 hour recovery from H_2O_2 treatment (Fig. 10B), there is a decrease in ATP-linked OXPHOS and total reserve capacity in both 15-minute and 60-minute H_2O_2-treated cells (Fig. 9B and 9C). This effect is greater in the 60-minute treated cells (38% decrease in ATP-linked OXPHOS and 62% decrease in total reserve capacity). By 4 hours after the H_2O_2 treatment (Fig. 10C), the 15-minute treated cells have nearly recovered their total reserve capacity to control levels, but their ATP-linked OXPHOS is still decreased (Fig. 9B and 9C).

This is in contrast to the 60-minute H_2O_2-treated cells, which did not recover ATP-linked OXPHOS or total reserve capacity to mock-treated levels (53% loss of ATP-linked OXPHOS and 68% loss of total reserve capacity). At 8 hours recovery (Fig. 10D), the 15-minute H_2O_2-treated cells have restored their ATP-linked OXPHOS to control levels, but the 60-minute H_2O_2-treated cells now show a 51% loss of ATP-linked OXPHOS and an 87% loss of total reserve capacity (Fig. 9B and 9C), in addition to a 40% increase in baseline glycolysis (Fig. 9F). The complete Seahorse profiles summarized in Fig. 9B and 9C are shown in Fig. 10A-D.

Figure 9A shows the mitochondrial pharmacologic profile of MMS- and control-treated cells at 8 hours after treatment. Unlike in 60-minute H_2O_2-treated cells, a 60 minute treatment with MMS did not cause massive mitochondrial dysfunction, and in fact only resulted in a 12% loss of ATP-linked OXPHOS (Fig. 9D) and total reserve capacity (Fig. 9E) at 8 hours recovery and no concomitant increase in glycolysis (Fig. 9G).

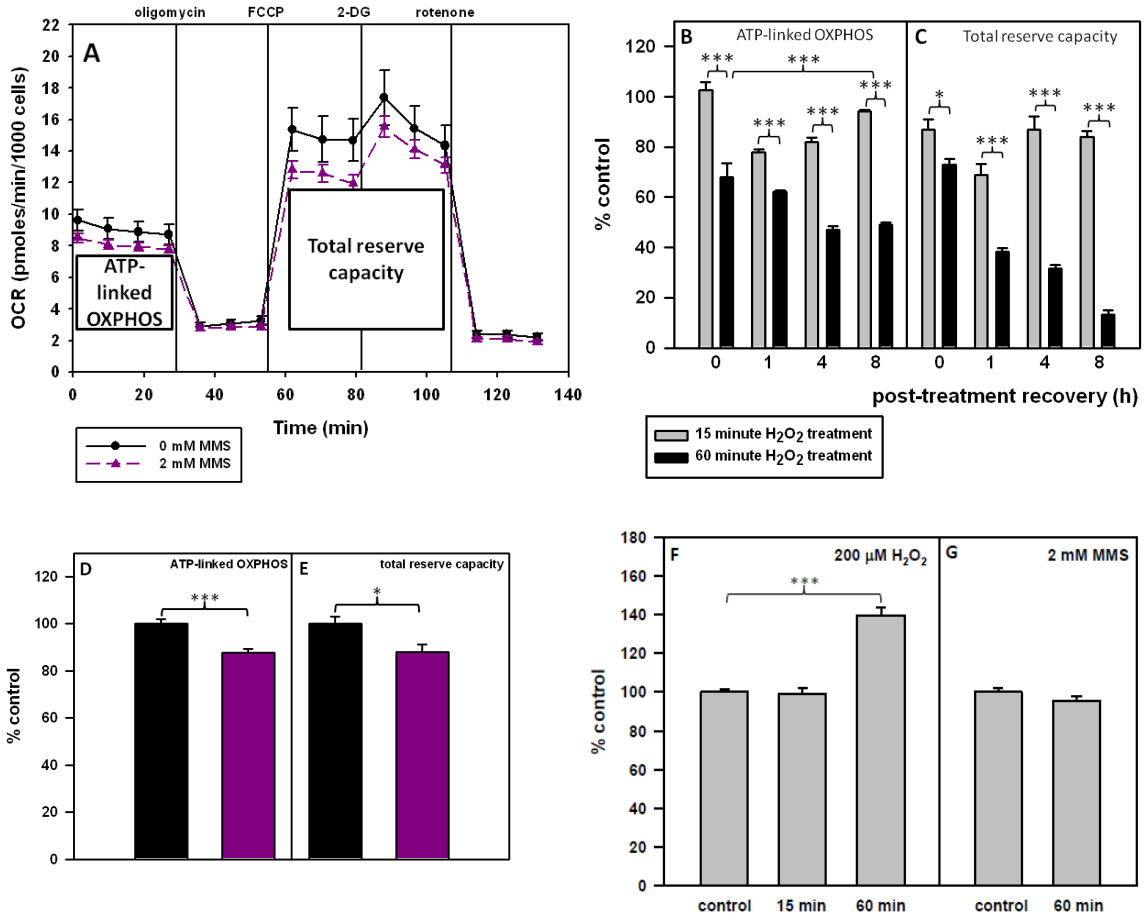

Figure 9. A 60-minute H_2O_2 treatment and not a 60-minute MMS treatment causes major mitochondrial dysfunction

Cells were plated and the following day were treated for 15 or 60 minutes with 200 µM H_2O_2 (Scheme 2, #1 and 2) or for 60 minutes with 2 mM MMS (Scheme 2, #3). ATP-linked OXPHOS is represented by $\overline{X}_{1\text{-}4}$ - $\overline{X}_{5\text{-}7}$ and total reserve capacity is represented by $\overline{X}_{8\text{-}13}$ - $\overline{X}_{5\text{-}7}$. (A) Pharmacologic profile of mitochondrial OXPHOS 8 hours after treatment with 2 mM MMS. Error bars represent the SEM of 2 Seahorse experiments with 6 replicates per run. (B) ATP-linked OXPHOS and (C) total reserve capacity of H_2O_2-treated cells at 0, 1, 4, and 8 hours as compared to control-treated cells. (D) ATP-linked OXPHOS and (E) total reserve capacity of MMS-treated cells at 8 hours compared to control-treated cells. Basal glycolysis at 8 hours after (F) H_2O_2 or (G) MMS treatment compared to control-treated cells.

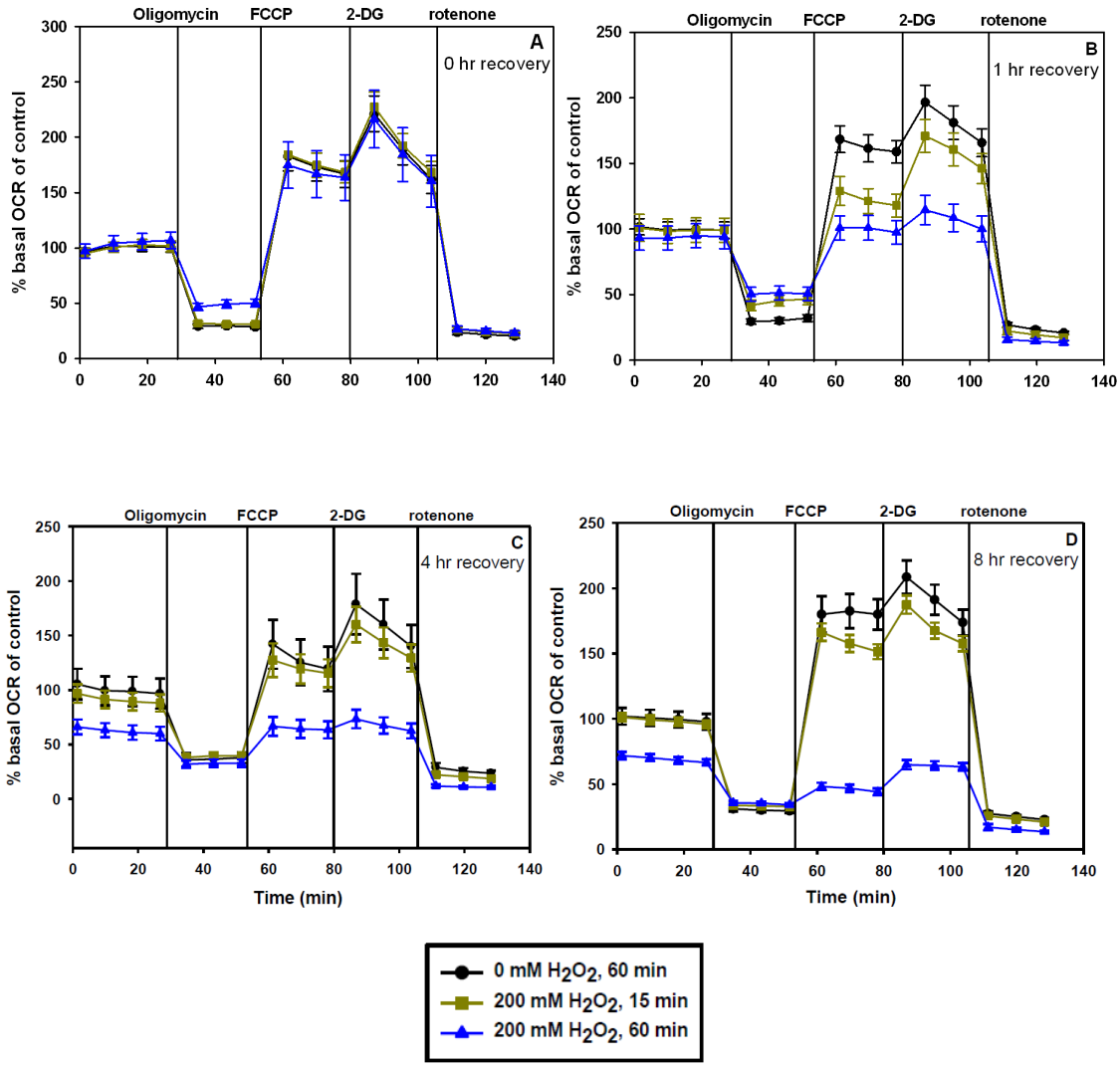

Figure 10. Time course of mitochondrial function after H_2O_2 treatment

Cells were plated and the following day were treated for 15 or 60 minutes with 200 μM H_2O_2 (Scheme 2, #1 and 2). Error bars represent the SEM of 2-3 Seahorse experiments with 6 replicates per run. (A) Pharmacologic profile of mitochondrial function immediately following H_2O_2 treatment, or after various recovery times ((B): 1 hr, (C): 4 hr, and (D): 8 hr). ATP-linked OXPHOS is represented by $\overline{X}_{1\text{-}4}$ - $\overline{X}_{5\text{-}7}$ and total reserve capacity is represented by $\overline{X}_{8\text{-}13}$ - $\overline{X}_{5\text{-}7}$. (E) ATP-linked OXPHOS and (F) total reserve capacity of H_2O_2-treated cells as compared to control-treated cells.

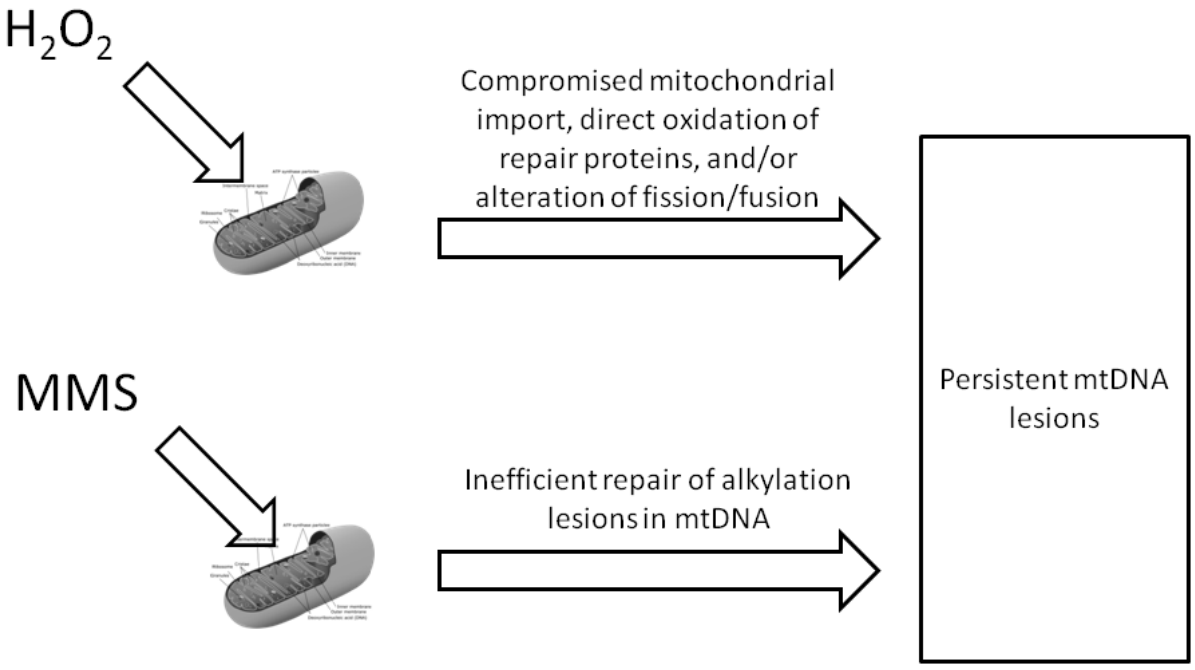

Figure 11. Model of mtDNA damage persistence in H_2O_2- versus MMS-treated cells

Mitochondrial DNA damage is predicted to persist in H_2O_2-treated cells due to oxidant-induced inhibition of mitochondrial protein import, direct oxidation of repair proteins, and/or perturbations in mitochondrial dynamics. MMS-induced mtDNA lesions are predicted to persist due to an insufficient alkylation repair pathway in mitochondria. As of yet, no proteins that recognize and repair alkylating lesions have been identified in mammalian mitochondria.

3.3 DISCUSSION

The purpose of this study was to better understand the relationship between persistent mtDNA damage and mitochondrial dysfunction. In this study we found that: (1) mtDNA damage persisted in cells treated with H_2O_2 or MMS for 60 minutes, but not in cells treated with H_2O_2 for 15 minutes; and that H_2O_2 damage persistence was not dependent upon the initial lesion frequency; (2) both the 15 minute and 60 minute H_2O_2 treatments caused a significant loss of mtDNA, but the 60 minute treatment with MMS did not result in mtDNA loss; (3) cells treated for 60 minutes with MMS had significantly decreased levels of the mitochondrially-encoded protein ND4 (35% loss) at 8 hours, while the 60-minute H_2O_2-treated cells showed a decrease in the nuclear-encoded complex V subunit α (58% loss) at 8 hours; (4) a 60 minute H_2O_2 treatment caused a 51% loss of ATP-linked OXPHOS and a plunge in mitochondrial function to 13% of the control total reserve capacity by 8 hours following treatment, unlike MMS-treated cells, which only resulted in a 12% loss of mitochondrial function at 8 hours. Collectively, these data suggest that persistent mtDNA damage is not sufficient to cause rapid mtDNA loss and mitochondrial dysfunction.

QPCR analysis indicated persistent mtDNA lesions at 8 hours following a 60 minute treatment with H_2O_2 or MMS. The persistence of the lesions is not dependent on initial lesion frequency but is dependent on treatment time; cells treated for 15 minutes with H_2O_2 did not have persistent mtDNA lesions at 8 hours. Although both DNA damaging agents H_2O_2 and MMS were able to induce persistent mtDNA damage, we suggest that persistent mtDNA damage may occur through two different mechanisms (Fig. 11). These differences may be due to one or more factors, including: (1) oxidation of mitochondrial proteins during H_2O_2 treatment that leads to a vicious cycle of ROS production and generation of mtDNA damage(32,66); (2) impaired

mitochondrial import of DNA repair proteins in H_2O_2- but not MMS-treated cells; (3) direct or indirect ROS-mediated inhibition of mtDNA repair during a crucial window of time for the initiation of repair; (4) high levels of oxidative DNA damage that does not stop the DNA polymerase and is therefore not detected by our assay (8-oxoG, for example); (5) insufficient alkylation repair pathway and/or (6) oxidant-induced alterations in mitochondrial dynamics of fission and fusion.

Oxidant treatments for 15- and 60-minutes led to a loss of mtDNA at 8 hours, but a 60-minute MMS treatment did not cause rapid mtDNA loss. Initial mtDNA lesion frequencies for the H_2O_2 and MMS treatments were similar, and these data indicate that mtDNA loss is not dependent on DNA lesion frequency. Likewise, mtDNA loss is not predictive for the persistence of mtDNA damage. Our data supports earlier work, which used different methods to suggest that oxidatively damaged mtDNA is degraded (65,213); in addition, it reproduces in mammalian cells the results of a study in yeast in which MMS treatment showed no loss of mtDNA (119).

Cells treated for 60 minutes with 200 μM H_2O_2 showed a 10% loss in the mitochondrially-encoded ND4 but a 58% decrease in the nuclear-encoded complex V subunit α. Conversely, cells treated with MMS for 60 minutes had a 35% loss in ND4 but no significant decrease in complex V α (Fig. 7). The decrease in complex V α in H_2O_2-treated cells could be due to (1) oxidant-impaired import of nuclear-encoded mitochondrial proteins (214,215) or (2) selective oxidative damage to the complex V subunit α gene (ATP5A1α) promoter, as suggested in a 2004 study (216).

A 60 minute H_2O_2 treatment led to a rapid and continual decrease in mitochondrial function. ATP-linked OXPHOS showed a 32% loss immediately following treatment, which

increased to a 51% loss of ATP-linked OXPHOS at 8 hours recovery. Startlingly, the initial 27% drop in total reserve capacity was exacerbated to 87% by 8 hours following H_2O_2 treatment. In contrast, MMS-treated cells only showed a 12% loss of mitochondrial function by 8 hours. Although the H_2O_2 treatment and the MMS treatment both had persistent mtDNA damage at 8 hours post-treatment, this was not sufficient to drive mitochondrial dysfunction. The difference in mitochondrial function between the 60 minute H_2O_2 treatment and the 60 minute MMS treatment may instead be due to other factors, including: (1) oxidant-impaired import of nuclear-encoded proteins, which is suggested by the 58% loss of complex V α subunit in the H_2O_2-treated cells, (2) selective oxidant damage to the promoter region of ATP5A1α, which can be tested by PCR amplifying this region of the nuclear genome, and/or (3) the excessive H_2O_2-induced loss of mtDNA (>50%), which is supported by the complete lack of OXPHOS seen in cells deficient in mtDNA (ρ^0 cells).

In this study we address two important questions: (1) Do persistent mtDNA lesions lead to rapid mtDNA loss and/or mitochondrial dysfunction? (2) What are the effects of MMS on mtDNA lesion levels, mtDNA loss and mitochondrial function? The results of this study demonstrate that persistent mtDNA damage is not sufficient to cause rapid mtDNA loss or mitochondrial dysfunction. In addition, we showed that MMS generates more nDNA lesions than mtDNA lesions. Importantly, the mtDNA lesion frequencies that a range of 1-3 mM MMS generates are similar to H_2O_2-induced lesion frequencies in our study. However, unlike H_2O_2, MMS causes no DNA loss and a modest (12%) decrease in mitochondrial function. The question of slow repair kinetics of MMS-induced mtDNA damage remains unresolved. Surprisingly little is known about the enzymology of alkylation repair in the mitochondria. Future studies are needed to address the mechanism and kinetics of alkylation repair in mtDNA.

This study suggests that mitochondrial dysfunction is not caused by initial mtDNA lesion frequency or by persistent mtDNA damage and may instead be influenced by mtDNA copy number. With the observation that a 15-minute 200 μM H_2O_2 treatment led to a 30% loss of mtDNA but a restoration of mitochondrial function by 8 hours, it would be predicted that a >50% loss of mtDNA would lead to the further decline of mitochondrial function as seen in cells treated with 200 μM H_2O_2 for 60 minutes. Similarly, MMS-treated cells show no loss of mtDNA and perhaps consequently, no loss of mitochondrial function. Future studies will address the cause of H_2O_2-induced mtDNA loss and the possible role of mitophagy and/or mitochondrial fission in this process.

4.0 MDIVI-1 PROTECTS CELLS AGAINST OXIDANT-INDUCED MTDNA DAMAGE INDEPENDENT OF DRP1

4.1 INTRODUCTION

Mitochondria are the major endogenous source and the main cellular target of reactive oxygen species (ROS)(217). Hydrogen peroxide (H_2O_2) has been extensively used as an agent to induce oxidative stress in cells. H_2O_2 is freely diffusible, unlike superoxide, which is the principal ROS produced during mitochondrial oxidative phosphorylation (OXPHOS) and cannot pass through membranes due to its negative charge (reviewed in (10)). H_2O_2 can cross the cell membrane and if it is not metabolized to H_2O in the cytosol, it can cross nuclear and mitochondrial membranes because it is uncharged. Thus, the effect of ROS on nuclear DNA (nDNA) and mitochondrial DNA (mtDNA) can be addressed. MtDNA is suggested to be more vulnerable to oxidative damage because of its proximity to superoxide production by OXPHOS complexes and a lack of protective histone structure. Past studies have shown that H_2O_2 causes more mtDNA damage than nDNA damage (32,66-68,218,219), persistent mtDNA damage (32,66,68,219) and mtDNA loss (65,219,220). In addition to H_2O_2, other oxidants such as menadione, an agent that generates superoxide in the cell, has been shown to induce persistent mtDNA damage (221) and mtDNA loss (213).

The observation that oxidants cause mtDNA loss led us to address the mechanism for this loss. We hypothesized that mitophagy was responsible for the oxidant-induced loss of mtDNA. In order to test this hypothesis, we treated SV40 large T antigen-immortalized mouse embryonic fibroblasts (92TAg MEFs) and human breast cancer cells (MCF7 cells) with H_2O_2 in the presence or absence of the pharmacologic fission inhibitor mitochondrial division inhibitor-1 (mdivi-1).

Mitochondrial fission results in the fragmentation of mitochondria and it exists in a balance with mitochondrial fusion, a process which generates a highly-interconnected mitochondrial network. Mitochondrial fission is mediated by the dynamin-related GTPase dynamin-related protein 1 (Drp1) and mitochondrial fission factor (Mff)(157,158,222). When the expression of Drp1 or Mff is decreased, mitochondria become hyperfused (157,158,223-225). Mitochondrial fission and fusion have been linked to mitophagy, the selective degradation of mitochondria (reviewed in(161)). Deleting Drp1 in mammalian cells or deleting Drp1's homolog mitochondrial division dynamin (Dnm1) in yeast resulted in the inhibition of mitophagy (175-177). Whereas fusion has been suggested to inhibit mitophagy (177), Drp1 and fission are proposed to promote mitophagy (175-177).

Mdivi-1 was established as a specific inhibitor of Drp1 based on the formation of a highly fused mitochondrial network during mdivi-1 treatment and on the mdivi-1-mediated inhibition of self-assembly and GTPase activity in Dnm1, the yeast homolog of Drp1 (224). Since the development of mdivi-1, it has been shown to inhibit mitochondrial cytochrome *c* release during apoptosis (224), improve cell survival after ischemia/reperfusion injury in the heart and retina in mouse studies (226,227) and rescue mitochondrial defects induced by a

mutant of the mitophagy protein PINK1 (228). These effects of mdivi-1 were purported to be due to the inhibition of Drp1 and thus the inhibition of fission (224,226-228).

The purpose of this study was to determine if mitophagy is the cause of oxidant-induced mtDNA loss. We predicted that the use of mdivi-1 would inhibit fission and thus, mitophagy. Therefore, we hypothesized that a treatment with H_2O_2 that normally results in a ~65% mtDNA loss at 8 hours in 92TAg MEFs would show no loss of mtDNA in the presence of mdivi-1. Our results indicate that pretreatment of cells with mdivi-1 is protective against H_2O_2-induced mtDNA damage. In fact, mdivi-1 reduces the amount of initial H_2O_2-induced mtDNA lesions several-fold. Mdivi-1 also rescues cells from the H_2O_2-induced loss of mitochondrial function. Mdivi-1 completely protected against the H_2O_2-induced loss of mtDNA at 8 hours, but this is likely due to the decrease in initial mtDNA lesions and not due to manipulation of fission/mitophagy levels. Mdivi-1 was not able to protect mtDNA or nDNA against lesions induced by the alkylating agent methyl methanesulfonate (MMS), however, which suggests a role for mdivi-1 in the oxidant-specific protection of mtDNA. To ascertain that the mdivi-1-mediated protection against H_2O_2-induced mtDNA was through Drp1 inhibition, Drp1 was knocked down ~88%; however, there was no change in the level of protection by mdivi-1 in the Drp1 knockdown, suggesting that mdivi-1 may be acting independently of Drp1 to protect mitochondria against oxidants.

4.2 RESULTS

The goal of this study was to determine if the oxidative stress-induced loss of mtDNA is due to mitochondrial fission and subsequent mitophagy. To accomplish this goal, we utilized a

pharmacologic inhibitor of fission, mdivi-1. Several endpoints were measured following treatment, including mtDNA damage and mtDNA copy number with QPCR, and mitochondrial function with the Seahorse Extracellular Flux Analyzer.

Mdivi-1 protects 92TAg MEFs and MCF7 human cells from H_2O_2-induced mtDNA damage and from mtDNA loss when present before and during H_2O_2 treatment. 92TAg MEFs or MCF7 human breast cancer cells were incubated for 60 minutes in serum-free media containing 50 or 25 μM mdivi-1, respectively. The media was removed and replaced with serum-free media containing 200 μM H_2O_2 and 25 or 50 μM mdivi-1. For the 92TAg MEF treatment, 50 μM mdivi-1 was also added into the conditioned growth media during the 8 hour recovery. A 1-hour pretreatment and co-treatment with 50 μM mdivi-1 reduced the initial mtDNA lesions in H_2O_2-treated 92TAg MEFs by 83%, from 3.7 lesions/10kb to 0.6 lesions/10kb (Fig. 12A). Similarly, a 1-hour pretreatment and co-treatment with 25 μM mdivi-1 reduced the initial lesions in H_2O_2-treated MCF7 cells by 92%, from 0.94 lesions/10kb to 0.07 lesions/10kb (Fig. 12B). By 8 hours after treatment in 92TAg MEFs, the remaining H_2O_2-induced lesions in mdivi-1-treated cells were almost completely repaired (Fig. 12A). This was similar to H_2O_2-treated MEFs, which showed almost complete repair of their mtDNA lesions at 8 hours (Fig. 12B). Mdivi-1 treatment alone did not cause any mtDNA lesions (Fig. 12A) or mtDNA loss (Fig. 12C). Mdivi-1 completely protected 92TAg cells (Fig. 12C) and MCF7 cells (Fig. 12D) against the H_2O_2-induced 62% and 16% loss of mtDNA at 8 hours, respectively.

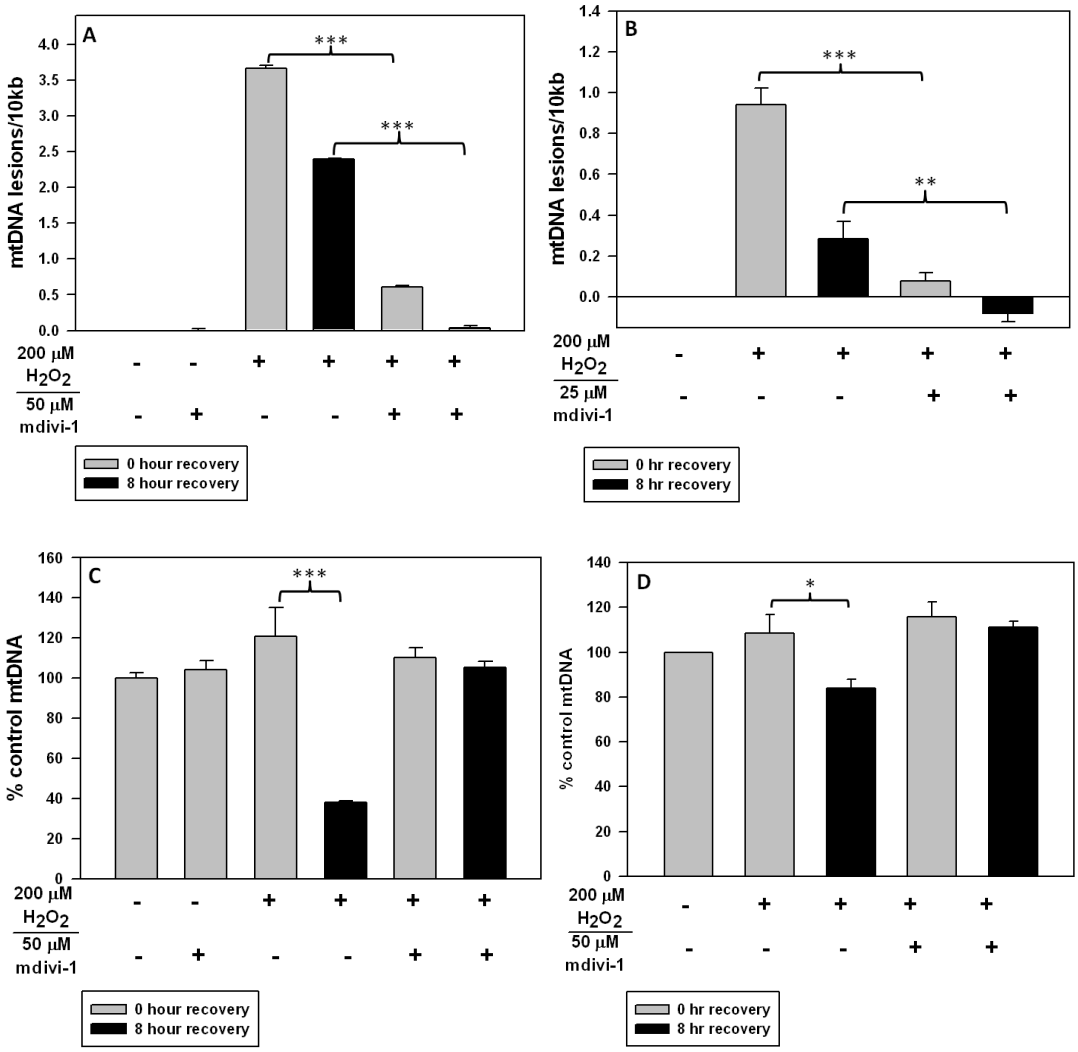

Figure 12. Mdivi-1 protects 92TAg MEFs and MCF7 human cells from H_2O_2-induced mtDNA damage and from mtDNA loss when present before and during H_2O_2 treatment

92TAg MEFs or MCF7 human breast cancer cells were treated with 50 or 25 μM mdivi-1, respectively, as in Scheme 2, #4. For the 92TAg MEF treatment, 50 μM mdivi-1 was added into the media during recovery. (A) MtDNA lesions and (C) mtDNA copy number in 92TAg MEFs at 0 and 8 hours following treatment with mdivi-1, mdivi-1/ H_2O_2, or H_2O_2. Error bars represent the SEM of n=2, with one experiment and 2 replicates per treatment type. (B) MtDNA lesions and (D) mtDNA copy number in MCF7 cells at 0 and 8 hours following treatment with mdivi-1/ H_2O_2 or H_2O_2.. Error bars represent the SEM of n=4, with 2 experiments and 2 replicates per treatment type.

Mdivi-1 does not enhance DNA repair when added after H_2O_2 treatment. Our previous results suggested that the presence of mdivi-1 in the recovery media was not needed for the near-complete mtDNA repair and for the attenuation of H_2O_2-induced mtDNA loss at 8 hours following H_2O_2 treatment. This led us to propose that adding mdivi-1 after treatment would not affect the level of H_2O_2-induced mtDNA lesions or mtDNA loss at 8 hours. 92TAg MEFs were incubated in 200 µM H_2O_2 in serum-free media for 60 minutes. The media was removed and replaced with conditioned growth media containing 50 µM mdivi-1 for the 8 hour recovery timepoint. When added after H_2O_2 treatment, mdivi-1 does not reduce the 2 mtDNA lesions/10kb remaining at 8 hours (Fig. 13A). It is also unable to prevent the ~70% loss of mtDNA at 8 hours (Fig. 13B). This is consistent with our hypothesis that mdivi-1 confers protection when added before and during H_2O_2 treatment.

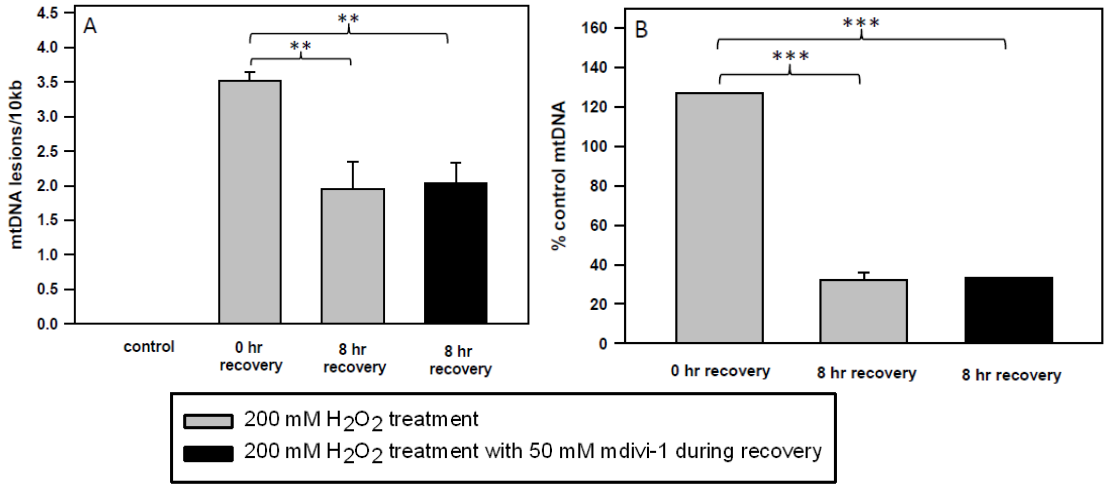

Figure 13. Mdivi-1 does not enhance DNA repair when added after H_2O_2 treatment

92TAg MEFs were treated with 200 µM H_2O_2 and 50 µM mdivi-1 for 60 minutes, as in Scheme 2, #5. (A) MtDNA lesions and (B) mtDNA copy number relative to control at 0 and 8 hr recovery. Error bars represent the SEM of n=4, with 2 experiments and 2 replicates per treatment type. One-sided ANOVA and a Tukey Test were used to analyze these data, $p < 0.05$ (*), < 0.01 (**), and < 0.001 (***).

Mdivi-1 protection against H_2O_2-induced mtDNA damage and loss is mdivi-1 dose-dependent. With the knowledge that 50 μM mdivi-1 was able to reduce by 6-fold the number of mtDNA lesions in 92TAg MEFs (Fig. 12A), we next wanted to determine if there were lower concentrations of mdivi-1 that could confer the same level of protection against H_2O_2-induced mtDNA damage and mtDNA loss. Using a lower concentration of mdivi-1 could also potentially reduce any off-target effects of higher concentrations. 92TAg MEFs were pre- and co-treated with either 10, 25, or 50 μM mdivi-1 and 200 μM H_2O_2 and were compared with H_2O_2 treatment and control treatment. We observed a dose-dependent increase in mtDNA lesions as the concentration of mdivi-1 was decreased, with 50, 25, and 10 μM mdivi-1 able to reduce the number of H_2O_2-induced lesions by 85%, 74%, and 35%, respectively (Fig. 14A). Likewise, the H_2O_2-induced mtDNA lesions remaining at 8 hours were reduced by 95%, 86%, and 31% in cells pre- and co-treated with 50, 25, and 10 μM mdivi-1, respectively (Fig. 14A).

We next wanted to determine the lowest concentration of mdivi-1 needed for the complete prevention of the H_2O_2-induced loss of ~70% mtDNA at 8 hours. Whereas 10 μM mdivi-1 was able to partially prevent the H_2O_2-induced loss (50% vs. 70% loss of mtDNA), it was 25 μM and 50 μM mdivi-1 that were able to completely prevent H_2O_2-induced loss (Fig. 14B).

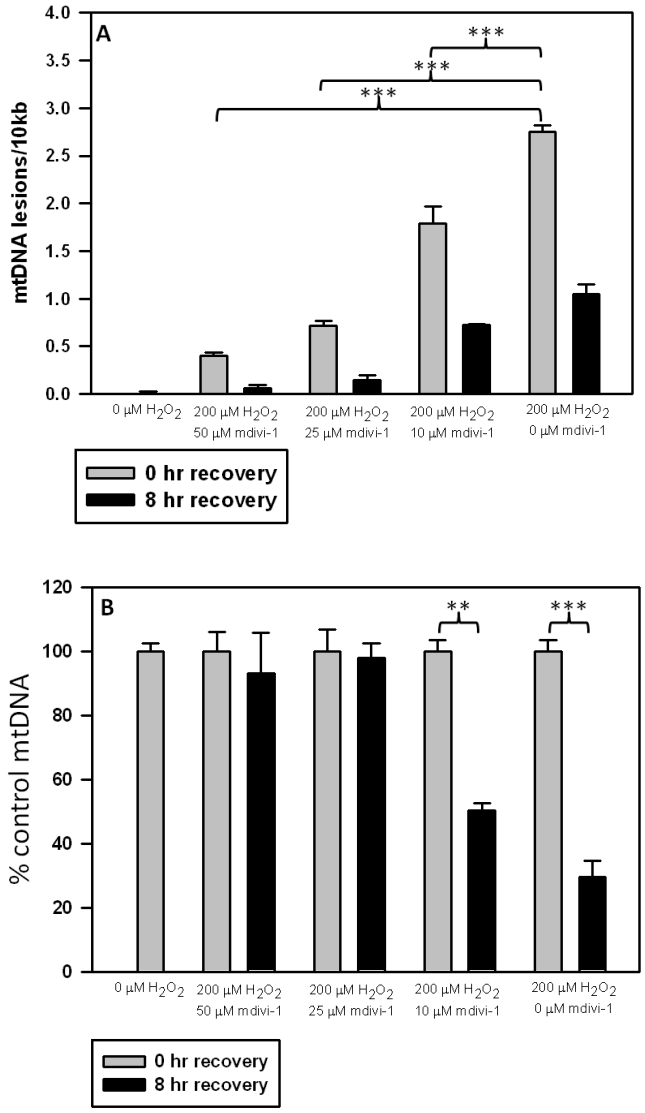

Figure 14. Mdivi-1 protection against H_2O_2-induced mtDNA damage and loss is mdivi-1 dose-dependent

92TAg MEFs were plated and the following day were treated with 10, 25, or 50 μM mdivi-1 and 200 μM H_2O_2 as in Scheme 2, #4. (A) MtDNA lesions at 0 and 8 hours after treatment with 10-50 μM mdivi-1 and/or 200 μM H_2O_2. (B) Change in mtDNA copy number at 0 and 8 hours following treatment with 10-50 μM mdivi-1 and/or 200 μM H_2O_2. Error bars represent the SEM of n=2, with one biological experiment and 2 replicates per treatment type. One-sided ANOVA and a Tukey Test were used to analyze these data, $p < 0.05$ (*), < 0.01 (**), and < 0.001 (***).

Mdivi-1 does not protect against MMS-induced lesions in either mtDNA or nDNA. The remarkable protection that mdivi-1 conferred against H_2O_2-treated cells led us to ask if the mdivi-1-mediated protection of mtDNA applied to other types of DNA damage. The observation that 25 μM mdivi-1 was just as protective against mtDNA loss as 50 μM mdivi-1 led us to use 25 μM mdivi-1 for this experiment. To affirm if the mtDNA protection of mdivi-1 was a general phenomenon, we used the alkylating agent methyl methanesulfonate (MMS). For this purpose, we performed a 1-hour pretreatment with 25 μM mdivi-1 followed by a co-treatment with 25 μM mdivi-1 and MMS at a concentration of 1, 2, or 3 mM and harvested cells at the 0 hour timepoint to determine the effect of mdivi-1 on MMS-induced lesions. Unlike with H_2O_2, mdivi-1 did not protect against MMS-induced mtDNA lesions for any of the MMS treatments (Fig. 15A). With the knowledge that mdivi-1 does not protect against initial MMS-induced mtDNA lesions, we next determined if mdivi-1 would protect against MMS lesions remaining at 8 hours. We performed a 1-hour pretreatment with 25 μM mdivi-1 followed by a co-treatment with 25 μM mdivi-1 and 2 mM MMS. Cells that were not harvested immediately following the treatment were put in conditioned growth media with no mdivi-1 and were allowed to recover for 8 hours. Not only did mdivi-1 not protect against mtDNA lesions at both 0 and 8 hours (Fig. 15B), but it did not confer protection against MMS-induced nDNA damage at these two timepoints (Fig. 15C). The effect of mdivi-1 on MMS-induced mtDNA loss could not be assessed because the 2 mM MMS treatment that was employed did not result in any mtDNA loss at 8 hours (Fig. 15D).

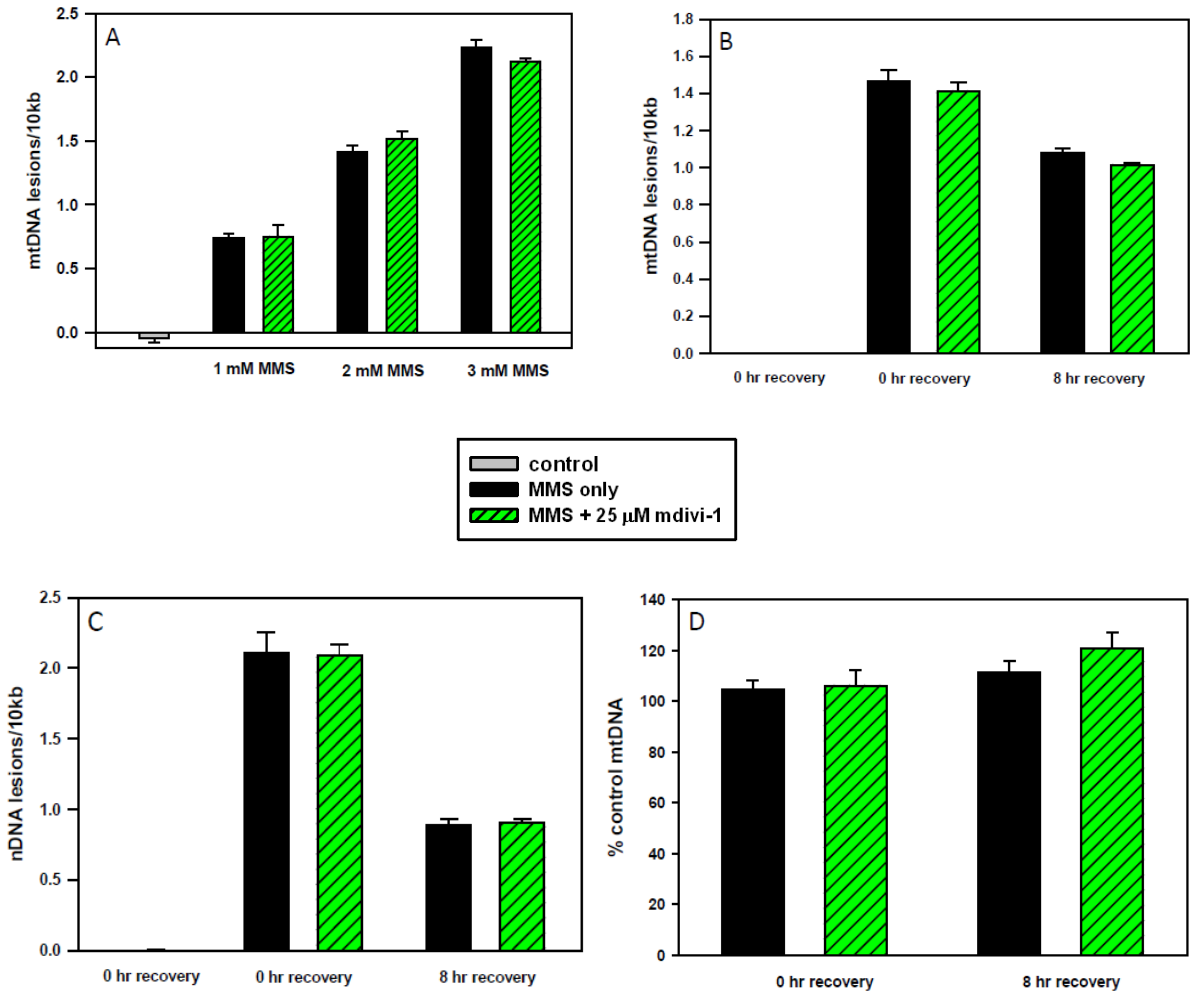

Figure 15. Mdivi-1 protection of DNA is not a general phenomenon – Mdivi-1 does not protect against MMS-induced lesions in either mtDNA or nDNA

92TAg MEFs were plated and the following day were pretreated with 25 µM mdivi-1 followed by a 1 hour co-treatment with 25 µM mdivi-1 and MMS at a concentration of 1, 2, or 3 mM (Scheme 2, #4). (A) MtDNA lesions at 0 hours after treatment with 1-3 mM MMS and/or 25 µM mdivi-1. (B) MtDNA lesions, (C) nDNA lesions, and (D) mtDNA copy number relative to control at 0 and 8 hours after treatment with 2 mM MMS and/or 25 µM mdivi-1. Error bars represent the SEM of n=4, with 2 biological experiments and 2 replicates per treatment type. One-sided ANOVA and a Tukey Test were used to analyze these data, $p < 0.05$ (*), < 0.01 (**), and < 0.001 (***).

Mdivi-1 does not increase the breakdown rate of H_2O_2. Our results indicated that mdivi-1 protects against H_2O_2-induced mtDNA damage but not against MMS-induced mtDNA damage. This observation led to the hypothesis that mdivi-1 treatment enhances the breakdown rate of H_2O_2. Similarly to the cellular antioxidant glutathione and the active site of peroxiredoxins, both which reduce H_2O_2 to water, mdivi-1 has an unblocked sulfhydryl group (224). The Amplex Red assay was performed to measure the breakdown rate of H_2O_2 in cells treated with either 200 µM H_2O_2 or concurrently with 200 µM H_2O_2 and 50 µM mdivi-1, and in cell-free media with the aforementioned treatments. Mdivi-1 did not increase the rate of H_2O_2 breakdown (Fig. 16). This indicates that mdivi-1 is not behaving as a general antioxidant and thus, the different effects of mdivi-1 on H_2O_2- and MMS-induced DNA damage are due to some other mechanism.

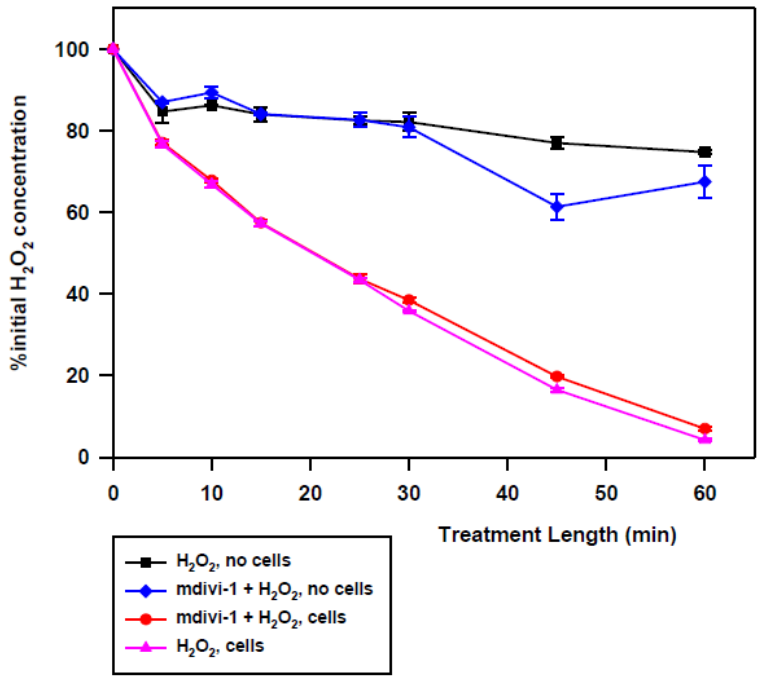

Figure 16. Mdivi-1 does not increase the breakdown rate of H_2O_2

92TAg MEFs were plated and the following day were treated concurrently with 200 µM H_2O_2 and 50 µM mdivi-1 for 1 hour. Percent of initial H_2O_2 concentration versus time in the presence or absence of mdivi-1 and in the presence or absence of cells.

Mdivi-1 still protects against H_2O_2 in Drp1 KD cells. It has been suggested that mdivi-1 is a specific inhibitor of Drp1 (224). Thus, if it is the inhibition of Drp1 that confers mdivi-1's protection against H_2O_2-induced mtDNA damage, it would be expected that knockdown of Drp1 would show a similar reduction of this mtDNA damage. Drp1 knockdown could not be accomplished in 92TAg MEFs. Mdivi-1 was shown to behave similarly in 92TAg MEFs and MCF7 cells in its protection against H_2O_2-induced mtDNA lesions (Fig. 12B). Thus, MCF7 cells were transfected with Drp1 siRNA. Three days after control or Drp1 siRNA transfection, cells were treated with 200 μM H_2O_2 or with a 25 μM mdivi-1 pre- and co-treatment with 200 μM H_2O_2. Immediately after the treatment, cells were harvested and the mtDNA lesions (Fig. 17B) and mtDNA copy number (Fig. 17C) were measured. Non-treated control siRNA and Drp1 siRNA-transfected cells were harvested on the same day as the treated samples to determine the level of Drp1 knockdown (Fig. 17A). Not only does Drp1 knockdown not behave like mdivi-1 in protecting against H_2O_2-induced mtDNA lesions, but mdivi-1 still confers protection to mtDNA even when Drp1 levels are reduced by ~88% (Fig. 17A). In addition, Drp1 knockdown cells show a 25% reduction in mtDNA copy number (Fig. 17C). This is inconsistent with mdivi-1 treatment, which does not show a difference in mtDNA copy number compared to control (Fig. 12C). These data suggest that mdivi-1's protection against H_2O_2-induced mtDNA damage is independent of its role in inhibiting Drp1.

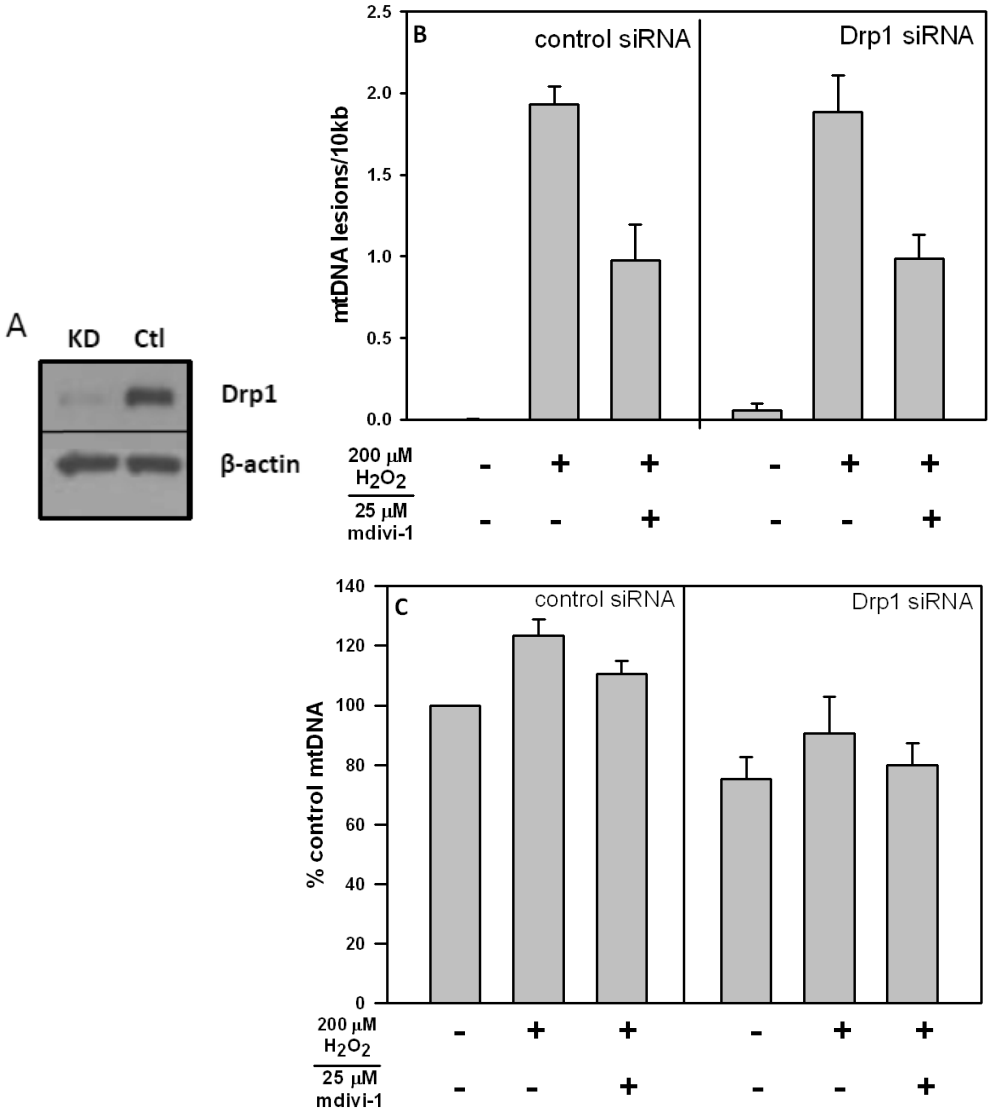

Figure 17. Mdivi-1 still protects against H_2O_2-induced mtDNA damage in Drp1 KD cells

MCF7 cells were transfected with Drp1 siRNA or control (scrambled) siRNA. On the third day after transfection, cells were treated as in Scheme 2, #4 with 200 μM H_2O_2 and 25 μM mdivi-1. Cells were harvested immediately following treatment and the (A) level of Drp1 knockdown, the (B) number of mtDNA lesions and (C) mtDNA copy number were measured. Error bars represent the SEM of n=4, with 2 biological experiments and 2 replicates per treatment type. One-sided ANOVA and a Tukey Test were used to analyze these data, $p < 0.05$ (*), < 0.01 (**), and < 0.001 (***).

Mdivi-1 protects against H_2O_2-induced mitochondrial dysfunction in 92TAg MEFs when present before/during H_2O_2 treatment but not when added after H_2O_2 treatment. With the observation that a 1-hour pretreatment and co-treatment with 50 μM mdivi-1 reduces H_2O_2-induced mtDNA lesions by 83%, we next sought to compare the mitochondrial function of the mdivi-1/H_2O_2 treatment to the H_2O_2 treatment at 8 hours following treatment.

In order to understand mitochondrial function, a combination of four pharmacological inhibitors was used consecutively during analysis with the Seahorse Extracellular Flux Bioanalyzer. The oxygen consumption rate (OCR) measurements before compound injections are referred to as the basal OCR. The first compound that is injected is oligomycin, which inhibits complex V in the electron transport chain and causes a decrease in respiration. The difference between the resulting OCR and the basal OCR is the ATP-linked OXPHOS (Fig. 18A). The second and third compounds, FCCP and 2-DG, uncouple the mitochondria and inhibit glycolysis, respectively, which drives mitochondrial respiration to its maximal capacity, referred to in this study as the total reserve capacity (Fig. 18A). Finally, rotenone inhibits oxidative phosphorylation at complex I and blocks all mitochondrial oxygen consumption.

92TAg MEFs were set up at 40,000 cells/well of a Seahorse plate and were treated the following day. On that day, cells were pretreated for 1 hour with either 50 μM mdivi-1 or serum-free media alone. The media was removed and serum-free media containing 50 μM mdivi-1 and 200 μM H_2O_2 was added back to the cells for 1 hour. After the treatment, conditioned growth media (without mdivi-1) was put back on the cells and placed in the incubator for 8 hours. The pharmacologic profile of the mitochondria at 8 hours is summarized in terms of ATP-linked OXPHOS and total reserve capacity in Fig. 18A. When cells were pretreated with mdivi-1 and co-treated with mdivi-1 during a 60 minute H_2O_2 treatment, the total

reserve capacity is two-fold higher than H_2O_2 alone and is comparable to the total reserve capacity of the control treated cells (Fig. 18A). This indicates that a pre- and co-treatment with mdivi-1 protects against H_2O_2-induced mitochondrial dysfunction.

Although MCF7 cells showed less initial H_2O_2-induced mtDNA lesions and a reduced loss of mtDNA compared to 92TAg MEFs (Fig. 12B and 12D), a 60-minute treatment with 200 μM H_2O_2 resulted in severe mitochondrial dysfunction (Fig. 18B). In this cell line, a pretreatment with 25 μM mdivi-1 and a co-treatment with 25μM mdivi-1 was not able to protect against H_2O_2-induced mitochondrial dysfunction (Fig. 18B).

Figure 18C shows the pharmacologic profile of mitochondria in which 92TAg MEFs were first treated with 200 μM H_2O_2 for 1 hour, with 50 μM mdivi-1 present in the conditioned media and in the Seahorse media for the 8 hour recovery. This treatment was already shown to confer no protection against mtDNA lesions and mtDNA loss at 8 hours. As was predicted, the mdivi-1 post-treatment is unable to protect against H_2O_2-induced mitochondrial dysfunction. Interestingly, the presence of mdivi-1 in the Seahorse media led to low basal OXPHOS, a 90% loss of ATP-linked OXPHOS compared to control, and a ~40% loss of total reserve capacity compared to control (Fig. 18D).

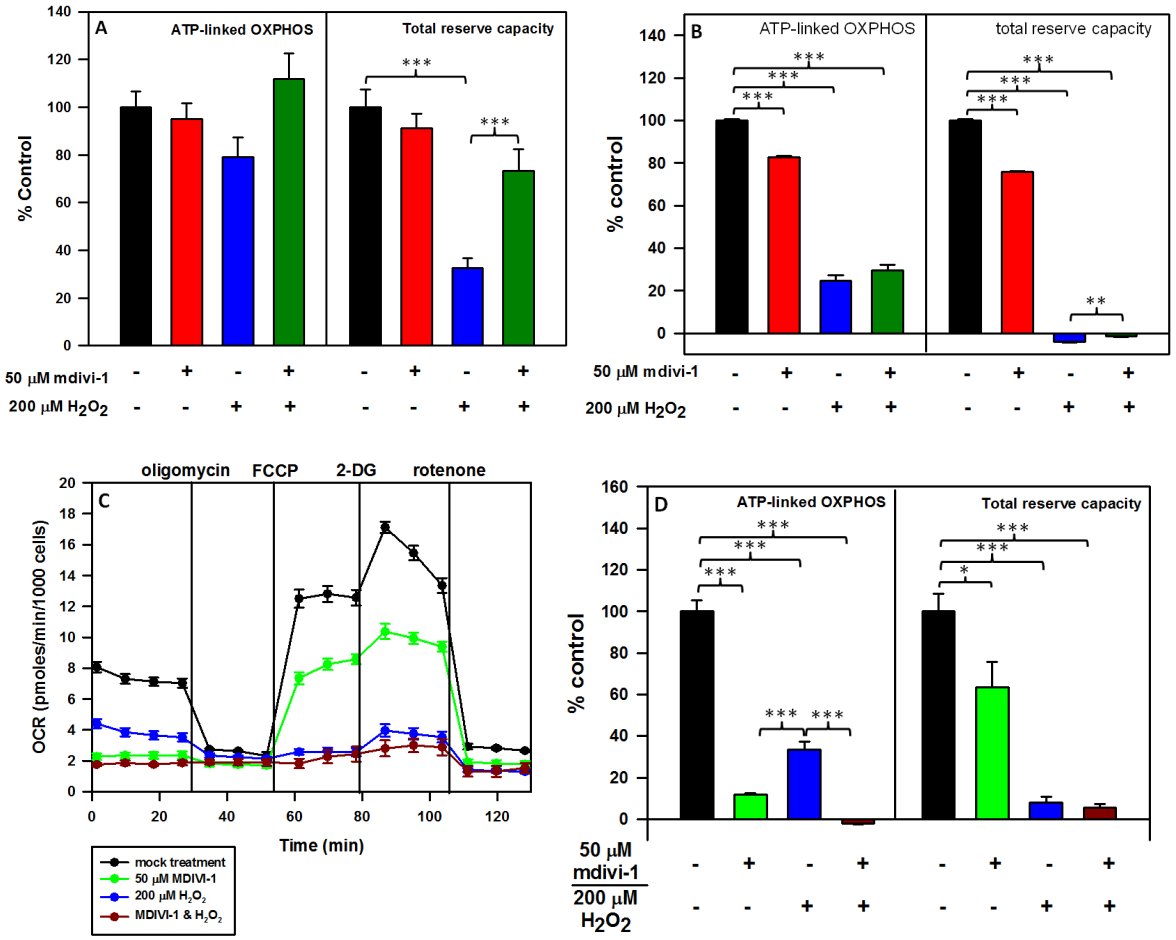

Figure 18. Mdivi-1 protects against H_2O_2-induced mitochondrial dysfunction in 92TAg MEFs when present before and during H_2O_2 treatment but not when added after H_2O_2 treatment

Cells in A-C were treated as in Scheme 2, #4, with 50 μM mdivi-1 and 25 μM mdivi-1, respectively, for 92TAg MEFs and MCF7 cells. Histogram of mitochondrial function in (B) 92TAg MEFs and (C) MCF7 cells. ATP-linked OXPHOS is represented by $\overline{X}_{1\text{-}4}$ - $\overline{X}_{5\text{-}7}$ and total reserve capacity is represented by $\overline{X}_{8\text{-}13}$ - $\overline{X}_{5\text{-}7}$. Error bars represent the SEM of n=8-10, with 2 experiments and 4-5 replicates per treatment type. (D) Pharmacologic profile of 92TAg MEFs treated as in Scheme 2 #5 with 50 μM mdivi-1 and 200 μM H_2O_2 and (E) histogram of the pharmacologic profile in 18D.

4.3 DISCUSSION

The purpose of this study was to use a pharmacologic inhibitor of mitochondrial fission (mdivi-1) to determine the role of fission and mitophagy in oxidant-induced mtDNA loss. In this study we found that: (1) mdivi-1 conferred protection against H_2O_2-induced mtDNA damage and mtDNA loss in both 92TAg MEFs and MCF7 cells; (2) mdivi-1 was only able to protect against H_2O_2-induced mtDNA damage and mitochondrial dysfunction when cells were pretreated with mdivi-1 and co-treated with mdivi-1 and H_2O_2; (3) mdivi-1 pretreatment and co-treatment with H_2O_2 was able to protect against H_2O_2-induced mitochondrial dysfunction in 92TAg MEFs but not in MCF7 cells; (4) mdivi-1 did not confer protection against MMS-induced mtDNA or nDNA lesions; (5) mdivi-1 did not increase the breakdown rate of H_2O_2. Our attempt to understand the mechanism of mdivi-1 protection against oxidant-induced mtDNA damage, led to the findings that: (1) siRNA-mediated knockdown of Drp1 did not mimic the effects of mdivi-1 on H_2O_2-induced mtDNA damage; and (2) mdivi-1 still conferred protection against H_2O_2-induced mtDNA damage with ~88% Drp1 knockdown. Collectively, these data suggest that mdivi-1 protects against oxidant-induced mtDNA damage and mitochondrial dysfunction and that this protection is independent of Drp1 inhibition.

The present study confirmed earlier findings that oxidants cause mtDNA loss (Fig. 12A and 12B)(65,213,219,220). In an attempt to inhibit oxidant-induced mtDNA loss, the fission inhibitor mdivi-1 was employed. Mdivi-1 has been shown to promote cell survival and normal mitochondrial function and inhibit apoptosis in models of ischemia/reperfusion and Parkinson's disease (226-229). The four aforementioned studies purport that the inhibition of Drp1-mediated mitochondrial fragmentation by mdivi-1 is the mechanism for the observed effect(s). Most of these studies employed a dominant-negative Drp1 (DrpK38A) defective in GTP binding (157) to

successfully reproduce the effects of mdivi-1 (227-229). They did not, however, treat cells with mdivi-1 in the presence of Drp1 knockdown or Drp1K38A to confirm that the observed effects of mdivi-1 were through Drp1.

This is the first study on the effects of mdivi-1 on mtDNA damage and mitochondrial function. Once we had observed that mdivi-1 reduced initial oxidant-induced mtDNA lesions by 83% in 92TAg MEFs (Fig. 12A), the human MCF7 breast cancer cell line was also tested, and it showed a similar reduction (92%) of initial mtDNA lesions by mdivi-1 (Fig. 12B). The prevention of mtDNA loss by mdivi-1 at 8 hours (Fig. 12C and 12D) cannot be attributed to its inhibition of fission (and therefore, mitophagy), but is instead likely due to the substantial reduction of initial mtDNA lesions. This is consistent with a previous study in our group suggesting that both initial lesions and treatment length drive mtDNA loss (219).

The observation that mdivi-1 is only able to protect against H_2O_2-induced mtDNA damage (Fig. 12A and 12B) and mitochondrial dysfunction (Fig. 18A and 18B) when mdivi-1 is present before and during oxidative insult but not after oxidative insult (Fig. 13A and 18C) suggest that mdivi-1 is acting during this time window. Interestingly, the pre- and co-treatment with mdivi-1 was able to protect against H_2O_2-induced mitochondrial dysfunction in 92TAg MEFs (Fig. 18A and 18B) but not in MCF7 cells (Fig. 18C).

The protection of mdivi-1 against oxidant-induced mtDNA damage that was observed is proposed to be due to the mdivi-1-mediated (1) prevention of oxidative stress-induced mitochondrial fission that enhances mtDNA damage, (2) alteration of the redox environment of the mitochondria towards a more reducing environment before and/or during oxidant treatment, (3) priming of mtDNA repair, and/or (4) inhibition of oxidative phosphorylation.

Mdivi-1 was developed as a specific inhibitor of Drp1 and thus, we hypothesized that it may be protecting cells from oxidant-induced mitochondrial fission that exacerbates mtDNA damage. To address this question, we knocked down Drp ~88% and treated these cells with mdivi-1 and H_2O_2 and found that mdivi-1 still protected against mtDNA lesions with the exact same ability as with control siRNA cells (Fig. 17A). In addition, we observed that Drp1 KD did not reproduce the protective effects of mdivi-1 treatment on mtDNA (Fig. 17A). This suggested that the mdivi-1 mediated protection of mtDNA against oxidant-induced damage may be independent of its role in inhibiting Drp1.

A possible role for mdivi-1 in redox balance is supported by the lack of mdivi-1 protection against alkylation-induced mtDNA or nDNA damage (Fig. 15A-C). It is apparent from our Amplex Red data, however, that mdivi-1 is not directly metabolizing H_2O_2 (Fig. 16). Mdivi-1 has an unblocked sulfhydryl group (224), and thus it may be acting as a reducing agent to return the oxidized sulfhydryl residue in the active site of peroxiredoxins back to its reduced state. Therefore, when H_2O_2 is added, a larger percentage of peroxiredoxins are in the reduced form and are thus more readily available to metabolize H_2O_2 to water.

Mdivi-1 may be damaging mtDNA and thus may preemptively draw DNA repair proteins to the mitochondria. This possibility will be discussed further in the conclusions and future directions chapter.

The data in Fig. 18D and Fig. 18E in which the presence of mdivi-1 during the Seahorse run led to a basal OXPHOS level significantly below levels in control-treated cells suggests that mdivi-1 may be inhibiting oxidative phosphorylation. If mdivi-1 inhibits oxidative phosphorylation, it may therefore inhibit a ROS-induced vicious cycle in which active OXPHOS leads to the exacerbation of ROS and ROS damage in mitochondria.

Though mdivi-1 is presumed to act solely through inhibition of the fission protein Drp1, our data suggest that the protection against oxidative damage to mitochondria may occur independently of Drp1 inhibition. Past studies have not utilized concurrent Drp1 knockdown and mdivi-1 treatment to ensure that the observed effects on cell survival and apoptosis inhibition are derived from the same pathway (224,226-228). Thus, it is possible that the protection mdivi-1 confers on cells after ischemia-reperfusion injury is due to a mechanism other than inhibition of mitochondrial fission. Future studies are needed to identify the mechanism of mdivi-1-mediated protection of mtDNA against oxidant-induced damage.

5.0 ROLE OF MITOCHONDRIAL DNA LIGASE IN CELL SURVIVAL AND MITOCHONDRIAL DNA REPAIR

5.1 INTRODUCTION

DNA Ligase III (Lig3) is the sole mitochondrial DNA ligase in mammalian mitochondria, generated from an alternative translation start site in the nuclear-encoded Lig3 gene. The mitochondrial form of Lig3 has a mitochondrial leader sequence that enables it to enter the mitochondria (94). Lig3 knockouts have been attempted, but they are embryonic lethal and their cells are not able to be cultured (230,231); thus, Lig3 is essential for cell viability. This study helps to answer the question as to whether it is the nuclear and/or mitochondrial form of Lig3 that is required for cell viability, and if mitochondrially targeted DNA ligase constructs can maintain mitochondrial DNA (mtDNA) integrity and mtDNA copy number.

5.2 RESULTS

To enable complete knockdown of Lig3, a pre-emptive complementation strategy in mouse embryonic stem cells was developed and employed by the laboratory of Dr. Maria Jasin (Memorial Sloan-Kettering Cancer Center) in this study (232)(see Appendix A). First, one allele of Lig3 was deleted and then cells were transfected with transgenes expressing various ligases

(Appendix 1, Fig. 1A). These included the following: (1) wild-type Lig3, (2) mitochondrial- or (3) nuclear-targeted Lig3, (4) Ligase I (Lig1) targeted to the mitochondria, (5) a mitochondrially-targeted minimal ligase from the chlorella virus, or Lig3 either missing (6) the domain that interacts with Parp1 and mitochondrial DNA (ΔZNF)(233,234) or (7) its Xrcc1-interaction domain (ΔBRCT)(235)(Appendix A, Figs 1A & 2A). The Cre-Lox system was then employed to knock out the second allele of Lig3, producing $Lig3^{KO/KO}$ (Appendix A, Fig. 1A). It was determined by the Dr. Jasin's laboratory that the BRCT and ZNF domains of Lig3 are not essential for cell viability (Appendix A, Fig. 1B). It was also shown by them that mitochondrially-targeted transgenes for Lig1, Lig3, and chlorella virus ligase could complement Lig3 in retaining cell viability (Appendix A, Fig. 1B & 2B). Complementation with nuclear-targeted Lig1 or Lig3, however, did not allow for the retention of viable cells (Appendix A, Fig. 1B). These data indicated that it is the mitochondrial function(s) of Lig3 that are essential for cell viability. The question that I addressed in my thesis work using a gene-specific QPCR assay for DNA damage, was whether these various ligase constructs could repair oxidative mtDNA damage and maintain mtDNA copy number similar to $Lig3^{KO/KO}$ pre-emptively complemented with a WTLig3-GFP transgene.

Mouse embryonic stem cells were treated with 175 μM H_2O_2 for 15 minutes and allowed to recover for 0 or 1.5 hours. They were then harvested and the DNA was subjected to QPCR analysis, with endpoints of mtDNA damage and mtDNA copy number. We found that the Lig3ΔBRCT, Lig3ΔZNF, and mitochondrially-targeted Lig1 and *Chlorella* virus ligase (ChVLig) could repair mtDNA damage at a similar rate to cells complemented with a wild type Lig3-GFP transgene (Lig3-/-, WTLig3-GFP)(Fig. 19A). The aforementioned ligases also

maintained mtDNA copy number at a level similar to Lig3$^{KO/KO}$ cells complemented with Lig3-GFP (Fig. 19B).

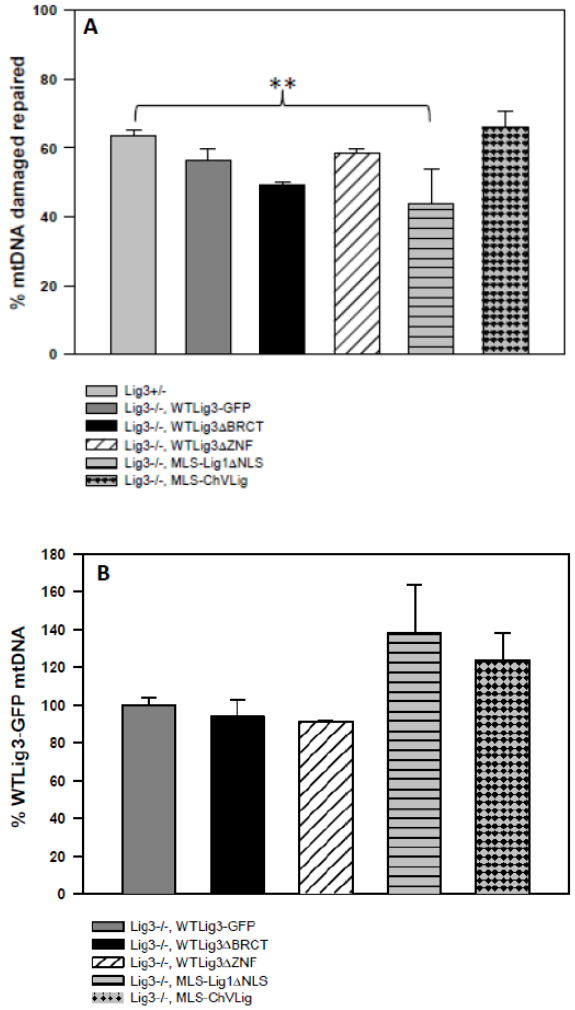

Figure 19. Cells expressing exogenous DNA ligases are competent to replicate and maintain mtDNA integrity

Cells were treated with 175 μM H_2O_2 for 15 minutes and allowed to recover for 0 or 1.5 hours. After the treatment, the cells were allowed to recover for 0 or 8 hrs. (A) Percent mtDNA damage repaired at 1.5 hours after treatment. (B) mtDNA copy number compared to control (WTLig3-GFP) immediately following control treatment. Error bars represent the SEM of n=2-6, with 1-3 biological experiments and 2 replicates per treatment type.

5.3 DISCUSSION

The goals of this study were to determine the following: (1) whether the nuclear and/or mitochondrial form of Lig3 was essential for cell viability; (2) what, if any, type of ligase activity could rescue cell survival in the absence of Lig3; and (3) the activities of various mitochondrial-targeted ligase transgenes compared to $Lig3^{KO/KO}$ complemented with WT Lig3-GFP, with endpoints of mtDNA repair and maintenance of copy number.

The results show that it is mitochondrial ligase activity that is essential for cell survival. Nuclear-targeted forms of Lig3 were not able to rescue cell viability in $Lig3^{KO/KO}$ cells, but the mitochondrially-targeted ligases they transfected were all able to produce viable clones. Even the smallest known eukaryotic ligase (ChVLig), which consists solely of a catalytic domain (236), can rescue the survival of $Lig3^{KO/KO}$ cells; thus, the only domain of Lig3 essential to cell survival is the ligase catalytic core.

Several ligase transgenes could pre-emptively complement $Lig3^{KO/KO}$ cells to rescue cell survival, including WT Lig3-GFP and mitochondrially-targeted Lig3ΔBRCT, Lig3ΔZNF, Lig1, and ChVLig. These transgenic cells were then treated with H_2O_2 and were harvested at two timepoints after treatment. We compared the mtDNA repair rates and control-treated mtDNA copy number of each ligase transgene to $Lig3^{KO/KO}$ complemented with WT Lig3-GFP to determine the extent of mtDNA ligase activity of each ligase. Both the mtDNA repair ability and the mtDNA copy number were not significantly different than $Lig3^{KO/KO}$ cells complemented with WT Lig3-GFP, indicating that these ligases function at a similar capacity to Lig3.

In summary, these results show the necessity of Lig3 for mammalian cell survival is due to its mitochondrial ligase activity and not its role in the nucleus. However, ligases such as Lig1

and the *Chlorella* viral ligase can replace Lig3 and maintain similar mitochondrial ligase activities as Lig3. Thus, we propose that the necessity for mitochondrial ligase in mammalian cell survival allows for a simple ligase catalytic domain to fulfill the requirements for mitochondrial DNA ligase activity.

6.0 CONCLUSIONS AND FUTURE DIRECTIONS

In this thesis I addressed the relationship between persistent mtDNA damage, mtDNA loss, and mitochondrial dysfunction. Previous studies have indicated a role for mtDNA damage, mtDNA loss and mitochondrial dysfunction in many human pathologies (reviewed in (8,69)). However, the cause and kinetics of persistent mtDNA damage, mtDNA loss and mitochondrial dysfunction is unknown.

Chapter 3 tested the hypothesis that persistent mitochondrial DNA (mtDNA) damage leads to mitochondrial dysfunction through a loss in mtDNA copy number. Our results show that persistent mtDNA damage is not sufficient to drive rapid mtDNA loss, loss of a mitochondrially-encoded protein or mitochondrial dysfunction. Instead, the damage-induced loss of mtDNA, proteins, and mitochondrial function appears to be dependent on the type of DNA damage. Treatment of cells with oxidants such as H_2O_2 but not the alkylating agent MMS leads to mtDNA loss and mitochondrial dysfunction. Hydrogen peroxide treatment led to a decrease in a nuclear-encoded subunit of complex V (complex V subunit α) but not the mitochondrially-encoded protein ND4, whereas MMS treatment caused no decrease in complex V subunit α but did show a decrease in ND4. These results indicate that the type of mtDNA damage sustained by the mtDNA leads to distinct outcomes.

Mitochondria are the major producer and target of reactive oxygen species, and so they utilize several nuclear-encoded glycosylases to remove oxidatively-induced mtDNA lesions

(reviewed in (89)). As a result, oxidant-induced lesions are repaired in mtDNA, which may therefore limit the effects of oxidants on the expression levels of mitochondrially-encoded proteins. Conversely, how alkylation lesions are repaired in mtDNA is largely unknown. It has been suggested in past studies that mitochondria are able to repair simple alkylation damage to mtDNA (65,116-119), but the mechanism and the effects of mtDNA alkylation damage have not been addressed. In this thesis, I addressed the effects of persistent mtDNA alkylation damage. Our results reveal that MMS-induced mtDNA damage only causes a modest (12%) loss of mitochondrial function and no loss of mtDNA at 8 hours in immortalized MEFs. Our results are consistent with a study in yeast mitochondria, which determined that MMS generated more nDNA damage compared to mtDNA damage and no loss of mtDNA (119).

MMS and H_2O_2 cause persistent mtDNA damage, but because of the differences in effects on mtDNA copy number and mitochondrial function, we propose that the persistence in mtDNA damage in MMS- and H_2O_2-treated cells may occur through two different mechanisms. The differences between MMS- and H_2O_2-induced persistent mtDNA damage may be due to one or more factors, including: (1) oxidation of mitochondrial proteins during H_2O_2 treatment that leads to a vicious cycle of ROS production and generation of mtDNA damage (32,66); (2) impaired mitochondrial import of DNA repair proteins in H_2O_2- but not MMS-treated cells; (3) direct or indirect ROS-mediated inhibition of mtDNA repair during a crucial window of time for the initiation of repair; (4) insufficient alkylation repair pathway and/or (5) oxidant-induced alterations in mitochondrial dynamics of fission and fusion.

Cysteine and methionine are the amino acids most prone to oxidation (reviewed in (237)). Oxidation of the mitochondrial proteins aconitase and citrate synthase have been shown to lead to decreased activity of these proteins (13,58). Oxidation of proteins can be reversible or

irreversible (reviewed in (237)). Irreversibly oxidized mitochondrial proteins have been suggested to be degraded by the Lon protease in the mitochondrial matrix (238). The oxidation of the sulfur-containing amino acids methionine and cysteine is reversible, and in fact mitochondria have several enzymes that reverse the oxidation of these two residues, including methionine sulfoxide reductase (Msr) A and B, thioredoxins, sulfiredoxins, and glutaredoxins (reviewed in (237)). If protein oxidation is responsible for the persistence of H_2O_2-induced mtDNA damage, then overexpressing an oxidation reversal enzyme such as Msr A or B or the Lon protease should lead to less persistent mtDNA lesions at 8 hours.

Mitochondrial import of DNA repair proteins requires mitochondrial membrane potential ($\Delta\Psi$)(239,240). Mitochondria with persistent DNA damage show a loss of $\Delta\Psi$ (32). If impaired mitochondrial import causes H_2O_2-induced mtDNA lesions to persist, then dissipating $\Delta\Psi$ with an uncoupler such as FCCP during H_2O_2 treatment should exacerbate the number of persistent mtDNA lesions at all timepoints after treatment.

The persistence of mtDNA lesions induced by MMS is hypothesized to be due to an insufficient alkylation repair pathway in mitochondria. Past studies have shown that mitochondria are able to repair simple alkylation damage to mtDNA (65,116-119), but the enzymes required for removal of alkylation lesions in mtDNA have not been identified. The two major enzymes that recognize and remove alkylation damage in DNA are O^6-methylguanine methyltransferase (MGMT) and *N*-methylpurine glycosylase (MPG)(reviewed in (241)). Although these enzymes have yet to be found in mitochondria, it is likely that one or both of these enzymes may remove alkylation damage in mitochondria. If the persistence of MMS-induced mtDNA lesions is due to insufficient alkylation repair in mtDNA, then knocking down MPG or MGMT should result in the exacerbation of persistent MMS-induced mtDNA lesions.

Additionally, it is predicted that targeting MGMT to the mitochondria would lead to a lower level of persistent mtDNA lesions.

Mitochondrial fission and fusion are antagonistic and must be tightly regulated to maintain appropriate mitochondrial morphology and dynamics (reviewed in (161)). Oxidants have been proposed to induce mitochondrial fission (38). We propose that our H_2O_2 treatment may be inducing pathological levels of fission that lead to persistent mtDNA damage and loss of mtDNA. If fission is responsible for the persistence of H_2O_2-induced mtDNA damage, then either inhibiting fission proteins or overexpressing fusion proteins should lead to a decreased amount of persistent mtDNA lesions. We tested this hypothesis by decreasing fission pharmacologically with mdivi-1, which was alleged to be a specific inhibitor of the fission protein Drp1 (224). We found that mdivi-1 not only decreased the amount of persistent mtDNA lesions at 8 hours, but also a decreased amount of initial H_2O_2-induced mtDNA lesions. These results are described in chapter 4 of the thesis.

Our data showed that H_2O_2 but not MMS treatment causes a decrease in mtDNA copy number at 8 hours after treatment. We hypothesized that this loss of mtDNA was due to mitophagy, and we tested this hypothesis by using an inhibitor of fission, which is believed to precede mitophagy (177). We proposed that if H_2O_2-induced mtDNA loss was due to mitophagy, then inhibiting mitochondrial fission should lead to no decrease of mtDNA copy number. In addition to causing no decrease of mtDNA copy number in H_2O_2-treated cells, the pharmacologic inhibitor of fission mdivi-1 decreased initial H_2O_2-induced lesions by ~90%. This result is discussed further in chapter 4. A more direct way to test the hypothesis that mitophagy is responsible for H_2O_2-induced mtDNA would be to knock down a mitophagy protein such as Beclin 1 or LC3. If H_2O_2-induced mtDNA loss is due to mitophagy, then

knocking down a mitophagy protein should lead to no loss of mtDNA copy number after H_2O_2 treatment.

Complex V subunit α is decreased at 8 hours after H_2O_2 treatment but not after MMS treatment. This could be due to (1) selective oxidation of the complex V subunit α (F1α1) promoter or (2) impaired mitochondrial import of complex V subunit α. A 2004 study in human brain tissue found that F1α1 expression is decreased 2.3-fold in aged human cortexes (216). They attributed this decrease in F1α1 expression to selective oxidative damage to the F1α1 promoter (216). If the H_2O_2-induced loss of complex V subunit α protein is due to selective oxidation of its promoter, then measuring the protein levels of a nuclear-encoded mitochondrial protein whose gene is not known to be selectively targeted by oxidants would remove this variable. For example, complex V subunit β is encoded by the nucleus and is part of the same moiety as subunit α of complex V (242). Conversely, if the H_2O_2-induced loss of complex V subunit α protein is due to the compromised mitochondrial import of this protein, then dissipating the $\Delta\Psi$ with an uncoupler such as FCCP should exacerbate the decrease in complex V α.

Our results indicate a loss of ND4 at 8 hours after MMS treatment but not after H_2O_2 treatment. This may be due to the specific alkylation and degradation of the ND4 protein by MMS. The effects of MMS on specific mitochondrial electron transport chain subunits are largely unknown. If ND4 is selectively targeted for MMS-induced alkylation and degradation, then measuring the levels of another mitochondrially-encoded protein (ATPase 6, for example) may not show this same drop in protein level at 8 hours after MMS treatment.

Treatment of 92TAg MEFs with H_2O_2 but not with MMS induces severe mitochondrial dysfunction at 8 hours after treatment. This may be due to (1) the oxidation of proteins in the

electron transport chain (ETC) or (2) excessive mtDNA loss after H_2O_2 treatment. If the oxidation of ETC proteins is the cause of H_2O_2-induced mitochondrial dysfunction, then overexpressing protein oxidation reversal enzymes should limit mitochondrial dysfunction at 8 hours. However, if excessive H_2O_2-induced mtDNA loss in 92TAg MEFs is responsible for the mitochondrial dysfunction at 8 hours, then it would be predicted that decreasing TFAM, a mitochondrial transcription factor that regulates mtDNA copy number (243,244), would lead to mitochondrial dysfunction in these cells. The MCF7 cells showed only a modest (~16%) loss of mtDNA 8 hours after H_2O_2 treatment but showed significantly decreased OXPHOS. This seems contradictory to the hypothesis that mtDNA loss drives mitochondrial dysfunction, but perhaps MCF7 cells depend more on their mitochondria and/or have less mitochondria than 92TAg MEFs. Thus, a small decrease in mtDNA copy number may affect the mitochondrial function of MCF7 cells more than 92TAg MEFs.

Our MMS study has implications in cancer chemotherapy, because alkylating agents are often used in the treatment of cancer. Alkylating agents have been studied extensively in the context of nuclear DNA damage, and in fact, the effects of alkylating agents on nDNA are implicated in the cellular toxicity of these agents. Our results show that the alkylating agent MMS induces persistent lesions in both nDNA and mtDNA and appears to preferentially target nDNA. The lack of rapid mtDNA loss and mitochondrial dysfunction support the idea that it is the effects on nDNA damage that drive alkylating agent toxicity, but it cannot be ruled out that loss of mtDNA and mitochondrial function occur at a later timepoint.

Chapter 5 of this thesis addresses the role of Lig3 in cell survival. Lig3 expression had been shown to be essential for mammalian cell survival (230), but it was yet unknown what of the two form(s) of Lig3 are vital and what activity and domains of the Lig3 protein are required

for life. We hypothesized that general mitochondrial DNA ligase activity is crucial for cell survival. Our study established that it is the mitochondrial form of Lig3 and mitochondrial DNA ligase activity alone that are crucial for cell survival and mtDNA maintenance (232)(Appendix A). This was exemplified by our use of a mitochondrially-targeted minimal eukaryotic *Chlorella* virus DNA ligase, which consists of a catalytic core but which was able to sustain cell survival and maintain mtDNA integrity and copy number in the absence of Lig3 (232). This study established the importance of mtDNA maintenance in mammalian cell survival.

Cells without mtDNA (ρ^0) have been generated by either chronic treatment with ethidium bromide or by targeting the restriction enzyme EcoRI to mitochondria, where it then destroys all mtDNA (245,246). Importantly, ρ^0 cells can survive if they are supplied with pyruvate and uridine; they cannot perform oxidative phosphorylation but can produce ATP through glycolysis (245). NAD^+ is normally generated by OXPHOS and is required for glycolysis (247). Thus, in the absence of OXPHOS, the conversion of pyruvate to lactate enables the oxidation of NADH to NAD^+. Uridine is required in ρ^0 media because the synthesis of thymine, cytosine, and uracil require uridine, a precursor of which is synthesized in active mitochondria (245,246). Lig3 was found to be essential for embryonic development and cell viability (232)(Appendix A). However, the fact that cells can survive without mtDNA led us to ask if Lig3 knockout cells can survive in ρ^0 media. If Lig3 KO reproduces a ρ^0 phenotype, then supplying cells with pyruvate and uridine should restore the cell viability of Lig3 knockout cells.

The last hypothesis addressed in this thesis was that mdivi-1, a compound that inhibits mitochondrial fission, was expected to prevent H_2O_2-induced mitochondrial dysfunction at 8 hours after H_2O_2 treatment by preventing mtDNA loss in H_2O_2-treated cells. Mdivi-1 was employed as a method to inhibit mitophagy, based on studies suggesting that mitochondrial

fission promotes mitophagy (175-177). Mdivi-1 was found to protect against initial H_2O_2-induced mtDNA lesions in both 92TAg MEFs and MCF7 cells. It was not, however, able to protect against MMS-induced mtDNA or nDNA lesions. Mdivi-1 also reduced the number of persistent mtDNA lesions and it inhibited mtDNA loss 8 hours after H_2O_2 treatment in the two aforementioned cell types, but this inhibition of mtDNA loss was most likely due to the reduction in initial mtDNA lesions and not prevention of mitophagy. When the fission protein Drp1, the target of mdivi-1, was knocked down ~88% in MCF7 cells, Drp1 knockdown did not reproduce the effects of mdivi-1. In addition, mdivi-1 was still able to protect against H_2O_2-induced mtDNA lesions in the Drp1 knockdown cells. This suggested that mdivi-1's protection against H_2O_2-induced mtDNA damage may be independent of Drp1. It is possible that the mdivi-1-mediated inhibition of Drp1 must be within an optimal range (for example, resulting in a 50% loss of Drp1 activity). Therefore, excessive loss of Drp1 (~88%) would not confer mitochondrial protection against oxidants. Interestingly, mdivi-1 was only able to rescue H_2O_2-induced mtDNA dysfunction in 92TAg MEFs.

Based on the data in Drp1 KD cells, mdivi-1 may be protecting against H_2O_2-induced mtDNA damage through a role independent of its role in Drp1 inhibition. If mdivi-1 is protecting against H_2O_2-induced mtDNA damage independent of Drp1, then the next question to address would be how mdivi-1 is protecting mtDNA. Possible mechanisms of mdivi-1-mediated protection against H_2O_2 include the (1) preemptive reduction of oxidized peroxiredoxins, (2) priming of DNA repair proteins to translocate to mitochondria, (3) direct interaction with the hydroxyl radical, or (4) inhibition of oxidative phosphorylation.

Oxidized peroxiredoxins utilize a second cysteine group on the enzyme to reduce the active site cysteine (19). The mdivi-1 compound contains an unblocked sulfhydryl moiety (224),

which may directly reduce the oxidized cysteine in the peroxiredoxin active site. This theory assumes that mdivi-1 is able to enter the mitochondria and to be transported to the matrix. Because mdivi-1 is proposed to act rapidly and reversibly (224), the Amplex Red experiment, which measures the rate of hydrogen peroxide breakdown, was performed using a simultaneous 1 hour mdivi-1/H_2O_2 co-treatment. This co-treatment did not show any increased rate in the breakdown of H_2O_2 in the presence of mdivi-1. However, the experiments showing mdivi-1-mediated protection against H_2O_2-induced mtDNA damage include a 1 hour mdivi-1 pretreatment. If a 1 hour pretreatment with mdivi-1 preemptively creates a reducing environment, then treating concurrently with mdivi-1 and H_2O_2 should decrease the protection of mdivi-1 against H_2O_2-induced mtDNA lesions. This has been suggested in preliminary studies by our group (data not shown).

All mitochondrial DNA repair proteins are expressed from the nuclear genome. These DNA repair proteins contain an MLS in their sequence (115) or an MLS is generated from an alternative splice site of the nuclear-targeted isoform of the gene (94,103,105,106,112). It was suggested in a 2006 study that the expression of nuclear-encoded mitochondrial proteins such as PolG and TFAM are controlled by nuclear respiratory factor (Nrf) 1 and 2, which bind to the promoter regions of these genes and upregulate their expression along with a coactivator such as PGC-1α (reviewed in (248)). In addition to genes involved in mtDNA maintenance and replication, the gene expression of mtDNA repair genes may also be controlled by Nrf1 or Nrf2. The 1-hour pretreatment with mdivi-1 may preemptively stimulate mtDNA repair gene expression and translocation to mitochondria, which may act as a defensive strategy against H_2O_2. If mdivi-1 stimulates DNA repair gene expression/mitochondrial translocation, then inhibiting mitochondrial protein import with an uncoupler during mdivi-1 pretreatment should

lead to no protection against H_2O_2-induced mtDNA lesions. How mdivi-1 would promote DNA repair gene expression/mitochondrial translocation during the 1 hour pretreatment is suggested in preliminary studies to be due to the induction of mtDNA damage by mdivi-1 (data not shown).

The sulfhydryl moiety of mdivi-1 may enable it to directly reduce the hydroxyl radical and thus prevent damage to other cellular targets such as DNA and proteins. This is supported by the mdivi-1-mediated decrease in H_2O_2-induced mtDNA damage but not MMS-induced damage.

In Fig. 18D and E, the basal OXPHOS at 8 hours after a control treatment with mdivi-1 present in the post-treatment media is 69% decreased compared to control treatment, suggesting that mdivi-1 may be inhibiting OXPHOS. In addition to the low basal OXPHOS rate in cells with mdivi-1 in the media, the ATP-linked OXPHOS and total reserve capacity of mdivi-1 treated cells is 88% and 47% reduced, respectively, compared to control. This suggests that mdivi-1 is inhibiting OXPHOS. Mdivi-1-mediated OXPHOS inhibition may protect mtDNA by preventing a vicious cycle of ROS. It is proposed that active OXPHOS is more heavily damaged by ROS than inactive OXPHOS. Once damaged, OXPHOS itself can produce ROS, which exacerbates mtDNA damage.

We found that a 1 hour pretreatment with mdivi-1 and a co-treatment with mdivi-1 and H_2O_2 was able to rescue H_2O_2-induced mitochondrial dysfunction in 92TAg MEFs, and yet, this same treatment schedule was unable to rescue H_2O_2-induced mitochondrial dysfunction in MCF7 cells. Importantly, 50 μM mdivi-1 was used for the pre- and co-treatment in the 92TAg MEFs, and 25 μM mdivi-1 was used for the pre- and co-treatment in the MCF7 cells. This different concentration of mdivi-1 had been utilized after observing that 25 μM still protected against mtDNA loss in 92TAg MEFs and against ~90% of the initial H_2O_2-induced mtDNA damage in

MCF7 cells. The difference observed in mdivi-1's effect on mitochondrial function in 92TAg MEFs and MCF7 cells could be due to the lower concentration of mdivi-1 used on the MCF7 cells (25 μM versus 50 μM) or it could be due to the specificity of mdivi-1 rescue of mitochondrial function in (1) fibroblasts, (2) p53-mutated/null cells, (3) mouse cells, and/or (4) cells with specific bioenergetics. If mdivi-1's rescue of H_2O_2-induced mitochondrial dysfunction is dependent upon its concentration being 50 μM, then treating MCF7 cells with 50 μM mdivi-1 in the treatment schedule detailed above should result in rescue of H_2O_2-induced mitochondrial dysfunction in these cells. If mdivi-1's protection against H_2O_2-induced mitochondrial dysfunction only occurs in fibroblasts, then treating normal human dermal fibroblasts (NHDFs) with 50 μM mdivi-1 should result in rescue of mitochondrial function. The treatment of NHDFs with mdivi-1 would also address whether p53 status or organism (mouse versus human) affects the rescue of mitochondrial function, because NHDFs have wild-type p53 like MCF7 cells and they are human cells. If mdivi-1 is able to rescue mitochondrial function in NHDFs, then its protection against H_2O_2-induced dysfunction is not affected by p53 status or organism source. It would instead suggest that mdivi-1 is able to rescue mitochondrial dysfunction in fibroblasts.

Cancer cells have been shown to have flexibility in their cellular bioenergetics (249,250). MCF7 cells are derived from luminal breast cancer, and thus, they may exhibit this same flexibility. Our results indicated a decline in OXPHOS at 8 hours after H_2O_2 addition in both MCF7 and 92TAg MEFs. The data indicated that at 8 hours after control treatment, the MCF7 cells were more dependent on glycolysis than the 92TAg MEFs. Thus, the decrease in OXPHOS seen at 8 hours after H_2O_2 addition in the MCF7 cells may be due to a different mechanism than the H_2O_2-induced in 92TAg MEFs. We hypothesize that the decrease in OXPHOS and increase in ECAR response in MCF7 cells is intentionally initiated as a mechanism of coping with

oxidative stress (the Crabtree effect) (249), whereas the decrease in OXPHOS in 92TAg MEF cells occurs as a result of mitochondrial dysfunction. MCF7 loss of mitochondrial function may be an intentional event after hydrogen peroxide insult. Thus, forcing the MCF7 cells to rely on OXPHOS with media containing galactose and pyruvate (250,251) should make the resultant H_2O_2-induced loss of OXPHOS due to mitochondrial dysfunction. Transmission electron microscope images were acquired from control- and H_2O_2-treated 92TAg MEFs, and it suggests that H_2O_2-induced mitochondrial dysfunction at 8 hours results in decreased OXPHOS in 92TAg MEFs (Fig. 20). These experiments have not been repeated for MCF7 cells or in the presence of mdivi-1, but these would be future avenues to pursue.

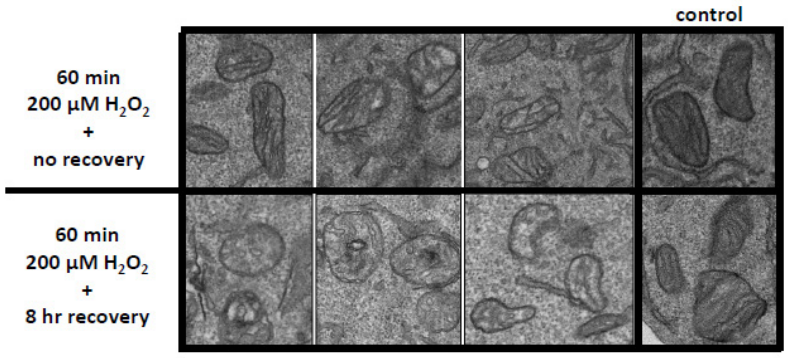

Figure 20. Transmission electron images of mitochondria at 0 and 8 hours following H_2O_2 treatment

92TAg MEFs were treated for 60 minutes with H_2O_2 and allowed to recover for 0 or 8 hours. A nontreated plate served as a control. At the harvest timepoint, cells were fixed and processed for TEM. Immediately after treatment, the mitochondrial matrix and membranes are less dense, and by 8 hours, the mitochondria are swollen, with absent or highly disorganized cristae, and the mitochondrial matrix and membranes are less dense than the 0 hour recovery cells.

This work demonstrates that persistent damage induced by oxidants and alkylating agents leads to divergent downstream events such as loss of mtDNA and mitochondrial dysfunction after oxidant treatment and no significant effect on mtDNA loss or function after treatment with MMS. The fission inhibitor mdivi-1 is able to protect against oxidant-induced effects on mtDNA and function but is unable to protect against MMS-induced mtDNA damage. Although we show that the maintenance of mtDNA copy number and mtDNA integrity is essential for cell survival, oxidants and alkylating agents affect mitochondria differently. These differences between oxidative mtDNA damage and alkylation mtDNA damage are exploited by mdivi-1. The mechanism for mdivi-1 action on oxidative mtDNA damage appears to be a role independent of its role in inhibiting mitochondrial fission.

BIBLIOGRAPHY

1. Ahting, U., Thieffry, M., Engelhardt, H., Hegerl, R., Neupert, W. and Nussberger, S. (2001) Tom40, the pore-forming component of the protein-conducting TOM channel in the outer membrane of mitochondria. *J Cell Biol*, **153**, 1151-1160.

2. Okado-Matsumoto, A. and Fridovich, I. (2001) Subcellular distribution of superoxide dismutases (SOD) in rat liver: Cu,Zn-SOD in mitochondria. *J Biol Chem*, **276**, 38388-38393.

3. Waterhouse, N.J. and Trapani, J.A. (2003) A new quantitative assay for cytochrome c release in apoptotic cells. *Cell Death Differ*, **10**, 853-855.

4. Wallace, D.C. (1994) Mitochondrial DNA sequence variation in human evolution and disease. *Proc Natl Acad Sci U S A*, **91**, 8739-8746.

5. Alam, T.I., Kanki, T., Muta, T., Ukaji, K., Abe, Y., Nakayama, H., Takio, K., Hamasaki, N. and Kang, D. (2003) Human mitochondrial DNA is packaged with TFAM. *Nucleic Acids Res*, **31**, 1640-1645.

6. Lambert, A.J. and Brand, M.D. (2009) Reactive oxygen species production by mitochondria. *Methods Mol Biol*, **554**, 165-181.

7. Yoshida, M., Muneyuki, E. and Hisabori, T. (2001) ATP synthase--a marvellous rotary engine of the cell. *Nat Rev Mol Cell Biol*, **2**, 669-677.

8. Van Houten, B., Woshner, V. and Santos, J. (2006) Role of mitochondrial DNA in toxic responses to oxidative stress. *DNA Repair*, **5**, 145-152.

9. Cadenas, E. and Davies, K.J. (2000) Mitochondrial free radical generation, oxidative stress, and aging. *Free Radic Biol Med*, **29**, 222-230.

10. Brand, M.D. (2010) The sites and topology of mitochondrial superoxide production. *Exp Gerontol*, **45**, 466-472.

11. Li, Y., Huang, T.T., Carlson, E.J., Melov, S., Ursell, P.C., Olson, J.L., Noble, L.J., Yoshimura, M.P., Berger, C., Chan, P.H. *et al.* (1995) Dilated cardiomyopathy and

neonatal lethality in mutant mice lacking manganese superoxide dismutase. *Nat Genet*, **11**, 376-381.

12. Lebovitz, R.M., Zhang, H., Vogel, H., Cartwright, J., Jr., Dionne, L., Lu, N., Huang, S. and Matzuk, M.M. (1996) Neurodegeneration, myocardial injury, and perinatal death in mitochondrial superoxide dismutase-deficient mice. *Proc Natl Acad Sci U S A*, **93**, 9782-9787.

13. Melov, S., Coskun, P., Patel, M., Tuinstra, R., Cottrell, B., Jun, A.S., Zastawny, T.H., Dizdaroglu, M., Goodman, S.I., Huang, T.T. *et al.* (1999) Mitochondrial disease in superoxide dismutase 2 mutant mice. *Proc Natl Acad Sci U S A*, **96**, 846-851.

14. Mitrunen, K., Sillanpaa, P., Kataja, V., Eskelinen, M., Kosma, V.M., Benhamou, S., Uusitupa, M. and Hirvonen, A. (2001) Association between manganese superoxide dismutase (MnSOD) gene polymorphism and breast cancer risk. *Carcinogenesis*, **22**, 827-829.

15. Nishida, T., Sugiyama, T., Kataoka, A., Tashiro, M., Yakushiji, M. and Ishikawa, M. (1993) Serum manganese superoxide dismutase (MnSOD) and histological virulence of ovarian cancer. *Asia Oceania J Obstet Gynaecol*, **19**, 427-431.

16. L'Abbe, M.R. and Trick, K.D. (1994) Changes in pancreatic glutathione peroxidase and superoxide dismutase activities in the prediabetic diabetes-prone BB rat. *Proc Soc Exp Biol Med*, **207**, 206-212.

17. Trimmer, C., Sotgia, F., Whitaker-Menezes, D., Balliet, R.M., Eaton, G., Martinez-Outschoorn, U.E., Pavlides, S., Howell, A., Iozzo, R.V., Pestell, R.G. *et al.* (2011) Caveolin-1 and mitochondrial SOD2 (MnSOD) function as tumor suppressors in the stromal microenvironment: a new genetically tractable model for human cancer associated fibroblasts. *Cancer Biol Ther*, **11**, 383-394.

18. Flohé, L. (1982) In Pryor, W. A. (ed.), *Free radicals in biology*. Academic Press, New York, pp. 223-275.

19. Banmeyer, I., Marchand, C., Clippe, A. and Knoops, B. (2005) Human mitochondrial peroxiredoxin 5 protects from mitochondrial DNA damages induced by hydrogen peroxide. *FEBS Lett*, **579**, 2327-2333.

20. Seo, M.S., Kang, S.W., Kim, K., Baines, I.C., Lee, T.H. and Rhee, S.G. (2000) Identification of a new type of mammalian peroxiredoxin that forms an intramolecular disulfide as a reaction intermediate. *J Biol Chem*, **275**, 20346-20354.

21. Wood, Z.A., Schroder, E., Robin Harris, J. and Poole, L.B. (2003) Structure, mechanism and regulation of peroxiredoxins. *Trends Biochem Sci*, **28**, 32-40.

22. Mari, M., Morales, A., Colell, A., Garcia-Ruiz, C. and Fernandez-Checa, J.C. (2009) Mitochondrial glutathione, a key survival antioxidant. *Antioxid Redox Signal*, **11**, 2685-2700.

23. Meredith, M.J. and Reed, D.J. (1982) Status of the mitochondrial pool of glutathione in the isolated hepatocyte. *J Biol Chem*, **257**, 3747-3753.

24. Han, D., Canali, R., Rettori, D. and Kaplowitz, N. (2003) Effect of glutathione depletion on sites and topology of superoxide and hydrogen peroxide production in mitochondria. *Mol Pharmacol*, **64**, 1136-1144.

25. Asensi, M., Sastre, J., Pallardo, F.V., Lloret, A., Lehner, M., Garcia-de-la Asuncion, J. and Vina, J. (1999) Ratio of reduced to oxidized glutathione as indicator of oxidative stress status and DNA damage. *Methods Enzymol*, **299**, 267-276.

26. Schaffer, S. and Suleiman, M. (eds.) (2007) *Mitochondria: the dynamic organelle*. Springer, NY.

27. Antunes, F., Han, D. and Cadenas, E. (2002) Relative contributions of heart mitochondria glutathione peroxidase and catalase to H(2)O(2) detoxification in in vivo conditions. *Free Radic Biol Med*, **33**, 1260-1267.

28. Radi, R., Turrens, J.F., Chang, L.Y., Bush, K.M., Crapo, J.D. and Freeman, B.A. (1991) Detection of catalase in rat heart mitochondria. *J Biol Chem*, **266**, 22028-22034.

29. Salvi, M., Battaglia, V., Brunati, A.M., La Rocca, N., Tibaldi, E., Pietrangeli, P., Marcocci, L., Mondovi, B., Rossi, C.A. and Toninello, A. (2007) Catalase takes part in rat liver mitochondria oxidative stress defense. *J Biol Chem*, **282**, 24407-24415.

30. Raha, S., McEachern, G.E., Myint, A.T. and Robinson, B.H. (2000) Superoxides from mitochondrial complex III: the role of manganese superoxide dismutase. *Free Radic Biol Med*, **29**, 170-180.

31. Hoppel, C. and Cooper, C. (1969) Studies on the nucleotide specificity of mitochondrial inner membrane particles. *Arch Biochem Biophys*, **135**, 184-193.

32. Santos, J.H., Hunakova, L., Chen, Y., Bortner, C. and Van Houten, B. (2003) Cell sorting experiments link persistent mitochondrial DNA damage with loss of mitochondrial membrane potential and apoptotic cell death. *J Biol Chem*, **278**, 1728-1734.

33. Okun, J.G., Lummen, P. and Brandt, U. (1999) Three classes of inhibitors share a common binding domain in mitochondrial complex I (NADH:ubiquinone oxidoreductase). *J Biol Chem*, **274**, 2625-2630.

34. Grigorieff, N. (1999) Structure of the respiratory NADH:ubiquinone oxidoreductase (complex I). *Curr Opin Struct Biol*, **9**, 476-483.

35. Turrens, J.F. and Boveris, A. (1980) Generation of superoxide anion by the NADH dehydrogenase of bovine heart mitochondria. *Biochem J*, **191**, 421-427.

36. Chen, Q., Vazquez, E.J., Moghaddas, S., Hoppel, C.L. and Lesnefsky, E.J. (2003) Production of reactive oxygen species by mitochondria: central role of complex III. *J Biol Chem*, **278**, 36027-36031.

37. Arai, M., Imai, H., Koumura, T., Yoshida, M., Emoto, K., Umeda, M., Chiba, N. and Nakagawa, Y. (1999) Mitochondrial phospholipid hydroperoxide glutathione peroxidase plays a major role in preventing oxidative injury to cells. *J Biol Chem*, **274**, 4924-4933.

38. Gleason, C., Huang, S., Thatcher, L.F., Foley, R.C., Anderson, C.R., Carroll, A.J., Millar, A.H. and Singh, K.B. (2011) Mitochondrial complex II has a key role in mitochondrial-derived reactive oxygen species influence on plant stress gene regulation and defense. *Proc Natl Acad Sci U S A*, **108**, 10768-10773.

39. Rustin, P., Munnich, A. and Rotig, A. (2002) Succinate dehydrogenase and human diseases: new insights into a well-known enzyme. *Eur J Hum Genet*, **10**, 289-291.

40. Mandavilli, B., Boldogh, I. and Van Houten, B. (2005) 3-nitropropionic acid-induced hydrogen peroxide, mitochondrial DNA damage, and cell death are attenuated by Bcl-2 overexpression in PC12 cells. *Mol Brain Res*, **133**, 215-223.

41. Sugioka, K., Nakano, M., Totsune-Nakano, H., Minakami, H., Tero-Kubota, S. and Ikegami, Y. (1988) Mechanism of O2- generation in reduction and oxidation cycle of ubiquinones in a model of mitochondrial electron transport systems. *Biochim Biophys Acta*, **936**, 377-385.

42. Trumpower, B.L. (1990) The protonmotive Q cycle. Energy transduction by coupling of proton translocation to electron transfer by the cytochrome bc1 complex. *J Biol Chem*, **265**, 11409-11412.

43. St-Pierre, J., Buckingham, J.A., Roebuck, S.J. and Brand, M.D. (2002) Topology of superoxide production from different sites in the mitochondrial electron transport chain. *J Biol Chem*, **277**, 44784-44790.

44. Demin, O.V., Westerhoff, H.V. and Kholodenko, B.N. (1998) Mathematical modelling of superoxide generation with the bc1 complex of mitochondria. *Biochemistry (Mosc)*, **63**, 634-649.

45. Gille, L. and Nohl, H. (2001) The ubiquinol/bc1 redox couple regulates mitochondrial oxygen radical formation. *Arch Biochem Biophys*, **388**, 34-38.

46. Han, D., Antunes, F., Canali, R., Rettori, D. and Cadenas, E. (2003) Voltage-dependent anion channels control the release of the superoxide anion from mitochondria to cytosol. *J Biol Chem*, **278**, 5557-5563.

47. Babcock, G.T. and Wikstrom, M. (1992) Oxygen activation and the conservation of energy in cell respiration. *Nature*, **356**, 301-309.

48. Babcock, G.T., Varotsis, C. and Zhang, Y. (1992) O2 activation in cytochrome oxidase and in other heme proteins. *Biochim Biophys Acta*, **1101**, 192-194.

49. Varotsis, C., Zhang, Y., Appelman, E.H. and Babcock, G.T. (1993) Resolution of the reaction sequence during the reduction of O2 by cytochrome oxidase. *Proc Natl Acad Sci U S A*, **90**, 237-241.

50. Dawson, T.L., Gores, G.J., Nieminen, A.L., Herman, B. and Lemasters, J.J. (1993) Mitochondria as a source of reactive oxygen species during reductive stress in rat hepatocytes. *Am J Physiol*, **264**, C961-967.

51. Drahota, Z., Chowdhury, S.K., Floryk, D., Mracek, T., Wilhelm, J., Rauchova, H., Lenaz, G. and Houstek, J. (2002) Glycerophosphate-dependent hydrogen peroxide production by brown adipose tissue mitochondria and its activation by ferricyanide. *J Bioenerg Biomembr*, **34**, 105-113.

52. Miwa, S. and Brand, M.D. (2005) The topology of superoxide production by complex III and glycerol 3-phosphate dehydrogenase in Drosophila mitochondria. *Biochim Biophys Acta*, **1709**, 214-219.

53. Imlay, J.A. (2008) Cellular defenses against superoxide and hydrogen peroxide. *Annu Rev Biochem*, **77**, 755-776.

54. Davies, M.J. (2005) The oxidative environment and protein damage. *Biochim Biophys Acta*, **1703**, 93-109.

55. Dean, R.T., Fu, S., Stocker, R. and Davies, M.J. (1997) Biochemistry and pathology of radical-mediated protein oxidation. *Biochem J*, **324 (Pt 1)**, 1-18.

56. Griffiths, S.W. and Cooney, C.L. (2002) Relationship between protein structure and methionine oxidation in recombinant human alpha 1-antitrypsin. *Biochemistry*, **41**, 6245-6252.

57. Winterbourn, C.C. and Metodiewa, D. (1999) Reactivity of biologically important thiol compounds with superoxide and hydrogen peroxide. *Free Radic Biol Med*, **27**, 322-328.

58. Schriner, S.E., Linford, N.J., Martin, G.M., Treuting, P., Ogburn, C.E., Emond, M., Coskun, P.E., Ladiges, W., Wolf, N., Van Remmen, H. *et al.* (2005) Extension of murine

life span by overexpression of catalase targeted to mitochondria. *Science*, **308**, 1909-1911.

59. Niki, E. (2009) Lipid peroxidation: physiological levels and dual biological effects. *Free Radic Biol Med*, **47**, 469-484.

60. Williams, M.V., Lee, S.H., Pollack, M. and Blair, I.A. (2006) Endogenous lipid hydroperoxide-mediated DNA-adduct formation in min mice. *J Biol Chem*, **281**, 10127-10133.

61. Blair, I.A. (2001) Lipid hydroperoxide-mediated DNA damage. *Exp Gerontol*, **36**, 1473-1481.

62. Moseley, R., Waddington, R., Evans, P., Halliwell, B. and Embery, G. (1995) The chemical modification of glycosaminoglycan structure by oxygen-derived species in vitro. *Biochim Biophys Acta*, **1244**, 245-252.

63. Henle, E.S., Han, Z., Tang, N., Rai, P., Luo, Y. and Linn, S. (1999) Sequence-specific DNA cleavage by Fe2+-mediated fenton reactions has possible biological implications. *J Biol Chem*, **274**, 962-971.

64. Imlay, J.A., Chin, S.M. and Linn, S. (1988) Toxic DNA damage by hydrogen peroxide through the Fenton reaction in vivo and in vitro. *Science*, **240**, 640-642.

65. Candeias, L. and Steenken, S. (1993) Electron transfer in di(deoxy)nucleoside phosphates in aqueous solution: rapid migration of oxidative damage (via adenine) to guanine. *J Am Chem Soc*, **115**, 2437-2440.

66. Shokolenko, I., Venediktova, N., Bochkareva, A., Wilson, G. and Alexeyev, M. (2009) Oxidative stress induces degradation of mitochondrial DNA. *Nuc Acids Res*, **37**, 2539-2548.

67. Yakes, F.M. and Van Houten, B. (1997) Mitochondrial DNA damage is more extensive and persists longer than nuclear DNA damage in human cells following oxidative stress. *Proc Natl Acad Sci U S A*, **94**, 514-519.

68. Ballinger, S.W., Patterson, C., Yan, C.N., Doan, R., Burow, D.L., Young, C.G., Yakes, F.M., Van Houten, B., Ballinger, C.A., Freeman, B.A. *et al.* (2000) Hydrogen peroxide- and peroxynitrite-induced mitochondrial DNA damage and dysfunction in vascular endothelial and smooth muscle cells. *Circ Res*, **86**, 960-966.

69. Ballinger, S.W., Van Houten, B., Jin, G.F., Conklin, C.A. and Godley, B.F. (1999) Hydrogen peroxide causes significant mitochondrial DNA damage in human RPE cells. *Exp Eye Res*, **68**, 765-772.

70. Barbi de Moura, M., Santana dos Santos, L. and Van Houten, B. (2010) Mitochondrial dysfunction in neurodegenerative diseases and cancer. *Environ Mol Mutagen*, **51**, 391-405.

71. Coskun, P.E., Beal, M.F. and Wallace, D.C. (2004) Alzheimer's brains harbor somatic mtDNA control-region mutations that suppress mitochondrial transcription and replication. *Proc Natl Acad Sci U S A*, **101**, 10726-10731.

72. Chatterjee, A., Mambo, E. and Sidransky, D. (2006) Mitochondrial DNA mutations in human cancer. *Oncogene*, **25**, 4663-4674.

73. Penta, J.S., Johnson, F.M., Wachsman, J.T. and Copeland, W.C. (2001) Mitochondrial DNA in human malignancy. *Mutat Res*, **488**, 119-133.

74. de la Monte, S.M., Luong, T., Neely, T.R., Robinson, D. and Wands, J.R. (2000) Mitochondrial DNA damage as a mechanism of cell loss in Alzheimer's disease. *Lab Invest*, **80**, 1323-1335.

75. Hirai, K., Aliev, G., Nunomura, A., Fujioka, H., Russell, R.L., Atwood, C.S., Johnson, A.B., Kress, Y., Vinters, H.V., Tabaton, M. *et al.* (2001) Mitochondrial abnormalities in Alzheimer's disease. *J Neurosci*, **21**, 3017-3023.

76. Khan, S.M., Cassarino, D.S., Abramova, N.N., Keeney, P.M., Borland, M.K., Trimmer, P.A., Krebs, C.T., Bennett, J.C., Parks, J.K., Swerdlow, R.H. *et al.* (2000) Alzheimer's disease cybrids replicate beta-amyloid abnormalities through cell death pathways. *Ann Neurol*, **48**, 148-155.

77. Trimmer, P.A., Swerdlow, R.H., Parks, J.K., Keeney, P., Bennett, J.P., Jr., Miller, S.W., Davis, R.E. and Parker, W.D., Jr. (2000) Abnormal mitochondrial morphology in sporadic Parkinson's and Alzheimer's disease cybrid cell lines. *Exp Neurol*, **162**, 37-50.

78. Betarbet, R., Sherer, T.B., MacKenzie, G., Garcia-Osuna, M., Panov, A.V. and Greenamyre, J.T. (2000) Chronic systemic pesticide exposure reproduces features of Parkinson's disease. *Nat Neurosci*, **3**, 1301-1306.

79. Testa, C.M., Sherer, T.B. and Greenamyre, J.T. (2005) Rotenone induces oxidative stress and dopaminergic neuron damage in organotypic substantia nigra cultures. *Brain Res Mol Brain Res*, **134**, 109-118.

80. Drolet, R.E., Cannon, J.R., Montero, L. and Greenamyre, J.T. (2009) Chronic rotenone exposure reproduces Parkinson's disease gastrointestinal neuropathology. *Neurobiol Dis*, **36**, 96-102.

81. Zhang, F., Bartels, M.J., Pottenger, L.H. and Gollapudi, B.B. (2005) Differential adduction of proteins vs. deoxynucleosides by methyl methanesulfonate and 1-methyl-1-nitrosourea in vitro. *Rapid Commun Mass Spectrom*, **19**, 438-448.

82. Barrows, L.R. and Magee, P.N. (1982) Nonenzymatic methylation of DNA by S-adenosylmethionine in vitro. *Carcinogenesis*, **3**, 349-351.

83. Bailey, E., Connors, T.A., Farmer, P.B., Gorf, S.M. and Rickard, J. (1981) Methylation of cysteine in hemoglobin following exposure to methylating agents. *Cancer Res*, **41**, 2514-2517.

84. Segerback, D., Calleman, C.J., Ehrenberg, L., Lofroth, G. and Osterman-Golkar, S. (1978) Evaluation of genetic risks of alkylating agents IV. Quantitative determination of alkylated amino acids in haemoglobin as a measure of the dose after-treatment of mice with methyl methanesulfonate. *Mutat Res*, **49**, 71-82.

85. Trezl, L., Park, K.S., Kim, S. and Paik, W.K. (1987) Studies on in vitro S-methylation of naturally occurring thiol compounds with N-methyl-N-nitrosourea and methyl methanesulfonate. *Environ Res*, **43**, 417-426.

86. Ralat, L.A., Manevich, Y., Fisher, A.B. and Colman, R.F. (2006) Direct evidence for the formation of a complex between 1-cysteine peroxiredoxin and glutathione S-transferase pi with activity changes in both enzymes. *Biochemistry*, **45**, 360-372.

87. Beranek, D.T. (1990) Distribution of methyl and ethyl adducts following alkylation with monofunctional alkylating agents. *Mutat Res*, **231**, 11-30.

88. Larson, K., Sahm, J., Shenkar, R. and Strauss, B. (1985) Methylation-induced blocks to in vitro DNA replication. *Mutat Res*, **150**, 77-84.

89. Casorelli, I., Russo, M.T. and Bignami, M. (2008) Role of mismatch repair and MGMT in response to anticancer therapies. *Anticancer Agents Med Chem*, **8**, 368-380.

90. Liu, P. and Demple, B. (2010) DNA repair in mammalian mitochondria: much more than we thought? *Environ Mol Mutagen*, **51**, 417-426.

91. Mason, P.A., Matheson, E.C., Hall, A.G. and Lightowlers, R.N. (2003) Mismatch repair activity in mammalian mitochondria. *Nucleic Acids Res*, **31**, 1052-1058.

92. Kajander, O.A., Karhunen, P.J., Holt, I.J. and Jacobs, H.T. (2001) Prominent mitochondrial DNA recombination intermediates in human heart muscle. *EMBO Rep*, **2**, 1007-1012.

93. Lakshmipathy, U. and Campbell, C. (1999) Double strand break rejoining by mammalian mitochondrial extracts. *Nucleic Acids Res*, **27**, 1198-1204.

94. Thyagarajan, B., Padua, R.A. and Campbell, C. (1996) Mammalian mitochondria possess homologous DNA recombination activity. *J Biol Chem*, **271**, 27536-27543.

95. Lakshmipathy, U. and Campbell, C. (1999) The human DNA ligase III gene encodes nuclear and mitochondrial proteins. *Mol Cell Biol*, **19**, 3869-3876.

96. Stierum, R.H., Dianov, G.L. and Bohr, V.A. (1999) Single-nucleotide patch base excision repair of uracil in DNA by mitochondrial protein extracts. *Nucleic Acids Res*, **27**, 3712-3719.

97. Taffe, B.G., Larminat, F., Laval, J., Croteau, D.L., Anson, R.M. and Bohr, V.A. (1996) Gene-specific nuclear and mitochondrial repair of formamidopyrimidine DNA glycosylase-sensitive sites in Chinese hamster ovary cells. *Mutat Res*, **364**, 183-192.

98. Bogenhagen, D. (1999) Repair of mtDNA in vertebrates. *Am J Human Genet*, **64**, 1276-1281.

99. Tann, A.W., Boldogh, I., Meiss, G., Qian, W., Van Houten, B., Mitra, S. and Szczesny, B. (2011) Apoptosis induced by persistent single-strand breaks in mitochondrial genome: critical role of EXOG (5'-EXO/endonuclease) in their repair. *J Biol Chem*, **286**, 31975-31983.

100. Liu, P., Qian, L., Sung, J.S., de Souza-Pinto, N.C., Zheng, L., Bogenhagen, D.F., Bohr, V.A., Wilson, D.M., 3rd, Shen, B. and Demple, B. (2008) Removal of oxidative DNA damage via FEN1-dependent long-patch base excision repair in human cell mitochondria. *Mol Cell Biol*, **28**, 4975-4987.

101. Copeland, W.C. and Longley, M.J. (2008) DNA2 resolves expanding flap in mitochondrial base excision repair. *Mol Cell*, **32**, 457-458.

102. Duxin, J.P., Dao, B., Martinsson, P., Rajala, N., Guittat, L., Campbell, J.L., Spelbrink, J.N. and Stewart, S.A. (2009) Human Dna2 is a nuclear and mitochondrial DNA maintenance protein. *Mol Cell Biol*, **29**, 4274-4282.

103. Kang, D., Nishida, J., Iyama, A., Nakabeppu, Y., Furuichi, M., Fujiwara, T., Sekiguchi, M. and Takeshige, K. (1995) Intracellular localization of 8-oxo-dGTPase in human cells, with special reference to the role of the enzyme in mitochondria. *J Biol Chem*, **270**, 14659-14665.

104. Nishioka, K., Ohtsubo, T., Oda, H., Fujiwara, T., Kang, D., Sugimachi, K. and Nakabeppu, Y. (1999) Expression and differential intracellular localization of two major forms of human 8-oxoguanine DNA glycosylase encoded by alternatively spliced OGG1 mRNAs. *Mol Biol Cell*, **10**, 1637-1652.

105. Hashiguchi, K., Stuart, J.A., de Souza-Pinto, N.C. and Bohr, V.A. (2004) The C-terminal alphaO helix of human Ogg1 is essential for 8-oxoguanine DNA glycosylase activity: the mitochondrial beta-Ogg1 lacks this domain and does not have glycosylase activity. *Nucleic Acids Res*, **32**, 5596-5608.

106. Nilsen, H., Otterlei, M., Haug, T., Solum, K., Nagelhus, T.A., Skorpen, F. and Krokan, H.E. (1997) Nuclear and mitochondrial uracil-DNA glycosylases are generated by alternative splicing and transcription from different positions in the UNG gene. *Nucleic Acids Res*, **25**, 750-755.

107. Ohtsubo, T., Nishioka, K., Imaiso, Y., Iwai, S., Shimokawa, H., Oda, H., Fujiwara, T. and Nakabeppu, Y. (2000) Identification of human MutY homolog (hMYH) as a repair enzyme for 2-hydroxyadenine in DNA and detection of multiple forms of hMYH located in nuclei and mitochondria. *Nucleic Acids Res*, **28**, 1355-1364.

108. Takao, M., Zhang, Q.M., Yonei, S. and Yasui, A. (1999) Differential subcellular localization of human MutY homolog (hMYH) and the functional activity of adenine:8-oxoguanine DNA glycosylase. *Nucleic Acids Res*, **27**, 3638-3644.

109. Hu, J., de Souza-Pinto, N.C., Haraguchi, K., Hogue, B.A., Jaruga, P., Greenberg, M.M., Dizdaroglu, M. and Bohr, V.A. (2005) Repair of formamidopyrimidines in DNA involves different glycosylases: role of the OGG1, NTH1, and NEIL1 enzymes. *J Biol Chem*, **280**, 40544-40551.

110. Karahalil, B., de Souza-Pinto, N.C., Parsons, J.L., Elder, R.H. and Bohr, V.A. (2003) Compromised incision of oxidized pyrimidines in liver mitochondria of mice deficient in NTH1 and OGG1 glycosylases. *J Biol Chem*, **278**, 33701-33707.

111. de Souza-Pinto, N.C., Wilson, D.M., 3rd, Stevnsner, T.V. and Bohr, V.A. (2008) Mitochondrial DNA, base excision repair and neurodegeneration. *DNA Repair (Amst)*, **7**, 1098-1109.

112. Ikeda, S., Kohmoto, T., Tabata, R. and Seki, Y. (2002) Differential intracellular localization of the human and mouse endonuclease III homologs and analysis of the sorting signals. *DNA Repair (Amst)*, **1**, 847-854.

113. Otterlei, M., Haug, T., Nagelhus, T.A., Slupphaug, G., Lindmo, T. and Krokan, H.E. (1998) Nuclear and mitochondrial splice forms of human uracil-DNA glycosylase contain a complex nuclear localisation signal and a strong classical mitochondrial localisation signal, respectively. *Nucleic Acids Res*, **26**, 4611-4617.

114. Takao, M., Aburatani, H., Kobayashi, K. and Yasui, A. (1998) Mitochondrial targeting of human DNA glycosylases for repair of oxidative DNA damage. *Nucleic Acids Res*, **26**, 2917-2922.

115. Nagelhus, T.A., Slupphaug, G., Lindmo, T. and Krokan, H.E. (1995) Cell cycle regulation and subcellular localization of the major human uracil-DNA glycosylase. *Exp Cell Res*, **220**, 292-297.

116. Wong, L.J., Naviaux, R.K., Brunetti-Pierri, N., Zhang, Q., Schmitt, E.S., Truong, C., Milone, M., Cohen, B.H., Wical, B., Ganesh, J. *et al.* (2008) Molecular and clinical genetics of mitochondrial diseases due to POLG mutations. *Hum Mutat*, **29**, E150-172.

117. Myers, K.A., Saffhill, R. and O'Connor, P.J. (1988) Repair of alkylated purines in the hepatic DNA of mitochondria and nuclei in the rat. *Carcinogenesis*, **9**, 285-292.

118. Pettepher, C.C., LeDoux, S.P., Bohr, V.A. and Wilson, G.L. (1991) Repair of alkali-labile sites within the mitochondrial DNA of RINr 38 cells after exposure to the nitrosourea streptozotocin. *J Biol Chem*, **266**, 3113-3117.

119. LeDoux, S.P., Wilson, G.L., Beecham, E.J., Stevnsner, T., Wassermann, K. and Bohr, V.A. (1992) Repair of mitochondrial DNA after various types of DNA damage in Chinese hamster ovary cells. *Carcinogenesis*, **13**, 1967-1973.

120. Acevedo-Torres, K., Fonseca-Williams, S., Ayala-Torres, S. and Torres-Ramos, C.A. (2009) Requirement of the Saccharomyces cerevisiae APN1 gene for the repair of mitochondrial DNA alkylation damage. *Environ Mol Mutagen*, **50**, 317-327.

121. Cai, S., Xu, Y., Cooper, R.J., Ferkowicz, M.J., Hartwell, J.R., Pollok, K.E. and Kelley, M.R. (2005) Mitochondrial targeting of human O6-methylguanine DNA methyltransferase protects against cell killing by chemotherapeutic alkylating agents. *Cancer Res*, **65**, 3319-3327.

122. Rasmussen, A.K. and Rasmussen, L.J. (2005) Targeting of O6-MeG DNA methyltransferase (MGMT) to mitochondria protects against alkylation induced cell death. *Mitochondrion*, **5**, 411-417.

123. Fishel, M.L., Seo, Y.R., Smith, M.L. and Kelley, M.R. (2003) Imbalancing the DNA base excision repair pathway in the mitochondria; targeting and overexpressing N-methylpurine DNA glycosylase in mitochondria leads to enhanced cell killing. *Cancer Res*, **63**, 608-615.

124. Yu, S.C., Qian, G.S., Li, Y.Y., Lu, W.Z., Li, J. and Huang, G.J. (2006) [Inhibitory effect of human mitochondria-targeted MPG recombinant on proliferation of human non-small cell lung cancer multidrug-resistant cell line A549/DDP]. *Ai Zheng*, **25**, 421-426.

125. Harrison, J.F., Rinne, M.L., Kelley, M.R., Druzhyna, N.M., Wilson, G.L. and Ledoux, S.P. (2007) Altering DNA base excision repair: use of nuclear and mitochondrial-targeted N-methylpurine DNA glycosylase to sensitize astroglia to chemotherapeutic agents. *Glia*, **55**, 1416-1425.

126. Coquerelle, T., Dosch, J. and Kaina, B. (1995) Overexpression of N-methylpurine-DNA glycosylase in Chinese hamster ovary cells renders them more sensitive to the production of chromosomal aberrations by methylating agents--a case of imbalanced DNA repair. *Mutat Res*, **336**, 9-17.

127. Demple, B., Herman, T. and Chen, D.S. (1991) Cloning and expression of APE, the cDNA encoding the major human apurinic endonuclease: definition of a family of DNA repair enzymes. *Proc Natl Acad Sci U S A*, **88**, 11450-11454.

128. Tell, G., Crivellato, E., Pines, A., Paron, I., Pucillo, C., Manzini, G., Bandiera, A., Kelley, M.R., Di Loreto, C. and Damante, G. (2001) Mitochondrial localization of APE/Ref-1 in thyroid cells. *Mutat Res*, **485**, 143-152.

129. Tomkinson, A.E., Bonk, R.T. and Linn, S. (1988) Mitochondrial endonuclease activities specific for apurinic/apyrimidinic sites in DNA from mouse cells. *J Biol Chem*, **263**, 12532-12537.

130. Li, M., Zhong, Z., Zhu, J., Xiang, D., Dai, N., Cao, X., Qing, Y., Yang, Z., Xie, J., Li, Z. *et al.* (2010) Identification and characterization of mitochondrial targeting sequence of human apurinic/apyrimidinic endonuclease 1. *J Biol Chem*, **285**, 14871-14881.

131. Chattopadhyay, R., Wiederhold, L., Szczesny, B., Boldogh, I., Hazra, T.K., Izumi, T. and Mitra, S. (2006) Identification and characterization of mitochondrial abasic (AP)-endonuclease in mammalian cells. *Nucleic Acids Res*, **34**, 2067-2076.

132. Frossi, B., Tell, G., Spessotto, P., Colombatti, A., Vitale, G. and Pucillo, C. (2002) H_2O_2 induces translocation of APE/Ref-1 to mitochondria in the Raji B-cell line. *J Cell Phys*, **193**, 180-186.

133. Tsuchimoto, D., Sakai, Y., Sakumi, K., Nishioka, K., Sasaki, M., Fujiwara, T. and Nakabeppu, Y. (2001) Human APE2 protein is mostly localized in the nuclei and to some extent in the mitochondria, while nuclear APE2 is partly associated with proliferating cell nuclear antigen. *Nucleic Acids Res*, **29**, 2349-2360.

134. Levin, C.J. and Zimmerman, S.B. (1976) A DNA ligase from mitochondria of rat liver. *Biochem Biophys Res Commun*, **69**, 514-520.

135. Pinz, K.G. and Bogenhagen, D.F. (1998) Efficient repair of abasic sites in DNA by mitochondrial enzymes. *Mol Cell Biol*, **18**, 1257-1265.

136. Levine, B. and Klionsky, D.J. (2004) Development by self-digestion: molecular mechanisms and biological functions of autophagy. *Dev Cell*, **6**, 463-477.

137. Ashford, T.P. and Porter, K.R. (1962) Cytoplasmic components in hepatic cell lysosomes. *J Cell Biol*, **12**, 198-202.

138. Lemasters, J.J. (2005) Selective mitochondrial autophagy, or mitophagy, as a targeted defense against oxidative stress, mitochondrial dysfunction, and aging. *Rejuvenation Res*, **8**, 3-5.

139. Youle, R.J. and Narendra, D.P. (2011) Mechanisms of mitophagy. *Nat Rev Mol Cell Biol*, **12**, 9-14.

140. Vives-Bauza, C., Zhou, C., Huang, Y., Cui, M., de Vries, R.L., Kim, J., May, J., Tocilescu, M.A., Liu, W., Ko, H.S. *et al.* (2010) PINK1-dependent recruitment of Parkin to mitochondria in mitophagy. *Proc Natl Acad Sci U S A*, **107**, 378-383.

141. Zhou, C., Huang, Y., Shao, Y., May, J., Prou, D., Perier, C., Dauer, W., Schon, E.A. and Przedborski, S. (2008) The kinase domain of mitochondrial PINK1 faces the cytoplasm. *Proc Natl Acad Sci U S A*, **105**, 12022-12027.

142. Narendra, D.P., Jin, S.M., Tanaka, A., Suen, D.F., Gautier, C.A., Shen, J., Cookson, M.R. and Youle, R.J. (2010) PINK1 is selectively stabilized on impaired mitochondria to activate Parkin. *PLoS Biol*, **8**, e1000298.

143. Matsuda, N., Sato, S., Shiba, K., Okatsu, K., Saisho, K., Gautier, C.A., Sou, Y.S., Saiki, S., Kawajiri, S., Sato, F. *et al.* (2010) PINK1 stabilized by mitochondrial depolarization recruits Parkin to damaged mitochondria and activates latent Parkin for mitophagy. *J Cell Biol*, **189**, 211-221.

144. Narendra, D., Tanaka, A., Suen, D.F. and Youle, R.J. (2008) Parkin is recruited selectively to impaired mitochondria and promotes their autophagy. *J Cell Biol*, **183**, 795-803.

145. Suen, D.F., Narendra, D.P., Tanaka, A., Manfredi, G. and Youle, R.J. (2010) Parkin overexpression selects against a deleterious mtDNA mutation in heteroplasmic cybrid cells. *Proc Natl Acad Sci U S A*, **107**, 11835-11840.

146. Geisler, S., Holmstrom, K.M., Skujat, D., Fiesel, F.C., Rothfuss, O.C., Kahle, P.J. and Springer, W. (2010) PINK1/Parkin-mediated mitophagy is dependent on VDAC1 and p62/SQSTM1. *Nat Cell Biol*, **12**, 119-131.

147. Kim, Y., Park, J., Kim, S., Song, S., Kwon, S.K., Lee, S.H., Kitada, T., Kim, J.M. and Chung, J. (2008) PINK1 controls mitochondrial localization of Parkin through direct phosphorylation. *Biochem Biophys Res Commun*, **377**, 975-980.

148. Kawajiri, S., Saiki, S., Sato, S., Sato, F., Hatano, T., Eguchi, H. and Hattori, N. (2010) PINK1 is recruited to mitochondria with parkin and associates with LC3 in mitophagy. *FEBS Lett*, **584**, 1073-1079.

149. Shiba, K., Arai, T., Sato, S., Kubo, S., Ohba, Y., Mizuno, Y. and Hattori, N. (2009) Parkin stabilizes PINK1 through direct interaction. *Biochem Biophys Res Commun*, **383**, 331-335.

150. Um, J.W., Stichel-Gunkel, C., Lubbert, H., Lee, G. and Chung, K.C. (2009) Molecular interaction between parkin and PINK1 in mammalian neuronal cells. *Mol Cell Neurosci*, **40**, 421-432.

151. Sha, D., Chin, L.S. and Li, L. (2010) Phosphorylation of parkin by Parkinson disease-linked kinase PINK1 activates parkin E3 ligase function and NF-kappaB signaling. *Hum Mol Genet*, **19**, 352-363.

152. Tanaka, A., Cleland, M.M., Xu, S., Narendra, D.P., Suen, D.F., Karbowski, M. and Youle, R.J. (2010) Proteasome and p97 mediate mitophagy and degradation of mitofusins induced by Parkin. *J Cell Biol*, **191**, 1367-1380.

153. Gegg, M.E., Cooper, J.M., Chau, K.Y., Rojo, M., Schapira, A.H. and Taanman, J.W. (2010) Mitofusin 1 and mitofusin 2 are ubiquitinated in a PINK1/parkin-dependent manner upon induction of mitophagy. *Hum Mol Genet*, **19**, 4861-4870.

154. Poole, A.C., Thomas, R.E., Yu, S., Vincow, E.S. and Pallanck, L. (2010) The mitochondrial fusion-promoting factor mitofusin is a substrate of the PINK1/parkin pathway. *PLoS One*, **5**, e10054.

155. Santel, A. and Fuller, M.T. (2001) Control of mitochondrial morphology by a human mitofusin. *J Cell Sci*, **114**, 867-874.

156. Alexander, C., Votruba, M., Pesch, U.E., Thiselton, D.L., Mayer, S., Moore, A., Rodriguez, M., Kellner, U., Leo-Kottler, B., Auburger, G. *et al.* (2000) OPA1, encoding a dynamin-related GTPase, is mutated in autosomal dominant optic atrophy linked to chromosome 3q28. *Nat Genet*, **26**, 211-215.

157. Delettre, C., Lenaers, G., Griffoin, J.M., Gigarel, N., Lorenzo, C., Belenguer, P., Pelloquin, L., Grosgeorge, J., Turc-Carel, C., Perret, E. *et al.* (2000) Nuclear gene OPA1, encoding a mitochondrial dynamin-related protein, is mutated in dominant optic atrophy. *Nat Genet*, **26**, 207-210.

158. Smirnova, E., Griparic, L., Shurland, D.L. and van der Bliek, A.M. (2001) Dynamin-related protein Drp1 is required for mitochondrial division in mammalian cells. *Mol Biol Cell*, **12**, 2245-2256.

159. Otera, H., Wang, C., Cleland, M.M., Setoguchi, K., Yokota, S., Youle, R.J. and Mihara, K. (2010) Mff is an essential factor for mitochondrial recruitment of Drp1 during mitochondrial fission in mammalian cells. *J Cell Biol*, **191**, 1141-1158.

160. Suen, D.F., Norris, K.L. and Youle, R.J. (2008) Mitochondrial dynamics and apoptosis. *Genes Dev*, **22**, 1577-1590.

161. Hales, K.G. and Fuller, M.T. (1997) Developmentally regulated mitochondrial fusion mediated by a conserved, novel, predicted GTPase. *Cell*, **90**, 121-129.

162. Westermann, B. (2010) Mitochondrial fusion and fission in cell life and death. *Nat Rev Mol Cell Biol*, **11**, 872-884.

163. Olichon, A., Emorine, L.J., Descoins, E., Pelloquin, L., Brichese, L., Gas, N., Guillou, E., Delettre, C., Valette, A., Hamel, C.P. *et al.* (2002) The human dynamin-related protein OPA1 is anchored to the mitochondrial inner membrane facing the inter-membrane space. *FEBS Lett*, **523**, 171-176.

164. Meeusen, S., McCaffery, J.M. and Nunnari, J. (2004) Mitochondrial fusion intermediates revealed in vitro. *Science*, **305**, 1747-1752.

165. Frezza, C., Cipolat, S., Martins de Brito, O., Micaroni, M., Beznoussenko, G.V., Rudka, T., Bartoli, D., Polishuck, R.S., Danial, N.N., De Strooper, B. *et al.* (2006) OPA1 controls apoptotic cristae remodeling independently from mitochondrial fusion. *Cell*, **126**, 177-189.

166. Koshiba, T., Detmer, S.A., Kaiser, J.T., Chen, H., McCaffery, J.M. and Chan, D.C. (2004) Structural basis of mitochondrial tethering by mitofusin complexes. *Science*, **305**, 858-862.

167. Chen, H., Detmer, S.A., Ewald, A.J., Griffin, E.E., Fraser, S.E. and Chan, D.C. (2003) Mitofusins Mfn1 and Mfn2 coordinately regulate mitochondrial fusion and are essential for embryonic development. *J Cell Biol*, **160**, 189-200.

168. Malka, F., Guillery, O., Cifuentes-Diaz, C., Guillou, E., Belenguer, P., Lombes, A. and Rojo, M. (2005) Separate fusion of outer and inner mitochondrial membranes. *EMBO Rep*, **6**, 853-859.

169. Roux, A., Uyhazi, K., Frost, A. and De Camilli, P. (2006) GTP-dependent twisting of dynamin implicates constriction and tension in membrane fission. *Nature*, **441**, 528-531.

170. Taguchi, N., Ishihara, N., Jofuku, A., Oka, T. and Mihara, K. (2007) Mitotic phosphorylation of dynamin-related GTPase Drp1 participates in mitochondrial fission. *J Biol Chem*, **282**, 11521-11529.

171. Chang, C.R. and Blackstone, C. (2007) Cyclic AMP-dependent protein kinase phosphorylation of Drp1 regulates its GTPase activity and mitochondrial morphology. *J Biol Chem*, **282**, 21583-21587.

172. Cereghetti, G.M., Stangherlin, A., Martins de Brito, O., Chang, C.R., Blackstone, C., Bernardi, P. and Scorrano, L. (2008) Dephosphorylation by calcineurin regulates translocation of Drp1 to mitochondria. *Proc Natl Acad Sci U S A*, **105**, 15803-15808.

173. Yoon, Y., Krueger, E.W., Oswald, B.J. and McNiven, M.A. (2003) The mitochondrial protein hFis1 regulates mitochondrial fission in mammalian cells through an interaction with the dynamin-like protein DLP1. *Mol Cell Biol*, **23**, 5409-5420.

174. Stojanovski, D., Koutsopoulos, O.S., Okamoto, K. and Ryan, M.T. (2004) Levels of human Fis1 at the mitochondrial outer membrane regulate mitochondrial morphology. *J Cell Sci*, **117**, 1201-1210.

175. Lee, Y.J., Jeong, S.Y., Karbowski, M., Smith, C.L. and Youle, R.J. (2004) Roles of the mammalian mitochondrial fission and fusion mediators Fis1, Drp1, and Opa1 in apoptosis. *Mol Biol Cell*, **15**, 5001-5011.

176. Nowikovsky, K., Reipert, S., Devenish, R.J. and Schweyen, R.J. (2007) Mdm38 protein depletion causes loss of mitochondrial K+/H+ exchange activity, osmotic swelling and mitophagy. *Cell Death Differ*, **14**, 1647-1656.

177. Parone, P.A., Da Cruz, S., Tondera, D., Mattenberger, Y., James, D.I., Maechler, P., Barja, F. and Martinou, J.C. (2008) Preventing mitochondrial fission impairs mitochondrial function and leads to loss of mitochondrial DNA. *PLoS One*, **3**, e3257.

178. Twig, G., Elorza, A., Molina, A.J., Mohamed, H., Wikstrom, J.D., Walzer, G., Stiles, L., Haigh, S.E., Katz, S., Las, G. *et al.* (2008) Fission and selective fusion govern mitochondrial segregation and elimination by autophagy. *EMBO J*, **27**, 433-446.

179. Van Laar, V.S., Arnold, B., Cassady, S.J., Chu, C.T., Burton, E.A. and Berman, S.B. (2010) Bioenergetics of neurons inhibit the translocation response of Parkin following rapid mitochondrial depolarization. *Hum Mol Genet*, **20**, 927-940.

180. Santos, J.H., Meyer, J.N., Mandavilli, B.S. and Van Houten, B. (2006) Quantitative PCR-based measurement of nuclear and mitochondrial DNA damage and repair in mammalian cells. *Methods Mol Biol*, **314**, 183-199.

181. Sugioka, R., Shimizu, S. and Tsujimoto, Y. (2004) Fzo1, a protein involved in mitochondrial fusion, inhibits apoptosis. *J Biol Chem*, **279**, 52726-52734.

182. Balaban, R., Nemoto, S. and Finkel, T. (2005) Mitochondria, oxidants, and aging. *Cell* **120**, 483-495.

183. LeDoux, S.P., Driggers, W.J., Hollensworth, B.S. and Wilson, G.L. (1999) Repair of alkylation and oxidative damage in mitochondrial DNA. *Mutat Res*, **434**, 149-159.

184. Wallace, D.C. (1992) Diseases of the mitochondrial DNA. *Annu Rev Biochem*, **61**, 1175-1212.

185. Salazar, J.J. and Van Houten, B. (1997) Preferential mitochondrial DNA injury caused by glucose oxidase as a steady generator of hydrogen peroxide in human fibroblasts. *Mutat Res*, **385**, 139-149.

186. Sawyer, D. and Van Houten, B. (1999) Repair of DNA damage in mitochondria. *Mutation Res*, **434**, 161-176.

187. Kujoth, G.C., Hiona, A., Pugh, T.D., Someya, S., Panzer, K., Wohlgemuth, S.E., Hofer, T., Seo, A.Y., Sullivan, R., Jobling, W.A. *et al.* (2005) Mitochondrial DNA mutations, oxidative stress, and apoptosis in mammalian aging. *Science*, **309**, 481-484.

188. Trifunovic, A., Wredenberg, A., Falkenberg, M., Spelbrink, J.N., Rovio, A.T., Bruder, C.E., Bohlooly, Y.M., Gidlof, S., Oldfors, A., Wibom, R. *et al.* (2004) Premature ageing in mice expressing defective mitochondrial DNA polymerase. *Nature*, **429**, 417-423.

189. Jarrett, S.G., Lin, H., Godley, B.F. and Boulton, M.E. (2008) Mitochondrial DNA damage and its potential role in retinal degeneration. *Prog Retin Eye Res*, **27**, 596-607.

190. de la Monte, S., Luong, T., Neely, T., Robinson, D. and Wands, J. (2000) Mitochondrial DNA damage as a mechanism of cell loss in Alzheimer's disease. *Lab Invest*, **80**, 1323-1335.

191. Yang, J., Weissman, L., Bohr, V. and Mattson, M. (2008) Mitochondrial DNA damage and repair in neurodegenerative disorders. *DNA Repair*, **7**, 1110-1120.

192. Durham, S., Krishnan, K., Betts, J. and Birch-Machin, M. (2003) Mitochondrial DNA damage in non-melanoma skin cancer. *Br J Cancer*, **88**, 90-95.

193. Parella, P., Xiao, Y., Fliss, M., Sanchez-Cespedes, M., Mazzarelli, P., Rinaldi, M., Nicol, T., Gabrielson, E., Cuomo, C., Cohen, D. *et al.* (2001) Detection of mitochondrial DNA mutations in primary breast cancer and fine-needle aspirates. *Cancer Res*, **61**, 7623-7626.

194. Sanchez-Cespedes, M., Parella, P., Nomoto, S., Cohen, D., Xiao, Y., Esteller, M., Jeronimo, C., Jordan, R., Nicol, T., Koch, W. *et al.* (2001) Identification of a mononucleotide repeat as a major target for mitochondrial DNA alterations in human tumors. *Cancer Res*, **61**, 7015-7019.

195. Lee, H., Yin, P., Chi, C. and Wei, Y. (2002) Increase in mitochondrial mass in human fibroblasts under oxidative stress and during replicative cell senescence. *J Biomed Sci*, **9**, 517-526.

196. Chen, Q. and Ames, B. (1994) Senescence-like growth arrest induced by hydrogen peroxide in human diploid fibroblast F65 cells. *Proc Natl Acad Sci*, **91**, 4130-4134.

197. Chen, Q., Bartholomew, J., Campisi, J., Acosta, M., Reagan, J. and Ames, B. (1998) Molecular analysis of H_2O_2-induced senescent-like growth arrest in normal human fibroblasts: p53 and Rb control G_1 arrest but not cell replication. *Biochem J*, **332**, 43-50.

198. Chen, Q., Fischer, A., Reagan, J., LJ, Y. and Ames, B. (1995) Oxidative DNA damage and senescence of human diploid fibroblast cells. *Proc Natl Acad Sci*, **92**, 4337-4341.

199. Barnouin, K., Dubuisson, M.L., Child, E.S., Fernandez de Mattos, S., Glassford, J., Medema, R.H., Mann, D.J. and Lam, E.W. (2002) H2O2 induces a transient multi-phase cell cycle arrest in mouse fibroblasts through modulating cyclin D and p21Cip1 expression. *J Biol Chem*, **277**, 13761-13770.

200. Bladier, C., Wolvetang, E.J., Hutchinson, P., de Haan, J.B. and Kola, I. (1997) Response of a primary human fibroblast cell line to H2O2: senescence-like growth arrest or apoptosis? *Cell Growth Differ*, **8**, 589-598.

201. Teramoto, S., Tomita, T., Matsui, H., Ohga, E., Matsuse, T. and Ouchi, Y. (1999) Hydrogen peroxide-induced apoptosis and necrosis in human lung fibroblasts: protective roles of glutathione. *Jpn J Pharmacol*, **79**, 33-40.

202. Zhang, H., Kong, X., Kang, J., Su, J., Li, Y., Zhong, J. and Sun, L. (2009) Oxidative stress induces parallel autophagy and mitochondrial dysfunction in human glioma U251 cells. *Toxicol Sci*, **110**, 376-388.

203. Lu, M. and Gong, X. (2009) Upstream reactive oxidative species (ROS) signals in exogenous oxidative stress-induced mitochondrial dysfunction. *Cell Biol Int*, **33**, 658-664.

204. Miguel, F., Augusto, A. and Gurgueira, S. (2009) Effect of acute vs chronic H_2O_2-induced oxidative stress on antioxidant enzyme activities. *Free Rad Res*, **43**, 340-347.

205. Nulton-Persson, A. and Szweda, L. (2001) Modulation of mitochondrial function by hydrogen peroxide. *J Biol Chem*, **276**, 23357-23361.

206. Hurley, L.H. (2002) DNA and its associated processes as targets for cancer therapy. *Nat Rev Cancer*, **2**, 188-200.

207. Loechler, E.L., Green, C.L. and Essigmann, J.M. (1984) In vivo mutagenesis by O6-methylguanine built into a unique site in a viral genome. *Proc Natl Acad Sci U S A*, **81**, 6271-6275.

208. Dosanjh, M.K., Galeros, G., Goodman, M.F. and Singer, B. (1991) Kinetics of extension of O6-methylguanine paired with cytosine or thymine in defined oligonucleotide sequences. *Biochemistry*, **30**, 11595-11599.

209. Wunderlich, V., Schutt, M., Bottger, M. and Graffi, A. (1970) Preferential alkylation of mitochondrial deoxyribonucleic acid by N-methyl-N-nitrosourea. *Biochem J*, **118**, 99-109.

210. Daugherty, J.P. and Clapp, N.K. (1985) Association of nitrosamine-derived radioactivity with nuclear and mitochondrial DNA in mice. *Jpn J Cancer Res*, **76**, 197-201.

211. Cadenas, E., Boveris, A., Ragan, C. and Stoppani, A. (1977) Production of superoxide radicals and hydrogen peroxide by NADH-ubiquinone reductase and ubiquinol-cytochrome c reductase from beef-heart mitochondria. *Arch Biochem Biophys*, **180**, 248-257.

212. Chance, B. and Williams, G. (1956) The respiratory chain and oxidative phosphorylation. *Advan Enzymol Relat Subj Biochem*, **17**, 65-134.

213. Bacman, S.R., Williams, S.L. and Moraes, C.T. (2009) Intra- and inter-molecular recombination of mitochondrial DNA after in vivo induction of multiple double-strand breaks. *Nucleic Acids Res*, **37**, 4218-4226.

214. Oka, S., Ohno, M., Tsuchimoto, D., Sakumi, K., Furuichi, M. and Nakabeppu, Y. (2008) Two distinct pathways of cell death triggered by oxidative damage to nuclear and mitochondrial DNAs. *EMBO J*, **27**, 421-432.

215. Wright, G., Terada, K., Yano, M., Sergeev, I. and Mori, M. (2001) Oxidative stress inhibits the mitochondrial import of preproteins and leads to their degradation. *Exp Cell Res*, **263**, 107-117.

216. Wright, G., Reichenbecher, V., Green, T., Wright, G.L. and Wang, S. (1997) Paraquat inhibits the processing of human manganese-dependent superoxide dismutase by SF-9 insect cell mitochondria. *Exp Cell Res*, **234**, 78-84.

217. Lu, T., Pan, Y., Kao, S.Y., Li, C., Kohane, I., Chan, J. and Yankner, B.A. (2004) Gene regulation and DNA damage in the ageing human brain. *Nature*, **429**, 883-891.

218. Cadenas, E. (1989) Biochemistry of oxygen toxicity. *Annu Rev Biochem*, **58**, 79-110.

219. Sawyer, D.E., Roman, S.D. and Aitken, R.J. (2001) Relative susceptibilities of mitochondrial and nuclear DNA to damage induced by hydrogen peroxide in two mouse germ cell lines. *Redox Rep*, **6**, 182-184.

220. Furda, A. and Van Houten, B. (2011) Oxidants but not alkylating agents induce rapid mtDNA loss and mitochondrial dysfunction. *submitted to DNA Repair*.

221. Noack, H., Bednarek, T., Heidler, J., Ladig, R., Holtz, J. and Szibor, M. (2006) TFAM-dependent and independent dynamics of mtDNA levels in C2C12 myoblasts caused by redox stress. *Biochim Biophys Acta*, **1760**, 141-150.

222. Rachek, L.I., Grishko, V.I., Alexeyev, M.F., Pastukh, V.V., LeDoux, S.P. and Wilson, G.L. (2004) Endonuclease III and endonuclease VIII conditionally targeted into mitochondria enhance mitochondrial DNA repair and cell survival following oxidative stress. *Nucleic Acids Res*, **32**, 3240-3247.

223. Gandre-Babbe, S. and van der Bliek, A.M. (2008) The novel tail-anchored membrane protein Mff controls mitochondrial and peroxisomal fission in mammalian cells. *Mol Biol Cell*, **19**, 2402-2412.

224. Mai, S., Klinkenberg, M., Auburger, G., Bereiter-Hahn, J. and Jendrach, M. (2010) Decreased expression of Drp1 and Fis1 mediates mitochondrial elongation in senescent cells and enhances resistance to oxidative stress through PINK1. *J Cell Sci*, **123**, 917-926.

225. Cassidy-Stone, A., Chipuk, J.E., Ingerman, E., Song, C., Yoo, C., Kuwana, T., Kurth, M.J., Shaw, J.T., Hinshaw, J.E., Green, D.R. *et al.* (2008) Chemical inhibition of the mitochondrial division dynamin reveals its role in Bax/Bak-dependent mitochondrial outer membrane permeabilization. *Dev Cell*, **14**, 193-204.

226. Smirnova, E., Shurland, D.L., Ryazantsev, S.N. and van der Bliek, A.M. (1998) A human dynamin-related protein controls the distribution of mitochondria. *J Cell Biol*, **143**, 351-358.

227. Park, S.W., Kim, K.Y., Lindsey, J.D., Dai, Y., Heo, H., Nguyen, D.H., Ellisman, M.H., Weinreb, R.N. and Ju, W.K. (2011) A selective inhibitor of drp1, mdivi-1, increases retinal ganglion cell survival in acute ischemic mouse retina. *Invest Ophthalmol Vis Sci*, **52**, 2837-2843.

228. Ong, S.B., Subrayan, S., Lim, S.Y., Yellon, D.M., Davidson, S.M. and Hausenloy, D.J. (2010) Inhibiting mitochondrial fission protects the heart against ischemia/reperfusion injury. *Circulation*, **121**, 2012-2022.

229. Cui, M., Tang, X., Christian, W.V., Yoon, Y. and Tieu, K. (2010) Perturbations in mitochondrial dynamics induced by human mutant PINK1 can be rescued by the mitochondrial division inhibitor mdivi-1. *J Biol Chem*, **285**, 11740-11752.

230. Brooks, C., Wei, Q., Cho, S.G. and Dong, Z. (2009) Regulation of mitochondrial dynamics in acute kidney injury in cell culture and rodent models. *J Clin Invest*, **119**, 1275-1285.

231. Puebla-Osorio, N., Lacey, D.B., Alt, F.W. and Zhu, C. (2006) Early embryonic lethality due to targeted inactivation of DNA ligase III. *Mol Cell Biol*, **26**, 3935-3941.

232. Tebbs, R.S., Flannery, M.L., Meneses, J.J., Hartmann, A., Tucker, J.D., Thompson, L.H., Cleaver, J.E. and Pedersen, R.A. (1999) Requirement for the Xrcc1 DNA base excision repair gene during early mouse development. *Dev Biol*, **208**, 513-529.

233. Simsek, D., Furda, A., Gao, Y., Artus, J., Brunet, E., Hadjantonakis, A., Van Houten, B., Shuman, S., McKinnon, P. and Jasin, M. (2011) Crucial role for DNA ligase III in mitochondria but not in Xrcc1-dependent repair. *Nature*, **471**, 245-248.

234. Rossi, M.N., Carbone, M., Mostocotto, C., Mancone, C., Tripodi, M., Maione, R. and Amati, P. (2009) Mitochondrial localization of PARP-1 requires interaction with mitofilin and is involved in the maintenance of mitochondrial DNA integrity. *J Biol Chem*, **284**, 31616-31624.

235. Leppard, J.B., Dong, Z., Mackey, Z.B. and Tomkinson, A.E. (2003) Physical and functional interaction between DNA ligase IIIalpha and poly(ADP-Ribose) polymerase 1 in DNA single-strand break repair. *Mol Cell Biol*, **23**, 5919-5927.

236. Caldecott, K.W., McKeown, C.K., Tucker, J.D., Ljungquist, S. and Thompson, L.H. (1994) An interaction between the mammalian DNA repair protein XRCC1 and DNA ligase III. *Mol Cell Biol*, **14**, 68-76.

237. Ho, C.K., Van Etten, J.L. and Shuman, S. (1997) Characterization of an ATP-dependent DNA ligase encoded by Chlorella virus PBCV-1. *J Virol*, **71**, 1931-1937.

238. Ugarte, N., Petropoulos, I. and Friguet, B. (2010) Oxidized mitochondrial protein degradation and repair in aging and oxidative stress. *Antioxid Redox Signal*, **13**, 539-549.

239. Bota, D.A. and Davies, K.J. (2002) Lon protease preferentially degrades oxidized mitochondrial aconitase by an ATP-stimulated mechanism. *Nat Cell Biol*, **4**, 674-680.

240. Geissler, A., Krimmer, T., Bomer, U., Guiard, B., Rassow, J. and Pfanner, N. (2000) Membrane potential-driven protein import into mitochondria. The sorting sequence of cytochrome b(2) modulates the deltapsi-dependence of translocation of the matrix-targeting sequence. *Mol Biol Cell*, **11**, 3977-3991.

241. Pfanner, N. and Truscott, K.N. (2002) Powering mitochondrial protein import. *Nat Struct Biol*, **9**, 234-236.

242. Friedberg, E.C., Walker, G.C., and Siede, W. (1995) *DNA Repair and Mutagenesis*. Am. Society Microbiol., Washington, D.C.

243. Abrahams, J.P., Lutter, R., Todd, R.J., van Raaij, M.J., Leslie, A.G. and Walker, J.E. (1993) Inherent asymmetry of the structure of F1-ATPase from bovine heart mitochondria at 6.5 A resolution. *EMBO J*, **12**, 1775-1780.

244. Guo, J., Zheng, L., Liu, W., Wang, X., Wang, Z., French, A.J., Kang, D., Chen, L. and Thibodeau, S.N. (2011) Frequent truncating mutation of TFAM induces mitochondrial DNA depletion and apoptotic resistance in microsatellite-unstable colorectal cancer. *Cancer Res*, **71**, 2978-2987.

245. Kang, D., Kim, S.H. and Hamasaki, N. (2007) Mitochondrial transcription factor A (TFAM): roles in maintenance of mtDNA and cellular functions. *Mitochondrion*, **7**, 39-44.

246. King, M.P. and Attardi, G. (1989) Human cells lacking mtDNA: repopulation with exogenous mitochondria by complementation. *Science*, **246**, 500-503.

247. Kukat, A., Kukat, C., Brocher, J., Schafer, I., Krohne, G., Trounce, I.A., Villani, G. and Seibel, P. (2008) Generation of rho0 cells utilizing a mitochondrially targeted restriction endonuclease and comparative analyses. *Nucleic Acids Res*, **36**, e44.

248. Martinus, R.D., Linnane, A.W. and Nagley, P. (1993) Growth of rho 0 human Namalwa cells lacking oxidative phosphorylation can be sustained by redox compounds potassium ferricyanide or coenzyme Q10 putatively acting through the plasma membrane oxidase. *Biochem Mol Biol Int*, **31**, 997-1005.

249. Scarpulla, R.C. (2006) Nuclear control of respiratory gene expression in mammalian cells. *J Cell Biochem*, **97**, 673-683.

250. Rodriguez-Enriquez, S., Juarez, O., Rodriguez-Zavala, J.S. and Moreno-Sanchez, R. (2001) Multisite control of the Crabtree effect in ascites hepatoma cells. *Eur J Biochem*, **268**, 2512-2519.

251. Warburg, O., Geissler, A.W. and Lorenz, S. (1967) On growth of cancer cells in media in which glucose is replaced by galactose. *Hoppe Seylers Z Physiol Chem*, **348**, 1686-1687.

252. Rossignol, R., Gilkerson, R., Aggeler, R., Yamagata, K., Remington, S.J. and Capaldi, R.A. (2004) Energy substrate modulates mitochondrial structure and oxidative capacity in cancer cells. *Cancer Res*, **64**, 985-993.

APPENDIX A

Reprinted from

Simsek, D., Furda, A., Gao, Y., Artus, J., Brunet, E., Hadjantonakis, A., Van Houten, B., Shuman, S., McKinnon, P., and Jasin, M. (2011) Crucial role for DNA ligase III in mitochondria but not in Xrcc1-dependent repair. *Nature*, 471, 245-248,

with permission (December 12th, 2011)

LETTER

doi:10.1038/nature09794

Crucial role for DNA ligase III in mitochondria but not in Xrcc1-dependent repair

Deniz Simsek[1,2], Amy Furda[3], Yankun Gao[4], Jérôme Artus[1], Erika Brunet[1,5,6,7], Anna-Katerina Hadjantonakis[1,2], Bennett Van Houten[3], Stewart Shuman[2,8], Peter J. McKinnon[4] & Maria Jasin[1,2]

Mammalian cells have three ATP-dependent DNA ligases, which are required for DNA replication and repair[1]. Homologues of ligase I (Lig1) and ligase IV (Lig4) are ubiquitous in Eukarya, whereas ligase III (Lig3), which has nuclear and mitochondrial forms, appears to be restricted to vertebrates. Lig3 is implicated in various DNA repair pathways with its partner protein Xrcc1 (ref. 1). Deletion of *Lig3* results in early embryonic lethality in mice, as well as apparent cellular lethality[2], which has precluded definitive characterization of Lig3 function. Here we used pre-emptive complementation to determine the viability requirement for Lig3 in mammalian cells and its requirement in DNA repair. Various forms of Lig3 were introduced stably into mouse embryonic stem (mES) cells containing a conditional allele of *Lig3* that could be deleted with Cre recombinase. With this approach, we find that the mitochondrial, but not nuclear, Lig3 is required for cellular viability. Although the catalytic function of Lig3 is required, the zinc finger (ZnF) and BRCA1 carboxy (C)-terminal-related (BRCT) domains of Lig3 are not. Remarkably, the viability requirement for Lig3 can be circumvented by targeting Lig1 to the mitochondria or expressing *Chlorella* virus DNA ligase, the minimal eukaryal nick-sealing enzyme[3], or *Escherichia coli* LigA, an NAD^+-dependent ligase[1]. *Lig3*-null cells are not sensitive to several DNA-damaging agents that sensitize Xrcc1-deficient cells[4–6]. Our results establish a role for Lig3 in mitochondria, but distinguish it from its interacting protein Xrcc1.

Biochemical and cell biological experiments implicate the nuclear Lig3–Xrcc1 complex in single-strand break repair, short patch base excision repair and nucleotide excision repair[1]. Lig3 and Xrcc1 interact through carboxy (C)-terminal BRCT domains found in each protein[7]. This interaction is important for the stability of Lig3 (ref. 7) and the recruitment of Lig3 to DNA damage foci[8]. Purified Lig3–Xrcc1 is proficient at nick sealing *in vitro*[9], and the complex associates with several other proteins involved in single-strand break repair, including Parp1 (ref. 10), aprataxin and TDP1 (ref. 1).

Lig3 also has a mitochondrial form due to an alternative translation start site, which results in a mitochondrial leader sequence (MLS)[11]. Mammals differ in this respect from budding yeast, where the Lig1 homologue, Cdc9, is the mitochondrial DNA ligase[12]. In mitochondria, Lig3 appears to act independently of Xrcc1, as Xrcc1 is not present in this organelle[13]. Disruption of the *Lig3* gene, like *Xrcc1*, results in early embryonic lethality in the mouse[2,5], and *Lig3*-null cell lines could not be established from these animals[2]. The similar timing of lethality of *Lig3* and *Xrcc1*-null embryos suggests that death could result from similar phenotypic consequences related to Lig3 nuclear functions in DNA repair. Alternatively, or in addition, the mitochondrial function of Lig3 may be critical for survival.

To determine whether *Lig3* is an essential gene because of its nuclear and/or mitochondrial function, we developed a pre-emptive complementation strategy in mES cells (Fig. 1a). A $Lig3^{KO/cKOneo+}$ cell line was constructed which contains one conditional *Lig3* allele with an intronic *Neo* selection marker and *LoxP* sites flanking exons 6 and 14 and a second allele in which these exons were already removed by Cre recombinase (Fig. 1a and Supplementary Fig. 1). These exons encode part of the DNA binding domain and the catalytic core of the protein. Cre recombinase was expressed in the $Lig3^{KO/cKOneo+}$ cells, and 145 clones were replica-plated in media with or without G418. No G418-sensitive clones (that is, $Lig3^{KO/KO}$) were obtained (Fig. 1b), consistent with the requirement for Lig3 for cellular viability. We then stably integrated transgenes expressing wild-type (WT), mitochondrial or nuclear Lig3; the nuclear (NucLig3) version lacked the MLS, and the mitochondrial (MtLig3) version contained the MLS but was mutated at the nuclear translation initiation site (M88T) (Fig. 1c and Supplementary Fig. 2). Green fluorescent protein (GFP) fusions of these proteins were also tested (Supplementary Fig. 3a).

To determine which *Lig3* transgenes allow the survival of cells deleted for endogenous *Lig3*, Cre recombinase was used to transform $Lig3^{KO/cKOneo+}$ cells to $Lig3^{KO/KO}$ cells. A large fraction of the post-Cre clones expressing WT Lig3 or MtLig3 were G418 sensitive (34–50%), whereas no G418-sensitive clones were obtained with NucLig3 (Fig. 1b and Supplementary Fig. 4). We confirmed that G418-sensitive cells were $Lig3^{KO/KO}$ (Fig. 1a) and that endogenous Lig3 was no longer present, with the only Lig3 present in the cells expressed from the transgene (Fig. 1d). Thus, cellular viability requires mitochondrial Lig3. To determine whether DNA ligase activity was essential for cell survival, we introduced a K508V mutation that abolishes ligase adenylylation and nick-sealing[1] into MtLig3. No G418-sensitive clones were derived from four independent transgenic cell lines (Fig. 1b), demonstrating that the requirement for mitochondrial Lig3 depends on its ligase activity.

BRCT domains are frequently involved in protein–protein interactions, and the BRCT domain of Lig3 is known to interact with Xrcc1 (ref. 7). However, as Xrcc1 is not found in mitochondria[13], the role of the BRCT domain for mitochondrial function of Lig3 is uncertain. Loss of the BRCT domain had no effect on the presence of Lig3 in mitochondria (Lig3-ΔBRCT and MtLig3-ΔBRCT; Supplementary Fig. 3a and data not shown). $Lig3^{KO/KO}$ clones expressing Lig3-ΔBRCT or MtLig3-ΔBRCT (Fig. 2a) were recovered as a substantial fraction of clones (39–49%; Fig. 2b), indicating that the BRCT domain is not required for viability. Thus, MtLig3 does not have a partner protein bound to its BRCT domain that is essential for its function.

A unique feature of Lig3 compared with the other mammalian DNA ligases is a ZnF at its amino (N) terminus. The Lig3 ZnF interacts with Parp1 (ref. 10), and this interaction is reported to be important for the association of Lig3 with mitochondrial DNA (mtDNA)[14]. Biochemical studies have shown that the ZnF promotes DNA nick recognition[15] and

[1]Developmental Biology Program, Memorial Sloan-Kettering Cancer Center, New York, New York 10065, USA. [2]Weill Cornell Graduate School of Medical Sciences, New York, New York 10065, USA. [3]Department of Pharmacology and Chemical Biology, University of Pittsburgh School of Medicine and The University of Pittsburgh Cancer Institute, Hillman Cancer Center, Pittsburgh, Pennsylvania 15213, USA. [4]Department of Genetics and Tumor Cell Biology, St Jude Children's Research Hospital, Memphis, Tennessee 38105, USA. [5]Museum National d'Histoire Naturelle, 43 rue Cuvier, F-75005 Paris, France. [6]CNRS, UMR7196, 43 rue Cuvier, F-75005 Paris, France. [7]Inserm, U565, 43 rue Cuvier, F-75005 Paris, France. [8]Molecular Biology Program, Memorial Sloan-Kettering Cancer Center, New York, New York 10065, USA.

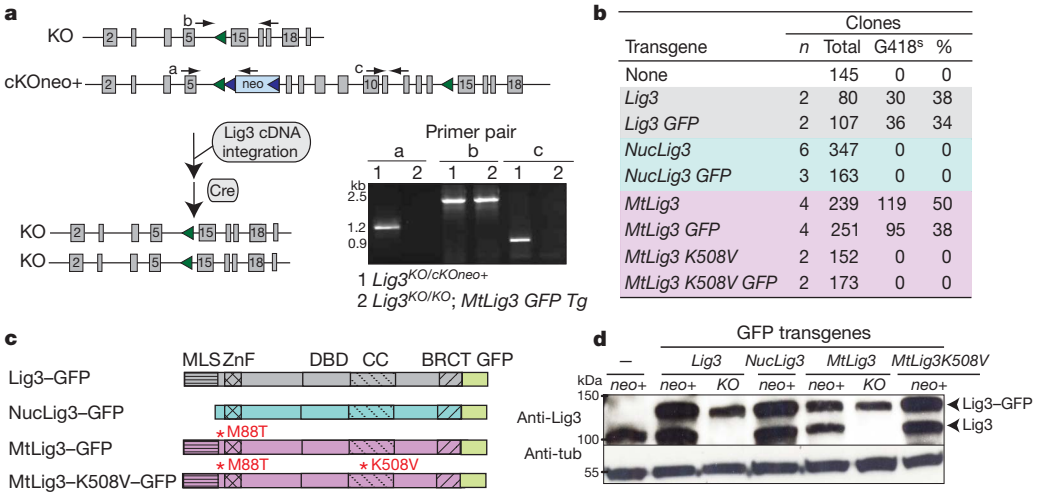

Transgene	Clones *n*	Total	G418^S	%
None		145	0	0
Lig3	2	80	30	38
Lig3 GFP	2	107	36	34
NucLig3	6	347	0	0
NucLig3 GFP	3	163	0	0
MtLig3	4	239	119	50
MtLig3 GFP	4	251	95	38
MtLig3 K508V	2	152	0	0
MtLig3 K508V GFP	2	173	0	0

Figure 1 | Mitochondrial Lig3 activity is critical for cellular viability. a, Pre-emptive complementation strategy for *Lig3* deletion. *Lig3*$^{KO/KO}$ clones were identified by their lack of growth in G418 (*neo*−). PCR confirmed the genotype, as indicated. KO, knockout; Tg, transgene. **b**, Mitochondrial Lig3 activity is critical for cellular viability. *n*, number of independently derived Lig3 transgenic cell lines analysed; Total, total number of post-Cre colonies analysed by replica plating with and without G418; G418^S, G418 sensitive; %, ratio of G418^S to Total. **c**, Lig3 proteins tested for pre-emptive complementation. DBD, DNA-binding domain; CC, catalytic core; *M88T, mutation of the nuclear translation initiation site. **d**, Western blot analysis showing the loss of endogenous Lig3 in *Lig3*$^{KO/KO}$ clones stably expressing GFP-tagged Lig3 or MtLig3. Lig3 is 105 kDa, whereas the GFP fusions are approximately 135 kDa. *neo*+, *Lig3*$^{KO/cKOneo+}$; *KO*, *Lig3*$^{KO/KO}$; α-tub, α-tubulin.

intermolecular ligation[16]. Nonetheless, *Lig3*$^{KO/KO}$ clones expressing Lig3-ΔZnF or MtLig3-ΔZnF (Fig. 2a) were efficiently recovered after Cre expression (37–38%; Fig. 2b).

Our results reveal that the catalytic activity of Lig3 is critical for cell survival, but that the ZnF and BRCT domains, which interact with various proteins, are dispensable, raising the question whether Lig3 itself is critical for mitochondrial function, or whether another DNA ligase would substitute. As the Lig1 homologue in yeast provides mitochondrial ligase function[12], we provided an MLS to murine Lig1 (Fig. 2a). GFP-tagged MtLig1, but not WT Lig1, was localized to mitochondria (Supplementary Fig. 3c), as expected. Stable *Lig3*$^{KO/cKOneo+}$ cell lines expressing MtLig1, but not WT Lig1, could be efficiently converted to *Lig3*$^{KO/KO}$ (35%; Fig. 2b). MtLig1 *Lig3*$^{KO/KO}$ clones were devoid of Lig3, and expressed instead a larger Lig1 protein due to the GFP tag (Fig. 3a). Thus, targeting Lig1 to mitochondria circumvents the viability requirement for Lig3, allowing the creation of *Lig3*-null cells. In this way, the DNA ligase repertoire of mammalian cells is converted to that of yeast.

Given that ZnF and BRCT-truncated forms of Lig3 and MtLig1 could rescue *Lig3*$^{KO/KO}$ cells, we investigated their proficiency in mtDNA maintenance and repair. The mtDNA copy number was maintained as well (or better) in these cell lines than in WT Lig3-expressing cells (Fig. 2c), indicating that cells expressing these altered ligases are competent to replicate their mtDNA during continued passage. A long-range quantitative PCR (qPCR) assay[17] was performed

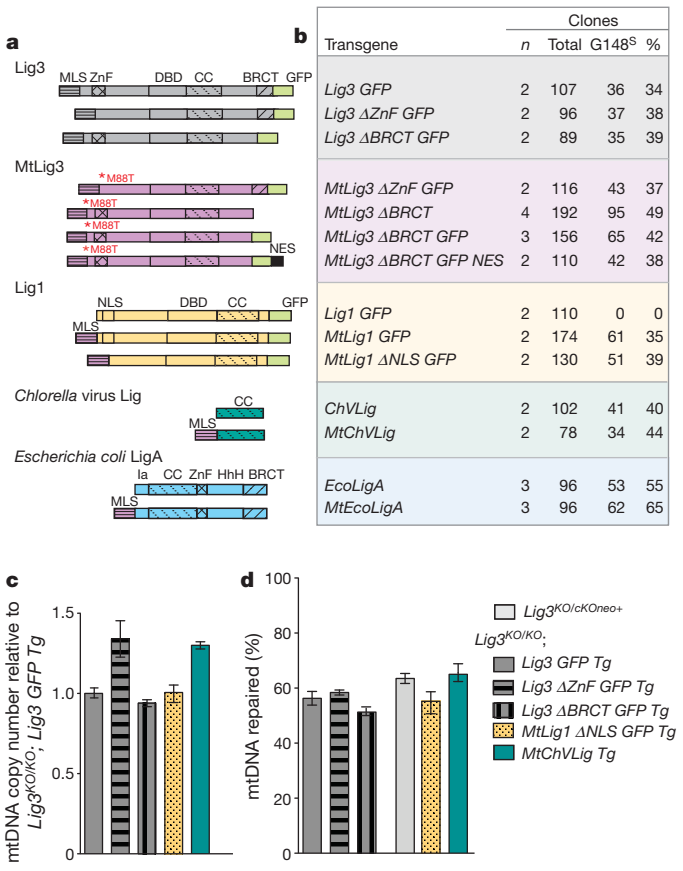

Transgene	Clones *n*	Total	G148^S	%
Lig3 GFP	2	107	36	34
Lig3 ΔZnF GFP	2	96	37	38
Lig3 ΔBRCT GFP	2	89	35	39
MtLig3 ΔZnF GFP	2	116	43	37
MtLig3 ΔBRCT	4	192	95	49
MtLig3 ΔBRCT GFP	3	156	65	42
MtLig3 ΔBRCT GFP NES	2	110	42	38
Lig1 GFP	2	110	0	0
MtLig1 GFP	2	174	61	35
MtLig1 ΔNLS GFP	2	130	51	39
ChVLig	2	102	41	40
MtChVLig	2	78	34	44
EcoLigA	3	96	53	55
MtEcoLigA	3	96	62	65

Figure 2 | Mitochondrial DNA ligase activity can be provided by a variety of DNA ligases. a, DNA ligases tested for pre-emptive complementation of *Lig3*$^{KO/KO}$ cells. ΔZnF, deletion of Lig3 amino acids 89–258; ΔBRCT, deletion of Lig3 amino acids 934–1009; ΔNLS, deletion of Lig1 amino acids 135–147; NES, nuclear export signal from MAPKK[21]; Mt, presence of Lig3 MLS; NLS, nuclear localization signal; HhH, helix–hairpin–helix. **b**, Mitochondrial DNA ligase activity can be provided by a variety of DNA ligases. ChVLig and EcoLigA presumably enter mitochondria without the requirement for an MLS. **c**, Cells expressing exogenous DNA ligases are competent to replicate and maintain mtDNA. mtDNA copy number was quantified by qPCR by amplifying a 117 base pair (bp) fragment from mtDNA. Values are presented relative to levels of mtDNA in *Lig3*$^{KO/KO}$; *Lig3 GFP Tg* cells. Data represent the mean of two biological repeats each determined twice by qPCR ± s.e.m. **d**, Cells expressing exogenous DNA ligases showed similar capacities for mtDNA repair after oxidative damage. Cells were treated with 175 μM hydrogen peroxide for 15 min and allowed to recover for 1.5 h. To measure repair, a 10-kb mtDNA fragment was amplified after damage and quantified by qPCR. Values were normalized to the amplification of a 117-bp mtDNA fragment. Percentage repair is 1 minus the amount of damage remaining after 1.5 h recovery divided by the initial damage. There was no significant difference between cell lines expressing WT Lig3 (parental cells and transgene-rescued cells) and the other ligase forms. For cells expressing MitLig1-ΔNLS and MtChVLig, two transgenic cell lines were analysed. Data represent the mean of two to four determinations on multiple clones with each qPCR performed twice ± s.e.m.

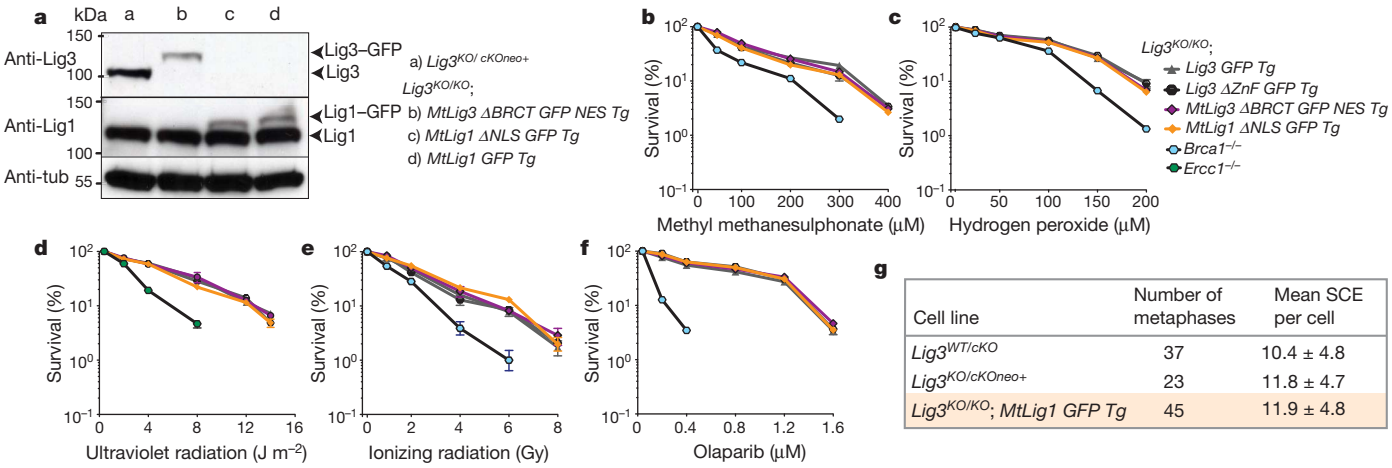

g

Cell line	Number of metaphases	Mean SCE per cell
Lig3$^{WT/cKO}$	37	10.4 ± 4.8
Lig3$^{KO/cKOneo+}$	23	11.8 ± 4.7
Lig3$^{KO/KO}$; *MtLig1 GFP Tg*	45	11.9 ± 4.8

Figure 3 | Loss of Lig3 is not associated with sensitivity to several DNA-damaging agents or with increased SCE. a, Western blot analysis showing the loss of endogenous Lig3 protein in *Lig3*$^{KO/KO}$ cells with the indicated transgenes. **b**–**f**, Sensitivity of *Lig3*$^{KO/KO}$ cell lines to the indicated DNA-damaging agents was measured using colony formation assays. *Brca1*$^{-/-}$ and *Ercc1*$^{-/-}$ cells are only shown on graphs when they are sensitive. For each cell line and agent, $n = 4$ and error bars show s.e.m.; error bars in some cases are smaller than the symbol. **g**, SCE analysis. The range of SCEs was between 5 and 21 per metaphase for each cell line. For cells expressing MtLig1, two transgenic cell lines were analysed. The differences between the cell lines are not significant using a two-tailed unpaired *t*-test. Values are presented with one s.d. from the mean.

to assess the mitochondrial base excision repair capacity of these cells in response to oxidative damage, and these altered ligases were similarly proficient in repairing mtDNA lesions compared with WT Lig3-expressing cells (Fig. 2d).

At 298 amino acids, *Chlorella* virus DNA ligase (ChVLig) is the smallest eukaryal ligase known, consisting solely of a catalytic core[3]. We expressed ChVLig and a modified form containing an MLS, MtChVLig (Fig. 2a), and found that expression of either allowed deletion of *Lig3* from the mouse genome (Fig. 2b). It is conceivable that ChVLig contains an internal sequence that allows translocation into mitochondria[18]. Thus, a minimal ATP-dependent ligase, devoid of auxiliary domains, rescues the survival of *Lig3*-null mammalian cells. Further, Lig3-null cells rescued by MtChVLig were proficient at mtDNA maintenance (Fig. 2c) and repair (Fig. 2d).

Whereas ATP-dependent ligases are widespread, ligases that use NAD^+ as a cofactor are usually restricted to bacteria[1]. *E. coli* DNA ligase, LigA, is NAD^+ dependent and has a distinctive domain organization compared with mammalian ligases[1]. LigA and a modified form with an MLS (Fig. 2a) were expressed from transgenes, and like ChVLig, both forms were found to allow the survival of Lig3-null cells (Fig. 2b). Hence, there is no essential functional distinction between NAD^+ and ATP-dependent ligases in the mammalian mitochondria, akin to swaps of NAD^+ and ATP-dependent ligases performed in bacteria[19] and yeast[20].

We demonstrated that nuclear Lig3 is not required for cell survival, as MtLig1 *Lig3*$^{KO/KO}$ cells are null for *Lig3*. To impair nuclear localization of MtLig1, we removed the Lig1 nuclear localization signal, creating MtLig1-ΔNLS *Lig3*$^{KO/KO}$ cells (Fig. 2a, b and Supplementary Fig. 3c). MtLig1-ΔNLS, like MtLig1, was expressed at a substantially lower level than endogenous Lig1 (Fig. 3a). As a complementary approach, we also created *Lig3*$^{KO/KO}$ cells expressing MtLig3-ΔBRCT-NES, whose interaction with Xrcc1 is abrogated and which is excluded from the nucleus by addition of a potent nuclear export signal (NES)[21] (Figs 2a, b and 3a and Supplementary Fig. 3b).

To assess the nuclear role of Lig3, we tested the sensitivity of *Lig3*-null (*Lig3*$^{KO/KO}$; MtLig1-ΔNLS) and nuclear Lig3-deficient (*Lig3*$^{KO/KO}$; MtLig3-ΔBRCT-NES) cells to a variety of DNA-damaging agents. Xrcc1-deficient cells are highly sensitive to alkylating agents like methyl methanesulphonate[4–6]. If the interaction of Xrcc1 with Lig3 is relevant to base excision repair, cells without nuclear Lig3 would also be expected to be sensitive to methyl methanesulphonate; however, we found that these cells were no more sensitive than transgenic cells expressing WT Lig3 (Fig. 3b) or the parental cells (Supplementary Fig. 5). Xrcc1-deficient cells are also sensitive to agents that produce DNA single- and double-strand breaks, including hydrogen peroxide and ionizing radiation[4–6], and to ultraviolet radiation[22]. By contrast, we found that cells without nuclear Lig3 were not any more sensitive to these agents than control cells (Fig. 3c–e and Supplementary Fig. 5). Thus, Lig3 appears to be dispensable for nuclear DNA damage repair that requires Xrcc1. Finally, we tested sensitivity to Parp inhibition, which causes the accumulation of single-strand breaks[23], and found that nuclear Lig3 was also not required for resistance of cells to Parp inhibition (Fig. 3f).

As the ZnF domain of Lig3 has been reported to be critical for its intermolecular ligation activity[16], we also investigated whether deletion of this domain in the context of an otherwise WT Lig3 would impair resistance of cells to ionizing radiation. As with the other mutants, Lig3-ΔZnF *Lig3*$^{KO/KO}$ cells were no more sensitive than control cells (Fig. 3e).

Xrcc1-deficient cells are notable for their high rate of spontaneous sister-chromatid exchange (SCE): both mouse and hamster Xrcc1 mutants have approximately tenfold higher SCE levels than control cells[4,5]. We examined spontaneous SCEs in MtLig1 *Lig3*$^{KO/KO}$ cells and found levels similar to control cells (Fig. 3g). Thus, the high level of SCEs found with Xrcc1 deficiency is not recapitulated with Lig3 deficiency.

The lack of Lig3 in many model organisms has limited their use to study its function. In mouse, disruption of any of the DNA ligase genes leads to embryonic death, but the most severe phenotype occurs with Lig3 disruption[2,24,25]. Lig1 has been considered to be the replicative ligase[1,26], but the earlier death associated with Lig3 disruption, together with the inability to obtain viable Lig3-null cells, left open the possibility that Lig3 could have a critical role in nuclear DNA metabolism. The generation of viable and healthy *Lig3*-null cells by providing a mitochondrial ligase conclusively rules out an essential role for Lig3 in the nucleus.

The well-documented interaction between Lig3 and Xrcc1 had suggested that Lig3 would be critical for the same nuclear DNA repair pathways as Xrcc1, similar to the Lig4–Xrcc4 complex in DSB repair[1]. However, the lack of sensitivity of Lig3-null cells to the spectrum of DNA-damaging agents that sensitize Xrcc1-deficient cells, as shown here in proliferating cells and in the accompanying paper in quiescent cells[27], together with a normal SCE frequency, provides strong evidence that Lig3 is not required for Xrcc1-dependent nuclear DNA repair, pointing instead to a role for Lig1.

Our results demonstrate instead that *Lig3* is an essential gene because of its requirement in mitochondria. However, Lig3 can be replaced in mitochondria with Lig1, the mitochondrial ligase in lower eukaryotes, with an algal viral ligase consisting solely of a catalytic core, and even the NAD^+-dependent *E. coli* LigA. Thus, these results attest to the requirement for a functional DNA ligase, which trumps even cofactor specificity. Why vertebrates developed a requirement for Lig3 is uncertain, but given our results, the additional domains found in Lig3 do not appear to be essential for mitochondrial function, including mtDNA maintenance or repair of oxidative damage. These results emphasize a surprising plasticity that mammalian cells have in their mitochondrial DNA ligase requirement.

METHODS SUMMARY

Cell culture. To construct stable cell lines expressing various DNA ligases, 5×10^6 $Lig3^{KO/cKOneo+}$ cells were electroporated with 12 μg ligase expression vector at 800 V, 3 μF. Hygromycin-resistant clones were picked after incubation for 10 days in 150 μg μl^{-1} hygromycin. Initial screening for exogenous ligase expression was performed by PCR with reverse transcription (RT–PCR) using specific primers, followed by western blotting. For deletion of the endogenous *Lig3* allele, 5×10^6 cells were electroporated with 5 μg Cre recombinase vector at 250 V, 950 μF. Cells were plated based on a serial dilution. After 7 days, colonies were picked and expanded, and then replica plated into two 96-well plates. One plate was cultured with 200 μg μl^{-1} G418, whereas the other plate was cultured in normal media. Clones that did not grow in G418, but grew in normal media, have converted the $Lig3^{cKOneo+}$ allele to a $Lig3^{KO}$ allele. The genotype of these clones was confirmed by PCR.

Western blotting. Whole-cell extracts were prepared with Nonidet-P40 buffer and were run on a 7.5% (w/v) Tris-HCl SDS page gel, blotted and then probed with Lig3 antibody clone 7 (BD Transduction Labs), which recognizes both the human and mouse Lig3 proteins, or Lig1 antibody N-13 (Santa Cruz). α-Tubulin (Sigma) was used as a loading control.

Full Methods and any associated references are available in the online version of the paper at www.nature.com/nature.

Received 29 April 2010; accepted 5 January 2011.

1. Ellenberger, T. & Tomkinson, A. E. Eukaryotic DNA ligases: structural and functional insights. *Annu. Rev. Biochem.* **77,** 313–338 (2008).
2. Puebla-Osorio, N., Lacey, D. B., Alt, F. W. & Zhu, C. Early embryonic lethality due to targeted inactivation of DNA ligase III. *Mol. Cell. Biol.* **26,** 3935–3941 (2006).
3. Ho, C. K., Van Etten, J. L. & Shuman, S. Characterization of an ATP-dependent DNA ligase encoded by *Chlorella* virus PBCV-1. *J. Virol.* **71,** 1931–1937 (1997).
4. Thompson, L. H., Brookman, K. W., Jones, N. J., Allen, S. A. & Carrano, A. V. Molecular cloning of the human XRCC1 gene, which corrects defective DNA strand break repair and sister chromatid exchange. *Mol. Cell. Biol.* **10,** 6160–6171 (1990).
5. Tebbs, R. S. *et al.* Requirement for the Xrcc1 DNA base excision repair gene during early mouse development. *Dev. Biol.* **208,** 513–529 (1999).
6. Lee, Y. *et al.* The genesis of cerebellar interneurons and the prevention of neural DNA damage require XRCC1. *Nature Neurosci.* **12,** 973–980 (2009).
7. Caldecott, K. W., McKeown, C. K., Tucker, J. D., Ljungquist, S. & Thompson, L. H. An interaction between the mammalian DNA repair protein XRCC1 and DNA ligase III. *Mol. Cell. Biol.* **14,** 68–76 (1994).
8. Mortusewicz, O., Rothbauer, U., Cardoso, M. C. & Leonhardt, H. Differential recruitment of DNA ligase I and III to DNA repair sites. *Nucleic Acids Res.* **34,** 3523–3532 (2006).
9. Chen, X. *et al.* Distinct kinetics of human DNA ligases I, IIIα, IIIβ, and IV reveal direct DNA sensing ability and differential physiological functions in DNA repair. *DNA Repair (Amst.)* **8,** 961–968 (2009).
10. Leppard, J. B., Dong, Z., Mackey, Z. B. & Tomkinson, A. E. Physical and functional interaction between DNA ligase IIIα and poly(ADP-ribose) polymerase 1 in DNA single-strand break repair. *Mol. Cell. Biol.* **23,** 5919–5927 (2003).
11. Lakshmipathy, U. & Campbell, C. The human DNA ligase III gene encodes nuclear and mitochondrial proteins. *Mol. Cell. Biol.* **19,** 3869–3876 (1999).
12. Willer, M., Rainey, M., Pullen, T. & Stirling, C. J. The yeast CDC9 gene encodes both a nuclear and a mitochondrial form of DNA ligase I. *Curr. Biol.* **9,** 1085–1094 (1999).
13. Lakshmipathy, U. & Campbell, C. Mitochondrial DNA ligase III function is independent of Xrcc1. *Nucleic Acids Res.* **28,** 3880–3886 (2000).
14. Rossi, M. N. *et al.* Mitochondrial localization of PARP-1 requires interaction with mitofilin and is involved in the maintenance of mitochondrial DNA integrity. *J. Biol. Chem.* **284,** 31616–31624 (2009).
15. Mackey, Z. B. *et al.* DNA ligase III is recruited to DNA strand breaks by a zinc finger motif homologous to that of poly(ADP-ribose) polymerase. Identification of two functionally distinct DNA binding regions within DNA ligase III. *J. Biol. Chem.* **274,** 21679–21687 (1999).
16. Cotner-Gohara, E., Kim, I. K., Tomkinson, A. E. & Ellenberger, T. Two DNA-binding and nick recognition modules in human DNA ligase III. *J. Biol. Chem.* **283,** 10764–10772 (2008).
17. Santos, J. H., Meyer, J. N., Mandavilli, B. S. & Van Houten, B. Quantitative PCR-based measurement of nuclear and mitochondrial DNA damage and repair in mammalian cells. *Methods Mol. Biol.* **314,** 183–199 (2006).
18. Neupert, W. & Herrmann, J. M. Translocation of proteins into mitochondria. *Annu. Rev. Biochem.* **76,** 723–749 (2007).
19. Park, U. E., Olivera, B. M., Hughes, K. T., Roth, J. R. & Hillyard, D. R. DNA ligase and the pyridine nucleotide cycle in *Salmonella typhimurium*. *J. Bacteriol.* **171,** 2173–2180 (1989).
20. Sriskanda, V., Schwer, B., Ho, C. K. & Shuman, S. Mutational analysis of *Escherichia coli* DNA ligase identifies amino acids required for nick-ligation *in vitro* and for *in vivo* complementation of the growth of yeast cells deleted for CDC9 and LIG4. *Nucleic Acids Res.* **27,** 3953–3963 (1999).
21. Henderson, B. R. & Eleftheriou, A. A comparison of the activity, sequence specificity, and CRM1-dependence of different nuclear export signals. *Exp. Cell Res.* **256,** 213–224 (2000).
22. Moser, J. *et al.* Sealing of chromosomal DNA nicks during nucleotide excision repair requires XRCC1 and DNA ligase IIIα in a cell-cycle-specific manner. *Mol. Cell* **27,** 311–323 (2007).
23. Farmer, H. *et al.* Targeting the DNA repair defect in BRCA mutant cells as a therapeutic strategy. *Nature* **434,** 917–921 (2005).
24. Bentley, D. *et al.* DNA ligase I is required for fetal liver erythropoiesis but is not essential for mammalian cell viability. *Nature Genet.* **13,** 489–491 (1996).
25. Frank, K. M. *et al.* Late embryonic lethality and impaired V(D)J recombination in mice lacking DNA ligase IV. *Nature* **396,** 173–177 (1998).
26. Barnes, D. E., Tomkinson, A. E., Lehmann, A. R., Webster, A. D. & Lindahl, T. Mutations in the DNA ligase I gene of an individual with immunodeficiencies and cellular hypersensitivity to DNA-damaging agents. *Cell* **69,** 495–503 (1992).
27. Gao, Y. *et al.* DNA ligase III is critical for mtDNA integrity but not Xrcc1-mediated nuclear DNA repair. *Nature* doi:10.1038/nature09773 (this issue).

Supplementary Information is linked to the online version of the paper at www.nature.com/nature.

Acknowledgements We thank K. Caldecott for the gift of the Lig3 expression vector, and M. Sanz for initial assistance with the SCE analysis. We also thank the members of Jasin laboratory, especially Y. Akamatsu, J. LaRocque, E. Kass and F. Vanoli, for discussions. This work was supported by PA CURE (to B.V.H.) and by National Institutes of Health grants ES019566 (to B.V.H.), NS37956 and CA21765 (to P.J.M.), and GM54668 (to M.J.).

Author Contributions D.S. performed most of the experiments. D.S. and M.J. designed the research and wrote the paper. A.F. performed the long-range qPCR assays to investigate mitochondrial BER and mitochondrial DNA maintenance, and with B.V.H. analysed the data. Y.G. and P.J.M. designed the initial *Lig3* targeting scheme and generated the $Lig3^{wt/cKO}$ embryonic stem cells. J.A. and A.-K.H. acquired confocal images for GFP-tagged proteins. E.B. contributed technical assistance and preparation of the manuscript. S.S. contributed discussions, provided reagents and shared unpublished data.

Author Information Reprints and permissions information is available at www.nature.com/reprints. The authors declare no competing financial interests. Readers are welcome to comment on the online version of this article at www.nature.com/nature. Correspondence and requests for materials should be addressed to M.J. (m-jasin@ski.mskcc.org).

METHODS

DNA constructs. A vector containing WT human Lig3 complementary DNA (cDNA) (with both mitochondrial and nuclear translation initiation sites), a gift from K.W. Caldecott, was digested with NheI and XbaI and subcloned into the NheI site of pCAGGS. As the cDNA contained a 51-bp linker located before the nuclear translation initiation site, it was modified by site-directed mutagenesis to remove the linker, with the primers 5′-GTGGCCCCTGTGAGATGGCTGAGCA ACG-3′ and 5′-CGTTGCTCAGCCATCTCACAGGGGCCAC-3′ to restore an unmodified Lig3 sequence, creating pCAGGS-Lig3. A Pgk-hygromycin resistance gene was inserted at the PsiI site to create pCAGGS-Lig3-hyg. MtLig3 was generated by using site-directed mutagenesis to generate an M88T mutation in pCAGGS-Lig3-hyg using the primers 5′-GAGAGGCCCCTGTGAGACCGCTGAGCA-3′ and 5′-GAGAGGATCCCTAGCAGGGAGCTACCAGTCTC-3′. For NucLig3, amino acids 1–87 were deleted by introducing NotI and BamHI sites into pCAGGS-Lig3-hyg by PCR using the primers 5′-GCATGCGGCCGCCTGTGAG ATGGCTGAGCAACGGT-3′, 5′-GGATGGATCCCTAGCAGGGAGCTACCA GTC-3′. For the ΔBRCT mutation, amino acids 934–1009 were deleted by introducing NheI and MfeI sites by PCR using the primers 5′-GGCCGCTAGCG GGCAGCTATATGTCTTTGGCTTTCAAGAT-3′ and 5′-GAGACAATTGTTA CTATACCTTTGTTTGGCACAGCGTC-3′. The ΔZnF mutation was generated by deleting amino acids 89–258 using site-directed mutagenesis with primers 5′-TGGCCCCTGTGAGATGAAGGACTGTCTGCTAC-3′ and 5′-GTAGCAG ACAGTCCTTCATCTCACAGGGGCCA-3′. For GFP tagging of the Mt-tagged constructs, SacII and AgeI sites were introduced and stop codons of the full-length or ΔBRCT proteins were converted into alanine codons by PCR and cloned in frame into SacII and AgeI sites of pEGFP-N1 (Clontech). PCR primers for full length were 5′-ACGGTACCGCGGCAGCTATATGTCTTTGG-3′and 5′-ACGG TACCGCGGCAGCTATATGTCTTTGG-3′, and for ΔBRCT were 5′-ACGGTAC CGCGGCAGCTATATGTCTTTGG-3′ and 5′-GGCGACCGGTGGTACCTTT GTTTGGCACAGCG-3′.

For other constructs with GFP fusions (NucLig3, Lig3, ΔZnF and K508V), plasmids were digested with PmlI and ligated into the vector backbone of MtLig3-GFP using the same enzyme. The MAPKK NES[21] was fused to the C terminus of GFP by PCR using the primers 5′-GCCCCCTCAGCCAGTACC AAGAA-3′ and 5′-GGCCAATTGGCCTTATTACTGCTGCTCGTCCAGCTC CAGCTCCTCCAGCTTCTTTTGGAGGTCCACGAGATTCTTGTACAGCTCG TCCAT-3′. Mouse Lig1 cDNA (Invitrogen) was amplified with primers introducing KpnI and AgeI sites and changing a stop codon into an alanine codon; this fragment was cloned in frame into the KpnI and AgeI sites of pEGFP-N1. The Lig3 MLS was amplified with the primers 5′-GGCGAATTCTATATGTCTTTGGC TTTCAAGATCTTCTTTC-3′and 5′-ATTGGTACCCCTCACAGGGGCCACTG CAG-3′ and cloned into the EcoRI and KpnI sites of Lig1-GFP-hyg vector. The *Chlorella* virus DNA ligase coding region was amplified with ChV-NheI and ChV-MfeI primers and cloned into the NheI and MfeI sites of the pCAGGS-Lig1-Hyg vector. ChV-NheI: 5′-GCCGCTAGCACCATGGCAATCACAAAGCCATT-3′; ChV-MfeI: 5′-GCCCAATTGTTAACGGTCTTCCTCGTGAC-3′. The *E. coli* DNA ligase coding region was amplified with LigA-NheI and LigA-MfeI primers and cloned into the NheI and MfeI sites of the pCAGGS-Lig1-Hyg vector. LigA-NheI: 5′-GCCGCTAGCACCATGGAATCAATCGAACAACAA-3′; LigA-MfeI: 5′-GCCCAATTGTCAGCTACCCAGCAAACG-3′.

RT–PCR. Hygromycin-resistant clones were screened by RT–PCR using primers specific to human Lig3. A primer pair was used with the forward primer to the pCAGGS backbone and the reverse primer to exon 3 of human Lig3, resulting in a size difference for mitochondrial and nuclear forms (Supplementary Fig. 3): pCAGRTfw 5′-CAACGTGCTGGTTATTGTGC-3′, hLig3Rv 5′-ACAGCTTTC TTCTTTGGTGTACCT-3′. A similar strategy was used for Lig1, with primers pCAGRTfw and Lig1RT_RV (5′-ACCGCTGAGCAACGGTTCT-3′), for *Chlorella* virus DNA ligase, with primers pCAGRTfw and chlRTPCR-RV1 (5′-CA GCACTTGTGGTGTCTTGAA-3′) and for *E. coli* DNA ligase, with primers pCAGRTfw and LigARTPCR-RV1 (5′-CCTGCACACGTTTGTTGAAA-3′). RNA was isolated using RNeasy Mini Kit (Qiagen) and cDNA was generated by the SuperScript III First-strand Synthesis system (Invitrogen).

Genotyping. Genomic DNA was isolated using the Genelute Mammalian Genomic DNA Miniprep Kit (Sigma). Each primer was named for the location on the genomic DNA (for example, Int5-6Fw means that the primer is at the intron between exons 5 and 6). Primer pairs used for genotyping were as follows: Exon 5Fw and Neo2Rv (primer pair 'a' in Fig. 1a), 5′-GGCTTTCACGGTG ATGTGTA-3′ and 5′-TCTGGATTCATCGACTGTGG-3′, using an annealing temperature of 62 °C; Int5-6Fw and Int16-17Rv (primer pair 'b' in Fig. 1a), 5′-CGGGTGTAGGGAGGTCATAA-3′, 5′-GAAGGAAGAGGTCTCCAGCA-3′, using an annealing temperature of 62 °C; Int10-11Fw and Int11-12Rv (primer pair 'c' in Fig. 1a), 5′-CACTAAACGTGGCAGAGCAA-3′, 5′-CCAGCCCA GACTACAGCTTC-3′, using an annealing temperature of 62 °C; Int5-6Fw2 and Int5-6Rv (Supplementary Fig. 1d), 5′-GCCAAGTGTGAATATACAGC-3′ and 5′-CAGGGAGCTTGGGACGGATGC-3′, using an annealing temperature of 64 °C; Int5-6 and Int16-17(Supplementary Fig. 1d), 5′-CGGGTGTAGGGA GGTCATAA-3′ and 5′-GAAGGAAGAGGTCTCCAGCA-3′, using an annealing temperature of 64 °C.

Microscopy. The subcellular localization of the various GFP fusion constructs was checked by Mitotracker Red CMXRos (Invitrogen) and Hoechst 33342 (Invitrogen) to stain mitochondria and nucleus, respectively. DNA constructs were transiently transfected with Lipofectamine 2000 (Invitrogen). After incubating cells with Opti-MEM (Invitrogen) containing 10 nM Mitotracker Red CMXRos and 2.5 μM Hoechst 33342 for 20 min at 37 °C, cells were monitored with a Zeiss LSM 510 META laser scanning microscope.

qPCR mtDNA repair assay. One million mES cells with the indicated genotypes were plated on 6-cm^2 plates. After 16 h, cells were cultured with 6.25 ml, 175 μM hydrogen peroxide for 15 min and then cultured with conditioned medium for 1.5 h. mtDNA copy number and mtDNA repair were determined by a long-range qPCR assay[17]. Basically, DNA was extracted from pellets of 1×10^6 cells with the DNeasy Blood and Tissue kit (Qiagen) by a QIAcube automated DNA extraction robot (Qiagen). Initial DNA concentration was measured using PicoGreen double-stranded DNA binding agent (Invitrogen) and a DNA standard curve. Total mouse genomic DNA at an approximate final concentration of 4.5 ng μl^{-1} was then digested with with HaeII (New England Biosciences) for 1 h at 37 °C in a reaction mixture containing1× NEBuffer 4, 1× BSA and 20 U undiluted HaeII enzyme. HaeII linearizes the mouse mtDNA by digesting once (2604) near the D-loop region. Linearization of mitochondrial DNA ensures efficient amplification and allows accurate determination of mtDNA copy number. After digestion, DNA concentration was measured with PicoGreen and an appropriate volume was directly removed from the digest to use for qPCR, with less than 5% variability in DNA concentration between samples.

The qPCR reaction was performed with the GeneAmp XL PCR kit (Applied Biosystems) as follows: 10–15 ng total DNA, in a reaction mix of 50 μl, with 1× buffer, 100 ng μl^{-1} BSA, dNTPs at 200 μM for each nucleotide, 1.2 and 1.1 mM $MgO(Ac)_2$ for the long and short fragments, respectively, and 20 pmol for each of two primers. Primer pairs for a 10-kb fragment of mtDNA (long) and for a 117-bp fragment of mtDNA (short) were used for calculating mtDNA damage and mtDNA copy number, respectively. Primer sequences are as described previously[17]. DNA polymerase was added at a concentration of 1 U per reaction. A 50% control and a 'no template' blank were used to ensure that the assay was within quantitative range and free of contamination, respectively. PCR products were quantified using fluorescence-blank measurements from the PicoGreen double-stranded DNA binding agent. PCR products from the long fragment were normalized to the short fragment to account for the effect of differing mtDNA copy number on amplification of the long fragment.

SCE. Five million mES cells with the indicated genotypes were plated on 10-cm^2 plates. After 24 h, cells were cultured with 10 μM bromodeoxyuridine for 20 h (approximately two cell-cycle periods) and pulsed with 0.03 μg ml^{-1} colcemid for the final 30 min. The cells were collected by centrifugation and exposed to 0.075 mM KCl hypotonic solution for 30 min at 25 °C. The cells were washed twice with the fixative (methanol:acetic acid = 3:1) and suspended in a small volume of the fixative. The cell suspension was dropped onto ice-cold glass slides and air-dried at 60 °C for 2 h. Two days later, slides were incubated with 1 μg ml^{-1} Hoechst 33258 in Sorensen's phosphate buffer (38 mM KH_2PO_4, 60 mM Na_2HPO_4, pH 7.0) for 10 min, rinsed with 2× SSC buffer (300 mM NaCl, 30 mM $Na_3C_6H_5O_7$, pH 7.0) and then overlaid with coverslips. Slides were exposed to black light ($\lambda = 352$ nm) at a distance of 1 cm for 20 min. After removal of coverslips, the slides were incubated in 2× SSC at 60 °C for 2 h and then stained with 4% (v/v) Giemsa solution in Sorensen's buffer for 10 min, rinsed in water and air-dried. A two-tailed unpaired *t*-test was used to analyse the data.

Drug sensitivity assays. Two thousand mES cells per well were seeded in 24-well plates in duplicate. After 24 h, cells were incubated with various drugs at the indicated concentrations (Fig. 3a) for 24 h in mES cell medium, except hydrogen peroxide which was for 1 h. For irradiation, plates were exposed to the X-ray source from an X-RAD 225C apparatus at a rate of 687 cGy min^{-1}. Six days later, cells were fixed with a solution of 12.5% (v/v) acetic acid, 12.5% (v/v) methanol for 15 min and then stained with 1% (w/v) crystal violet. Afterwards, stained cells were treated with 0.1% SDS in methanol and the absorbance was measured at 595 nm. Each point in the plots was the average of two experiments where each experiment had a duplicate and was a percentage of the absorbance from untreated embryonic stem cells. For *Lig3*-null cells expressing the Lig3 ΔZNF-GFP, MtLig3-ΔBRCT-GFP-NES and MtLig1 GFP transgenes, two independent null clones were used for each. For the colony formation assays (Fig. 3b), 2×10^3 embryonic stem cells were plated in 10-cm^2 plates and exposed to ionizing radiation or ultraviolet C radiation. Eight days later, surviving colonies were fixed with methanol and stained with 3% (v/v) Giemsa.